NATIONAL ADVISORY COMMITTEE FOR AERONAUTICS

TECHNICAL NOTE 2662

A SUMMARY OF DIAGONAL TENSION

PART II - EXPERIMENTAL EVIDENCE

By Paul Kuhn, James P. Peterson,
and L. Ross Levin

Langley Aeronautical Laboratory
Langley Field, Va.

Washington

May 1952

CONTENTS

NATIONAL ADVISORY COMMITTEE FOR AERONAUTICS

TECHNICAL NOTE 2662

A SUMMARY OF DIAGONAL TENSION

PART II - EXPERIMENTAL EVIDENCE

By Paul Kuhn, James P. Peterson,
and L. Ross Levin

SUMMARY

Methods of analyzing web systems working in diagonal tension have been given in Part I of this paper. Part II presents the experimental evidence.

INTRODUCTION

Methods of analyzing plane or curved shear webs in incomplete diagonal tension have been presented in Part I of this paper (reference 1). These methods make liberal use of empirical relations, and a rather large amount of space was devoted in Part I to general discussions of the test results in order to furnish the background knowledge that was felt to be desirable for anybody concerned with the application of the methods.

Part II presents the test information in greater detail. It is intended primarily for those who are interested in improving the methods. It should also be useful in interpreting specific tests such as might be made in the course of demonstrating the strength of a specific airplane.

All references to numbered formulas in the text refer to formulas given in Part I; a list of symbols is also given in Part I.

PLANE-WEB SYSTEMS

The methods for analyzing plane diagonal-tension webs presented in Part I may be considered to consist of a basic stress theory and of a strength theory which is based on the basic stress theory.

The experimental evidence concerning the stress theory was obtained mainly from NACA tests on beams, involving extensive strain measurements. These tests are presented in some detail.

The experimental evidence on the strength theory is based on NACA tests, including those just mentioned, and on tests made by aircraft manufacturers. The main series of NACA tests comprised about 50 beams; the manufacturers furnished a total of about 140 tests. Some of these test results were given to the NACA with the stipulation that no test details be published. For this reason, and also because a detailed presentation of the data would be rather voluminous, the data from manufacturers' tests are presented only in summary form. The cooperation extended by the manufacturers was very valuable, because many of the strength formulas are partly or wholly empirical, and the large number of additional tests greatly increases the confidence that may be placed in the formulas.

Data from the following manufacturers were used:

Boeing Aircraft Co.
Consolidated Aircraft Corp.
Douglas Aircraft Co., Inc.
The Glenn L. Martin Co.
Vultee Aircraft Corp.

1. Stresses and Deflections

1.1. General discussion of NACA test procedures.- The beams tested by the NACA may be divided into three groups as far as test technique is concerned: medium-size beams, which formed the largest group, small but heavily loaded beams, and very large beams.

A typical test setup for a medium-size beam is shown in figure 1. Beams having depths of 25 and 40 inches were tested in the manner shown as cantilevers fastened to a heavy universal support. The load is applied by means of a hydraulic jack, with rollers interposed in order to give freedom of extension to the beam flange. Stabilization against torsional failure of the beam and against lateral buckling of the compression flange is effected by horizontal guide arms (extending to the left in fig. 1) which are pivoted at both ends and form a series of parallel-motion guides.

The dial gages used to measure beam deflections are supported by a steel truss above the beam. The truss is welded to a vertical post which in turn is securely fastened to the top and bottom flanges of the beam at the root end of the test section, where a web doubler plate begins. This method of supporting the dial gages was found necessary because the angles used to attach the beam to the support deformed under the pull of

the tension flange. Although the attachment angles were made of the heaviest steel angles rolled (7/8 in. thick) and were reinforced by welded gussets, they deformed sufficiently to almost double the deflection at the tip of the beam in some cases.

The beam is shown after failure, and after the strain-gage leads had been removed; the strain gages are not visible in this view. The failure is typical of upright failure by column buckling: Although the uprights have large permanent over-all deformations, no local deformations of the cross sections are evident.

A typical setup for a small but heavy beam is shown in figure 2. (The beam is 12 in. deep and has a depth-thickness ratio of 120.) The beam is simply supported in an inverted position; the reaction supports are visible above the two ends. Because the beam is heavily loaded, the compression flange is heavily stressed and requires closely spaced supports to prevent lateral buckling. For beams of the proportions shown $\left(\frac{h}{t} \approx 120\right)$, round steel rods were satisfactory as supports. Heavier beams $\left(\frac{h}{t} \approx 60\right)$ were found to twist with sufficient force (due to torsional instability) to set up as much as 15 percent friction by rubbing of the beam flanges against the guide bars. For these beams, the round bars were replaced by square bars, and rollers were placed on each bar to reduce the friction to a negligible amount.

A typical setup for a large beam (74 in. deep) is shown in figure 3. The electric resistance strain gages may be seen on the three middle uprights. Figure 4 shows a different view of the same setup; in this view, the parallel-motion guide bars may be seen, as well as the structure necessary to support them.

Figure 5 shows column failure of the uprights on one of these large beams; no distortion of the cross sections of the uprights is evident. By contrast, figure 6 shows forced-crippling failures of large but frail uprights. The attached legs of the Z-section stiffeners are badly deformed, while the free legs show only a barely visible buckle. It might be noted that the junction line between the attached leg and the web of the Z-section is also kinked, while the explanation of forced-crippling failure given in Part I stated that this line remains straight. However, the kink in this line occurred only at the instant of final failure, while the explanation in Part I referred to the deformation pattern that begins to develop as soon as the buckling load of the web is exceeded.

On the first beam tested, an extensive strain survey was made with Tuckerman strain gages in order to provide a check against the electric resistance gages, which were being introduced at this time. The tests

with Tuckerman gages required loading the beam repeatedly to a fairly high percentage of its ultimate load. On all other beams, electric resistance gages were used exclusively, and no repeated loads were applied; the load was increased in increments until failure occurred.

1.2. Basic data on NACA test beams.- The main NACA beam tests were made over a period of several years in five groups; for convenience of reference, the groups have been designated as series I to V.

Series I consisted of beams 40 inches or 25 inches deep with double uprights. Series II consisted of 25-inch beams with single uprights. In series I and II, the material was 24S-T3 aluminum alloy (with one exception as noted).

Series III consisted of 25-inch beams made of 75S-T6 alloy. Single as well as double uprights were used.

Series IV consisted of very large beams (74 in. deep) made of 24S-T3 alloy.

Series V was a series of thick-web beams $\left(\frac{h}{t} \approx 120\right)$ made of 24S-T3 alloy.

Each beam carries a code designation such as I-25-4D, with the following meaning:

I	test series I
25	approximate depth of beam in inches
4	number of beam within the series
D	double uprights (S for single uprights)

The basic data on dimensions and materials are given in tables 1 and 3; calculated and test data are given in tables 2 and 4. Figures 7 to 10 give information not covered by the tables.

A comprehensive report on series I to IV was published as reference 2, which gives also the original references. The results for series V were published in reference 3.

1.3. Web buckling.- When the loading ratio τ/τ_{cr} is large, the diagonal-tension factor k is insensitive to small changes in τ/τ_{cr}; even for a ratio as low as 10, a 10-percent change in τ/τ_{cr} produces

only a 3.5 percent change in k. An accurate estimate of the buckling stress τ_{cr} is therefore not important when the beam fails at high loading ratios, and consequently no concerted efforts were made to measure the buckling stresses for thin webs (with high h/t ratios).

Observations in this range were made mostly by two simple methods:

(1) Observing the reflections of windows on the web

(2) Checking the web for out-of-flatness with a straight edge

The first method is a good one under favorable circumstances, but such circumstances often do not prevail in beam tests.

Another method employed was to take strain readings on a 2-inch Tuckerman strain gage placed at right angles across an expected buckle. The gage, having a rigid body, measures the geometric shortening due to buckle curvature in addition to the strain; thus, deviation of the load-strain plot from a straight line indicates buckling. This method was employed very successfully on curved sheet and proved satisfactory on flat thick sheet.

All measurements of buckling stress made on the web have a defect: The first buckle noted may be merely a local buckle. This defect could be overcome to some extent by using a large number of gages, but this was considered an undesirable complication for beam tests.

The method considered to be the most desirable one (in general) was to utilize the measured upright stresses. As long as the web is not buckled, the uprights are unstressed (unless there are bending effects due to unsymmetrical construction). The appearance of compressive stresses in the uprights marks the beginning of diagonal-tension action and thus indicates that the web has buckled. From a plot of upright stress against load, the buckling load can generally be determined fairly accurately on web systems for which it needs to be known accurately.

The curves of empirical restraint coefficients for buckling calculations (Part I, fig. 12(b)) were drawn as weighted average curves for buckling data obtained from beam tests and from miscellaneous other tests. Table 4 lists buckling stresses calculated with the aid of these curves and buckling stresses determined experimentally by the last-mentioned method (appearance of upright stresses) for the beams of series V. These beams failed at loading ratios ranging approximately from 1.1 to 2.2; they are thus in a range where a rather accurate estimate of the buckling stress is desirable. The fourth column of the table shows that the ratio of experimental to calculated buckling stress ranges from 0.77 to 1.24, with an average value of 0.95. For tests on medium-thick webs, the ratios

fell in about the same scatter band. For thin webs, on which only simple visual observations were made, the ratio ranged up to 1.5, but this was undoubtedly due to inadequate sensitivity of the test methods under unfavorable conditions.

1.4. Upright stresses.- The measurements of upright stresses were guided by the following considerations:

(1) Built-up structures exhibit more or less irregular stress distributions due to imperfect construction.

(2) The stress in an upright varies along the length of the upright.

(3) Single uprights are subjected to eccentric loading and thus to bending in addition to compression.

(4) Any upright of practical size is subjected to local deformations caused by the shear buckles in the web; these deformations may become very severe at high loads.

In view of the first consideration, stresses were measured on three uprights except on beams with large upright spacing where only two uprights were usable for measurements because the others were adjacent to the stiffened end bays and thus worked under different conditions.

In order to take care of the second consideration, a number of gage stations were distributed along the length of each upright. The number ranged from 9 stations for 25-inch beams to 13 for 74-inch beams.

The third consideration introduces a difficulty. The calculated stress σ_U for a single upright is the sum of compressive stress and bending stress for the fibers in the plane of the web in a vertical strip adjacent to the upright. The gages are necessarily in a different plane - on the exposed face of the attached leg of the upright. The calculated stresses therefore had to be adjusted to the plane of the gages. For Z-section uprights, the adjustment is small, but for uprights of angle section it is fairly large (of the order of 25 percent). The "plane of the web" was assumed to be defined by the midplane of the web.

In double uprights, bending would be only of an accidental or secondary nature, and its effect was eliminated by using a pair of gages back to back at each gage station.

The last consideration - local deformations - is also fairly effectively eliminated for double uprights by using a pair of gages at each station. For single uprights, however, it is the largest source of uncertainty. The most effective method of reducing this uncertainty

would be to use a single gage extending over the full length of the upright; with such an arrangement, the effect of the local deformations would be fairly well averaged out because the shear buckles have a regular pattern, and their wave length is short. This method was not used because it would require special strain gages. It was felt, however, that the number of gages used was sufficient to give a reasonable approximation to σ_U if they were averaged, and the results appear to vindicate this point of view.

Figure 11 shows on the left the distribution of σ_U for three beams with double uprights and at three different loads. Each test point represents an average obtained as follows: First, readings of each pair of gages were averaged. Next, corresponding stations were averaged for the two (or three) test uprights. Finally, stations above the neutral axis of the beam were averaged against corresponding stations below the neutral axis; the points are shown in the figure at the stations below the neutral axis. Each point thus represents the average of 8 or 12 gages. The curves faired through the points were also plotted for the upper half of the beam in order to permit easier visualization of the complete curve. As predicted by the theory, the stress was a maximum at midheight.

The right-hand side of figure 11 shows test points and curves obtained in the same manner for the two 74-inch beams having double uprights. The pronounced local minimum, instead of a maximum, at midheight of the curves shows that the web splice along the neutral axis (fig. 9(a)) had a distinct effect on the action of the web.

Figures 12 to 15 show upright stresses plotted against load. For beams with double uprights, the maximum value $\sigma_{U_{max}}$ is shown as well as the average value σ_U, unless the difference was too small to show on the plots. The experimental value of $\sigma_{U_{max}}$ represents the average (for 2 or 3 uprights) estimated from distribution curves such as shown in figure 11. The experimental value σ_U represents the average of all gages on the beam; the number of gages averaged ranges from a minimum of 36 (2 uprights with 9 stations each) to a maximum of 78 (3 uprights with 13 stations each).

On beams with single uprights, the stresses caused by the local deformations make the determination of the stress distribution and of the maximum stress $\sigma_{U_{max}}$ too uncertain to be worthwhile. Consequently, only the average stress σ_U is shown. In addition, however, a horizontal line terminated by tick marks shows the range from the lowest individual gage reading to the highest individual value in the entire group of gages. The deviations from the mean values depend on the relative sturdiness of the upright and increase with increasing load. The large spread between

highest and lowest gage reading found in a number of cases demonstrates clearly that isolated strain measurements on structures of this type are quite useless; correlation with any kind of theory can be expected only if a large number of gages is used to permit local stress effects to be averaged out.

Inspection of figures 12 to 15 shows that the engineering theory of incomplete diagonal tension gives no unconservative predictions of upright stress at loads less than about two-thirds ultimate except for the first beam tested (I-40-1D). As stated in Part I, this conservativeness is the result of the policy followed in choosing the empirical relation between the factor k and the ratio τ/τ_{cr}. The exception for the first beam was permitted because this beam had been subjected to repeated loading (section 1.1), and repeated buckling lowers the buckling stress below the calculated value, as discussed in section 9.10 of Part I. It may also be noted that the unconservativeness on beam I-40-1D (fig. 12), although amounting to about 20 percent for $\sigma_{U_{max}}$, is very small for σ_U.

The poorest agreement is exhibited by the stresses for beam IV-72-4S in figure 15. This beam was deliberately designed with very thin uprights in order to demonstrate, by direct comparison with beam IV-72-2S, the fallacy of designing uprights simply for a large moment of inertia (Part I, section 3.9, closing paragraph). The local deformations consequently were very large (see fig. 6), so that an extremely large range of measured stresses resulted (fig. 15). It may be noted that this is the only test beam for which some individual upright gages showed tension stresses about as large as the highest individual compression stresses. Under these conditions, the upright stress obtained by averaging gage readings obviously cannot be regarded as reliable in spite of the fairly large number of gages averaged.

On a number of beams, the predictions are unconservative for the high loads. The load at which the prediction begins to become unconservative coincides in most cases quite closely with the load at which the web stress reaches the yield value, as indicated by a dash-dot line in the figures. The explanation is probably that yielding of the web has a two-fold effect: The diagonal tension develops more rapidly, and the contribution of the web to the effective area of the upright decreases more rapidly than in the elastic range. At present, it does not seem justifiable to attempt any correction for this effect, because the accuracy with which the strength of the uprights can be predicted is not high enough. (Note, for instance, that beam II-25-5S in figure 13 shows the largest excess of measured over calculated stress in the upright as the failing load is approached, but table 2 shows that the strength prediction is conservative by about the same amount as the average for all tests.)

Unconservative predictions of the upright stresses were also noted in the beams of series V. These beams failed at high web stresses, ranging from 22 to 38 ksi, and at low ratios τ/τ_{cr}, ranging from 1.1 to 2.2. Thus, by the time the upright stresses were of any magnitude, the web was well in the plastic range, the proportional limit of the web material being 12.5 ksi and the yield stress less than 24 ksi. The upright

stresses themselves were relatively low, because the ratios τ/τ_{cr} were low; on the other hand, there were very high local stresses due to severe forced crippling, because the uprights were thinner than the web in most cases. In view of all these factors, the lack of agreement between measured and calculated stresses was not surprising, and a presentation of the results was not considered worthwhile. It might be noted, however, that the predictions of ultimate strength for the beams of series V show no more scatter than those for the other series.

1.5. Indefinite-width uprights.- In box beams, bulkheads formed from sheet are sometimes flanged over, and the flanges are riveted to the shear webs of the box. Formally, such a bulkhead constitutes a "single upright" for the shear web. It is evident, however, that the bulkhead will not bend like an ordinary single upright; the flanged edge of the bulkhead will remain straight and will thus behave like a double upright in this respect. On the other hand, it is equally obvious that the compressive load introduced by the shear web into the upright will not be distributed uniformly over the entire bulkhead; only a portion of the bulkhead next to the attached flange will participate in carrying the compressive load.

In order to provide some information on this problem, three box beams were built, with shear webs 25 inches deep and separated by about 25 inches. Bulkheads formed from solid sheet were flanged over and riveted to the webs, and stress measurements were made on the attached flanges with the box subjected to vertical shear loads. From these measurements, it was concluded that the effective upright area A_{U_e} consisted of the attached leg and an additional area equal to $12t_U^2$, or in other words, the effective width furnished by the bulkhead is equal to $12t_U$. The results obtained from the three tests were fairly consistent.

The effective width of $12t_U$ is the one acting at and near the failing load. At low loads, the effective width was found to be 2 to 3 times as large; the decrease with load was roughly linear. The failing stresses in the uprights ranged from 15 to 30 ksi and fell within the scatter band established from tests with conventional uprights.

1.6. Beam deflections.- A complete set of deflection measurements was taken on the beams of series I. The test section was taken as the region over which the thickness of the web was constant; that is, the end bays with doubler plates were excluded. The measurements were taken with respect to the tangent at the inboard end of the test section; they can therefore be compared directly with the computed deflections.

The deflections were computed in the usual manner as the sum of bending deflection and shear deflection, with the latter computed by the expression

$$\delta = \frac{PL}{htG_e}$$

where L is the length of the test section.

Figure 16 shows the measured and the calculated deflections. As a matter of some interest, the following calculated curves are also shown:

(1) The bending deflections alone. It may be seen that they are relatively small.

(2) Deflections calculated on the assumption that the web did not buckle $(G_e = G)$.

(3) Deflections calculated with allowance for buckling, but without allowance for plasticity effects $(G_e = G_{IDT})$.

A comparison of the curves calculated with the final value G_e and those calculated with G_{IDT} shows that the plasticity effect can be so large as to double the deflection.

The curve giving the plasticity correction for the shear modulus (fig. 22(b), Part I) was derived from a series of 10 tests on square webs in a pin-jointed frame under diagonal pull (reference 4). The webs were of different thicknesses and carried varying amounts of stiffening in order to produce varying amounts of diagonal tension. The ratio G_e/G_{IDT} did not appear to depend on the amount of diagonal tension within the rather wide scatter limits of the tests. The average curve shown in the figure should therefore be approximately valid for a web without diagonal tension, that is to say, it should be about the same as the shear stress-strain curve of the material. Application of a recent empirical method of deducing the shear stress-strain curve from the tensile and the compressive stress-strain curves also gave reasonable agreement with the curve.

2. Ultimate Strength

2.1. General discussion.- In most web systems, the web weighs more than twice as much as the uprights; the achievement of structural efficiency depends therefore chiefly on an accurate knowledge of web strength. A series of special shear tests was consequently made in order to establish the failing stresses for webs made of the two most widely used aluminum alloys; these tests are discussed in section 2.2. The following sections give information, derived from beam tests made by the NACA and by the manufacturers listed previously, on the strength of the web, the uprights, and the rivet connections.

Out of a total of 144 tests made by manufacturers, only four were rejected. A group of three tests on 10-inch beams was rejected outright. The reported test loads were more than twice the predicted loads.

Examination of the test report showed that wooden guide posts were used to prevent twisting of the beam; in such a setup, there is always danger that the beam flanges may hang up in the guides, and it was considered probable that hanging-up was responsible for the extremely high loads reported. The fourth test was rejected after a duplicate beam had been built and tested by the NACA; this case is discussed in section 2.5.

2.2. Strength of webs tested in pure shear.- Tests made to establish the failing stresses of shear webs made of 24S-T3 and 75S-T6 aluminum alloys have been reported in references 5 and 6. The jig used for most of the tests is shown in figure 17. The two long edges of the web were bolted to steel plates, which in turn were bolted between heavy steel bars. These bars were very heavy (2 by 4 in.) in order to reduce the nonuniformity of shear strain caused by longitudinal strain in the bars. The nuts on the bolts going through the sheet were "just snug" in order to keep friction to a minimum. Angles were riveted to the short edges of the webs in order to enable the web to carry shear stresses over its full length. (The length of the ineffective zone caused by a free end can be estimated for nonbuckled sheet but not for buckled sheet.)

Figure 17 shows that the "uprights" used to separate the flanges were hinged in order to eliminate portal-frame effects. Webs intended to develop a high buckling stress (and thus a low value of k) had closely spaced stiffeners riveted to them. These stiffeners had semicircular ends bearing on the flanges but not connected to them, again in order to eliminate portal-frame effects.

Either one or two rows of bolts were used. The pitch of the bolts was 1 inch; the diameter of the bolts was varied. Heavy washers were used to protect the sheet from direct contact with the bolt heads.

The results of the main tests are shown in tables 5 and 6. The nominal shear stress is given in two forms: the stress τ_g computed for the gross section (Lt), and the stress τ_n computed for the net section between rivet holes (along one line of rivets). The actually observed failing stresses have been corrected to a "specification ultimate strength" given in the figures (on the usual assumption of direct proportionality). Figures 18 and 19 show that the stress based on the net section (shown by square symbols) varies greatly, contrary to the assumption commonly made in design work. Apparently, a stress-concentration factor operates which increases as the rivet factor C_r (ratio of net to gross section) increases, at least up to a certain point. For the two materials tested, this change in stress-concentration factor just about offsets the change in net section. As a result, the stress based on the gross section (shown by circles) is practically independent of the rivet factor C_r. For the tests at the two lower values of the

factor k ($k \approx 0.04$ and 0.4), the deviations from the average of τ_g are mostly within ±5 percent; for the tests at the two higher values of k, the deviations are mostly within ±10 percent. This spread is about the same as that due to changing other factors while keeping C_r constant and is only about twice the spread found in groups of four nominally identical specimens.

The tests thus indicate that, for the two alloys tested at least, it is convenient to abandon the usual method of computing the allowable web stress for the net section between rivet holes and to use instead the stress based on the gross section. The allowable stress derived in this manner naturally does not represent the true shear strength of the material.

The tests on 24S-T3 webs with $C_r \approx 0.81$ show a slight loss (at least relatively) if only one row of bolts is used instead of two. Examination of the data shows that the allowable bearing stresses for the sheet are exceeded. The allowable shear stresses derived from the tests should therefore be considered as valid only under the proviso that the allowable bearing stresses are not exceeded; the latter were taken from reference 7 when the analysis was originally made, but the substitution of currently valid allowable bearing stresses would not change the picture significantly.

In one of the test series (fig. 18(a)), a few tests were made on square webs in a pin-jointed "picture frame," with the webs sandwiched between the flange angles and the nuts "just snug." As expected, these tests gave the same results as the main tests. In another series, long webs were tested with the washers under the bolt heads omitted (fig. 18(a)). In this condition, the allowable stress was reduced about 10 percent.

Comparisons with earlier tests in the picture-frame jig (reference 6) indicate that riveted webs will carry 10 to 15 percent higher stresses than bolted webs with the nuts just snug, because friction carries part of the load. At very low values of k (≈ 0.1) and for one thickness of sheet, the increase was somewhat less; however, this slight deficiency may be attributed to the fact that the picture-frame jig does not give a very uniform stress. It is believed, therefore, that a 10-percent increase in allowable stress for riveted webs (over the "basic-allowable" values valid for bolted webs with nuts just snug) is justified. Under some conditions, however, consideration should be given to the question of whether the rivets will remain sufficiently tight throughout the service life of the structure to justify the increase.

2.3. Strength of beam webs.- The allowable shear stress for beam webs given in figure 19 of Part I is based on the pure-shear tests described in the preceding section. The tests showed a scatter band of ±10 percent,

and the allowable stress is based on the lower edge of the scatter band. Consequently, strength predictions for beams failing by web rupture would be expected to average 10 percent conservative, provided that the allowable stress is corrected to the actual properties of the web material. This practice was followed for all the predictions discussed here; where actual properties were not known, typical properties were used. While this practice is not in accord with the aeronautical one of using minimum guaranteed or probability values, it is felt to be more significant here where the point at issue is the reliability of the basic method.

The last column of table 2 and table 4 gives the ratio of failing load to the load predicted to cause web rupture. In these calculations, the allowable strength was assumed to be increased 5 percent by the bolts being tight. It will be noted that the majority of these ratios are in parentheses. These parentheses denote that the observed web rupture is considered to be a secondary failure, because according to the predictions failure of the upright was the primary failure. The column averages shown disregard the values in parentheses. If tables 2 and 4 are combined, the average ratio of actual to predicted load becomes 1.07, which is reasonably close to the expectation in spite of the fact that only 5 tests are averaged. Inspection of the tables shows also that most of the ratios in parentheses are above unity; therefore, most webs were developing somewhat more than their rated strengths at the instant when upright failures precipitated failures of the entire systems with ensuing web ruptures.

For beam III-25-8S, the prediction was 5 percent unconservative; a prediction based on the minimum guaranteed or the probability value therefore would have been conservative, because even the latter value differs from the actual one by more than 5 percent.

In the group of older tests (mostly 24S-T material) by manufacturers, six web failures were noted, with the ratio of actual to predicted load being 1.14 ± 0.06, which is again reasonably well in line with the expectation.

In the more recent group (mostly 75S-T6 material) of manufacturers' tests, 45 web ruptures were noted; of these, only 16 are considered to be primary web failures. For these primary web failures, the average ratio of actual to predicted load was 1.05. This is lower than expected; the three lowest ratios are 0.92, 0.93, and 0.95. In these beams, the end bays were not reinforced; for the beam that failed at the lowest ratio, a photograph was available which showed that the failure originated in an end bay. As pointed out in Part I, unreinforced end bays will generally have less than 90 percent efficiency. The fact that the average ratio was only 1.05 instead of the expected 1.10 can therefore probably be explained by end-bay failures which lowered the average.

A "hidden factor of safety" is furnished by the portal-frame effect (Part I, appendix). For the NACA beams, this effect was estimated to be less than 5 percent for most tests and less than 1 percent for many; the four cases in which it was estimated to be about 10 percent are discussed in section 2.4.

2.4. Upright failure by column buckling.- The column failures of double uprights listed in table 2 were used to plot figure 20, which shows the computed upright stress σ_U at failure as a function of the effective slenderness ratio L_e/ρ. The effective length L_e is computed with the aid of the empirical formulas (35). The Euler curve agrees quite well with the lower limit of the scatter band; formulas (35) therefore appear to give an acceptable estimate of the effective column length. The number of tests is too small to consider formulas (35) as firmly established; it appears to be large enough, however, to establish fairly well that Wagner's theoretical curves for effective column length are definitely too high. (See fig. 6(b), Part I, for comparison between theoretical and empirical curve.)

The very small number of column failures out of a total of nearly 200 beam tests reflects the fact that most practical web systems are in the range where the uprights fail by forced crippling rather than by column bowing (see Part I, discussion of fig. 23). The 144 beams tested by manufacturers may be presumed to cover fairly well the range encountered in practice; among these, not one upright failure was attributed to column buckling. Such column failures as were observed took place in NACA beams deliberately designed with very slender uprights in order to produce column failure.

The ratios of actual to predicted beam failing loads are shown in the third-from-the-last column of table 2. The low strength developed by the first beam is attributed in part to the effects of the previous repeated loadings applied (section 1.1). For the two beams showing the highest ratios (I-25-2D and -3D), the portal-frame effect (Part I, appendix) was estimated to be about 10 percent, which may have contributed to the high value of the ratio.

The portal-frame effect was also estimated to be about 10 percent for beams I-25-5D and I-25-1D. The former could not be carried to failure because of interference with the dial-gage truss; the highest load applied was 1.19 times the predicted failing load. The latter, on the other hand, failed by web rupture at a load only 1 percent in excess of the predicted one. For the time being, then, it is concluded that it would not be wise to make an allowance for portal-frame effect in routine strength predictions.

2.5. Upright failure by forced crippling.- The plots from which the empirical formulas for forced crippling were established are shown in

figures 21 to 23. Calculated values of $\sigma_{U_{max}}$ are plotted against a parameter which involves the diagonal-tension factor k and the "relative sturdiness" t_U/t of the upright with respect to the web. The plots include manufacturers' and NACA tests.

In all three plots, shaded symbols indicate tests in which the web ruptured. It is not possible to determine accurately whether the web or the upright was the primary cause of failure. It is possible, of course, that some of the uprights in these cases would have carried a somewhat higher stress if the web had been stronger. However, inspection of the three figures shows that the design allowable curves deduced would not be changed if the shaded symbols were omitted.

Figure 21 shows the plot for single uprights for web systems made of 24S-T3 aluminum alloy. The full-line curve represents the formula recommended for design (formula (37a), Part I), with the plasticity correction made as recommended in section 4.10 of Part I. The short dashed and the long-and-short-dashed curves represent, respectively, 1.25 and 1.5 times the design allowable value, corrected for plasticity effect. The former represents fairly well the middle of the scatter band, the latter the upper edge, except at the right-hand end, where the formulas become more conservative. (Taken at face value, the test points may suggest that it would be better to omit the plasticity correction. On general principles, however, it is clear that such an omission would be unsafe.)

Figure 22 shows the plot for double uprights on web systems made of 24S-T3 aluminum alloy. The number of tests is small but may be considered adequate to establish the design allowable value based on the lower edge of the scatter band (full-line curve). The width of the scatter band cannot be established because of the small number of tests, but it appears to be of the same order of magnitude as that for single uprights shown in figure 21.

Figure 23 shows the plot for single uprights made of 75S-T6 or Alclad 75S-T6 alloy and used on webs made of Alclad 75S-T6. The width of the scatter band appears to be slightly less than for 24S-T3 alloy, but possibly only because the number of tests is smaller.

Few tests are available on Alclad 75S-T6 web systems with double uprights. The allowable value of upright stress given in Part I was obtained from the allowable value for single uprights of the same alloy on the assumption that the ratio of allowable stress for double uprights to allowable stress for single uprights is identical for the two aluminum alloys.

The fact that figure 23 shows a much larger percentage of tests with web failures than figures 21 and 22 may be explained as follows: The beams made of 24S-T alloy were designed at a time when little was known about upright failure; many of them were therefore deliberately designed with overstrength webs in order to obtain information on upright failure. The 75S-T beams were designed much later, when enough information was available to insure a reasonable balance between web strength and upright strength.

In the NACA test beams, upright cross sections were either plain angles or plain Z-sections. The manufacturers' tests on 24S-T beams included also a large number of lipped Z-sections and some lipped angles. Manufacturers' tests on 75S-T beams were mostly lipped Z-sections and J-sections. No effect of lips could be deduced from separate plots made for each type of section; it is possible, however, that tests made specifically to investigate this question would show a strengthening effect of lips.

Previously published plots corresponding to figure 21 (as in references 2 and 3) showed one point about 25 percent below the lower edge of the scatter band. Careful examination of the test report did not disclose any reason for suspecting faulty test technique or workmanship. Consequently, a duplicate of the beam was built and tested by the NACA. The uprights were of lipped-angle section. In the NACA test, the lip at the free edge of one upright kinked badly at a load about 11 percent higher than the "test load" given in the manufacturers' test report. However, the NACA beam continued to carry load and did not collapse until the load was 73 percent higher than the test load reported for the manufacturers' beam. The manufacturer's test was therefore rejected. It might be noted that, aside from the local kink mentioned, the deformations of the NACA beam were of the same order of magnitude as on many other beams; this fact would seem to remove the - rather remote - possibility that the manufacturer's test was stopped short of ultimate load because of excessive web or over-all deformations.

2.6. Web-to-flange rivets.- In the NACA tests, the web was generally attached by bolts in order to facilitate re-use of the flanges. No bolt failures were expected or experienced.

In the manufacturers' tests prior to 1942 (which constitute the majority of the data available), the rivet design tended to be rather conservative. The rivet loads were usually computed on the assumption of complete diagonal tension, which is always conservative. The allowable rivet strengths were based on the nominal rivet area and the shear strength of the rivet wire. The first of these practices is conservative because the rivet hole is always drilled oversize; the second, because the driving operation tends to increase the shear strength of the rivet. The actual

rivet strengths were therefore usually from 20 to 40 percent above the nominal values used at that time. As a result of these conservative practices, and because failure was often caused by weak uprights, very few rivet failures occurred in the manufacturers' tests.

Failures did occur in five tests at loads ranging from 3 percent lower to 16 percent higher than predicted with formula (34) used to calculate the loads on the rivets and special tests to determine the actual strengths of the rivets. On the average, the predictions were 7 percent conservative; this result may be attributed to friction relieving the rivet loads.

In the discussion of formula (34) in Part I, mention was made of a "more rational" version of the formula, but it was pointed out that this purported greater rationality is spurious. If the "more rational" formula had been used, the predictions for the five beams would have been unconservative by 2 percent on the average and by 12 percent in the extreme case.

Among the new manufacturers' tests, one group showed positive margins ranging from 10 percent on up, based on actual rivet strengths estimated on the basis of information given in reference 8. (Currently valid design allowables are about 15 percent lower.) No failures were recorded in this group.

The latest group differed markedly in that it showed consistently much lower margins; the margins also computed on the basis of actual rivet strengths ranged from -10 to 10 percent. No failures were recorded for several beams with negative margins, but failures were noted for two beams which had essentially zero margins.

For the limiting cases of a shear-resistant and a pure-diagonal-tension web, the formula for rivet load is a straightforward application of statics; this consideration, together with the test evidence presented, is felt to justify the belief that the method of computing the rivet load is fairly accurate. Results obtained in individual tests should be judged with due consideration given to the difference between true and nominal rivet strength and the possible existence of hidden factors of safety.

2.7. Upright-to-flange rivets.- In practically all test beams, the upright-to-flange rivets were considerably overstrength; therefore, practically no failures were experienced. This overstrength can be attributed either to the use of very conservative design formulas based on simple diagonal-tension theory, or to deliberately conservative design on test beams intended to furnish information on other items.

For beams with double uprights, one rivet failure was recorded. The existing nominal rivet strength was only about 5 percent below the required

strength and the existing actual rivet strength was therefore probably above the required strength; however, the calculated upright stress was very uncertain because of a peculiar design feature. In two beams, no failures were recorded, although the estimated true rivet strengths were 10 to 20 percent below the required strength.

For beams with single uprights, there were two records of failure although the rivet strengths were appreciably greater than required; the analyses were very uncertain, however, because several important dimensions of the beams were not given and had to be estimated or inferred. There are two records of successful joints in which the ratio of estimated true rivet strength to required strength was less than unity (0.98 and 0.83), and several records of successful joints with essentially zero margin.

The very scanty direct test evidence is thus divided into two groups, for double as well as for single uprights. The smaller group indicates that the formula for rivet load may be somewhat unconservative, the larger group indicates the opposite. However, the analysis of all the tests in the former group is so uncertain that very little significance can be attached to it.

Formulas (39) give the rivet load as the product of upright stress σ_U and upright area. The method of calculating the stress σ_U has been extensively verified by tests and is somewhat conservative (section 1.4). Furthermore, the stress at the ends of an upright is less than σ_U, although the difference is small when the diagonal tension is highly developed. The large amount of strain-gage evidence concerning σ_U, coupled with the favorable portion of the strength-test evidence, is felt to be sufficient to allay any concern that might be felt as a result of the three unfavorable strength-test results.

2.8. Upright-to-web rivets.- The criterion for shear strength required in double uprights is based on a series of column tests (reference 9).

The criteria for the required tensile strengths of rivets (formulas (41) and (42)) are attempts to provide a safeguard against a type of failure that has been observed in tests. Because no tests have been made to check specifically on this item, the available evidence is rather sketchy and largely negative; that is, in most tests no failures were observed (or at least none were recorded). An additional difficulty is that rivet failures are often found after the failure of the beam, and it is then impossible to state whether the rivet failure was a primary one responsible for the beam failure or a secondary one that took place while the beam was failing for other reasons. In view of all these uncertainties, the coefficients given in formulas (41) and (42) should be considered only as tentative values.

On beams with single uprights, a total of five rivet failures have been recorded. The ratios of actual to required rivet tensile strength (with the latter based on formula (42)) were: 0.46, 0.59, 0.73, 0.90, and 0.92.

On beams with double uprights, two failures were observed, with ratios of actual to required rivet tensile strength of 0.60 and 0.87.

On most of the manufacturers' beams analyzed, there was a positive margin against tensile failure of the (protruding-head type) rivets, averaging about 15 percent. The criterion therefore appears to require rivet sizes that are fairly well in accord with the riveting practices followed by several manufacturers. It should be well-noted, however, that the riveting criteria followed in the past were usually couched in terms of shear strength. Rules of this type may (and generally will) result in adequate tensile strengths of the rivets if the rivets are of the protruding-head type, but they are likely to fall down if rivets of another type, such as the flush type, are used. The inadequacy of a shear criterion alone becomes evident if one considers what would happen if a shear web were attached to the uprights by dowel pins which have shear strength but no tensile strength.

There were a small number of cases where no rivet failures were observed (on single as well as on double uprights) in spite of the fact that the criterion for tensile strength indicated negative margins, some quite large. In most of these cases, weakness of the uprights precipitated failures at loads well below the potential strengths of the webs. The criterion should evidently be regarded as establishing the tensile rivet strength needed for a beam of balanced design, in which the web and the uprights fail simultaneously.

A few failures were encountered in cases where the rivets had adequate tensile strengths but inadequate shear strengths; therefore, both should be checked.

CURVED-WEB SYSTEMS

Almost all the information available on curved-web systems in diagonal tension has been obtained on circular cylinders tested in torsion. Because cylinders are more expensive to manufacture and to test than plane-web beams, the total number tested so far is rather small; however, because the theory is an extension of the well-substantiated theory of plane systems and because an effort was made to check doubtful points on specimens with rather extreme proportions, it is felt that the theory of the primary stresses is fairly well established. The strength theory, on the

other hand, is not so well established as for plane systems, and very little is known about the secondary stresses except in the special case of floating rings.

3. Stresses and Deflections

3.1. Test specimens and procedures.- The extension of the engineering theory of incomplete diagonal tension to curved webs discussed in Part I was first presented in reference 10. The tests utilized included 8 tests made by the NACA and 4 made at the Research Laboratories of the Aluminum Company of America (reference 11). Since then, 4 additional tests have been made by the NACA in order to check some doubtful items in the theory.

The basic data for the NACA cylinders are given in figure 24 and in table 7. The unconventional arrangement of double stringers was used because it not only keeps the bending stresses in the stringers small but also permits their effective elimination by the device of averaging pairs of symmetrically located strain gages. The locations of the electric resistance strain gages on the cross sections of the stringers and rings are shown in figure 25. Strain gages were applied to three or four stringers in the middle bay of each cylinder. The total number of stringer gages was 50 for cylinder 1 and varied from 62 to 96 for the remaining cylinders.

The rings of the NACA cylinders were made rather large in order to preclude ring failure. For this reason, and because the angle of diagonal tension in curved webs is fairly flat, the ring stresses were small; they were therefore considered a minor issue, and no effort was made to measure them accurately. For the sake of simplicity, the gages were located at middepth on each ring, although this is not the neutral axis because some effective width of skin cooperates with the ring. On cylinders 1 to 8, only 3 gages were used; on cylinders 9, 11, and 12, the number was increased to 12 or 16; on cylinder 10, a total of 96 gages was used because the measurements covered ring bending moments as well as axial forces.

The setup for the NACA tests is shown in figure 26. The particular test illustrated is one under combined torsion and compression. All strain-gage wiring has been removed in order to show the cylinder more clearly. The torque-loading jig illustrated was used in all tests except the first one; the jig used for cylinder 1 was found to have insufficient throw, and the torque values are in doubt for torques larger than about 95 percent of the failing value. In all tests, the load was increased in steps until failure occurred; there was no decrease of load during a test except for small unavoidable drops caused by skin buckling.

The cylinders tested at the Aluminum Research Laboratories (hereafter referred to as ARL) differed from the NACA cylinders chiefly in the type of stringers and rings used. The stringers of the ARL cylinders were of inverted Ω-section and were located on the outside of the cylinders; the rings were of solid rectangular section. The stringer strains were measured partly with electric resistance gages, partly with 10-inch Whittemore gages. Measurements were also made of skin strains, of the angles of twist of the cylinders, and of the buckle patterns of the skin. The latter measurements, presented in reference 11 in the form of contour maps, are especially interesting because they are quite detailed; the only other set of comparable measurements (reference 12) was much less detailed.

The different types of measurements taken on the ARL cylinders required repeated loadings of the cylinders; this repeated loading may have had some influence on the measured strains, angles of twist, and ultimate loads (see discussion in section 9.10, Part I).

3.2. Buckling of skin.- The buckling stress of the skin can be determined by several methods, three of which are:

(1) Visual observation of skin panels

(2) Deviation of torque-twist curve from initial straight line

(3) Deviation of torque - stringer-stress curve from zero axis (The ring stresses could also be used but are often much less reliable.)

The first method gives values of buckling stress for individual panels. Because of manufacturing imperfections, these individual values differ; the maximum deviations from the final mean value for an entire cylinder are seldom less than ±5 percent, and deviations of ±15 percent have been observed a number of times. The accuracy depends on whether the buckles form slowly or suddenly.

The second and the third methods give automatically averaged values. The second method averages over the entire cylinder surface; the third method averages over the region that affects the strain gages.

For purposes of diagonal-tension design, average values are more significant than individual values, except perhaps in extreme cases where failure is expected at very low loading ratios $\left(\text{say } \frac{\tau}{\tau_{cr}} < 1.5\right)$.

In the NACA tests of cylinders 1 to 11, no twist measurements were made.

The stringer and ring stresses are shown in figures 27 and 28. Inspection of the stringer stresses (and the ring stresses, if reliable) shows that there is in general very close agreement between the calculated

and the "observed" buckling stress. The largest discrepancy appears to be for cylinder 7, where the observed stress is about 8 percent lower than the calculated value.

For the ARL tests, reference 11 tabulates average observed values deduced from the visual observations. The following tabulation shows the ratios of these observed stresses to the theoretical values:

Cylinder	Ratio
14	1.06
15	1.15
19	.94
20	1.02
21	1.20
Average	1.07

The ratios tabulated for cylinders 14 and 15 agree roughly with similar ratios that could be deduced from the curves of stringer stress (fig. 29). For cylinders 20 and 21, the stringer stresses indicate buckling stresses about 20 percent lower than the average values deduced from the visual observations; by this criterion, the theoretical buckling stress is roughly 20 percent unconservative for cylinder 20 and very close for cylinder 21.

(Cylinder 19 does not appear in fig. 29 because it failed before any stress measurements could be taken.)

Viewed as a whole, the test evidence appears to justify the conclusion that the theoretical formula for buckling gives quite accurate (on the average perhaps slightly conservative) values of the average buckling stress, which determines the diagonal-tension effects. However, experience with flat sheets suggests that some modifications may be necessary for panels with lower curvature than that in the test specimens (Part I, section 9.1).

3.3. Stresses in stringers and rings.- Plots of the stresses in stringers and rings are shown in figures 27 and 28 for the NACA cylinders.

For the original group (cylinders 1 to 8, from reference 10), the range from lowest to highest individual gage reading is also indicated for stringer stress.

For cylinders 1 to 8, the agreement between calculated and measured stresses is reasonably satisfactory as long as the load is not too high, except for the ring stresses of cylinders 2 and 4, which are so low as to create the suspicion that the gages might not have been operating properly. At high loads, the ring stresses show a tendency to increase precipitately beyond the calculated values for cylinders 1 and 6. This increase is analogous to that noted for upright stresses on plane-web systems, but there are some unexplained anomalies. The precipitous increase in ring stress would be expected to be accompanied by a corresponding decrease in stringer stress (because the angle of diagonal tension is expected to become steeper). Such a decrease of stringer stress is noted only on cylinder 1, not on cylinder 6. Conversely, cylinder 5 shows a decrease of stringer stress at high loads, but no corresponding increase in ring stress.

The additional NACA cylinders 9 to 12 were designed to have the value of one parameter well beyond the range of the previous tests, in an effort to insure that the methods of analysis would not break down in such cases. Cylinder 9 had only 4 stringers (longerons) and thus had panels long in the circumferential direction $\left(\frac{h}{d} = 3.16\right)$; moreover, the cylinder did not comply with the restriction of close ring spacing $\left(d < \frac{1}{3} R\right)$ placed by Wagner on this case, the ratio d/R being 0.5. Cylinder 10 had rings floating on top of the stringers. In cylinder 11, the skin panels were long in the axial direction, with an aspect ratio d/h equal to 4. This test was considered important as a check on the validity of the cut-off rule applied to the ratio d/h in the determination of the diagonal-tension factor k (see fig. 13, Part I). Finally cylinder 12 had large stiffening ratios in both directions (see table 7).

Inspection of figure 28 shows that, in this special group of tests, the stress predictions were in some cases less accurate than in the original group, but such errors as exist are on the conservative side.

Figure 29 shows the stringer stresses in the ARL cylinders. Except for cylinder 15, the predictions are somewhat unconservative, contrary to the tendency noted for the NACA cylinders.

3.4. Angle of folds.- According to the theory of incomplete diagonal tension of Part I, the angle of diagonal tension in curved-web systems is only a few degrees initially; as the load increases, the angle increases, at first very rapidly, then at a decreasing rate, and approaches an angle

somewhere near 45° as the shear stress increases indefinitely (see fig. 28, Part I). In the limiting case of pure diagonal tension, the skin buckles form a pattern of straight and parallel folds; the direction of these folds coincides with the direction of the diagonal tension. Immediately after buckling, the buckle pattern cannot be described by straight lines, and consequently, the term "angle of folds" has no meaning. However, when the incomplete diagonal tension is reasonably well developed, the pattern assumes such a shape that it may be said to consist of straight folds.

On the ARL cylinders, the shape of the buckled skin was determined by dial-gage surveys at several loads (reference 11); from the contour maps, the angle of the folds can be established rather accurately. In figure 30, these angles are plotted as test points; also shown is a curve of the computed angle of diagonal tension. Furthermore, a vertical line indicates the angle corresponding to a diagonal line running from corner to corner in the panel. In all cases, the diagonal-tension field is less than two-thirds fully developed ($k < 0.67$).

With two exceptions, the angle of folds is somewhat larger than the angle of diagonal tension. The two exceptions (on cylinders 20 and 21) appear to indicate a phenomenon also observed qualitatively in some NACA tests: The angle of the folds stops increasing when it has reached the corner-to-corner direction. The differences between angles of folds and angles of diagonal tension do not appear to bear any relation to the differences between measured and calculated stringer stresses on any cylinder; it is therefore not obvious at present that any practical significance attaches to the phenomenon.

3.5. Angle of twist.- Measurements of the angle of twist were made on NACA cylinder 12. Figure 31 shows the measured and the computed angles. The discrepancies that may be noted can be explained qualitatively as follows:

At torques just beyond the critical value, the computed twists are too large because the theory assumes that the flattening to the polygon cross section takes place instantaneously on buckling. At torques high enough to bring the skin into the plastic region, the computed twists are too low because the plasticity correction factor (fig. 22(b) of Part I) holds good only for plane-web systems. In curved-web systems, the angle α is usually much lower and the stress distribution is less uniform than in plane systems; both these considerations indicate that the plasticity correction factor for curved systems should deviate more from unity than that for plane systems.

There appears to be no practical need for high accuracy in the calculation of twists in the plastic range; the problem of improving the

agreement in this range may therefore be regarded as academic. In the region of practical interest, the agreement may be considered as satisfactory except perhaps for torques just beyond the buckling value. However, the evidence discussed in the next section makes it appear somewhat dubious at present that such satisfactory agreement will always be found.

3.6. Effects of repeated buckling.- Section 9.10 of Part I quotes experimental evidence that repeated buckling, even at nominal stresses well within the elastic range, will produce a significant lowering of the buckling stress (presumably because of the formation of "plastic hinge lines") and discusses some of the probable effects on strength predictions.

In order to obtain some more information on this problem, a duplicate of NACA cylinder 12 was built and designated cylinder 12a. This cylinder was loaded 63 times to a torque of 660 inch-kips, or 68 percent of the failing load of cylinder 12 (corresponding closely to the limit load). Readings were taken at the first and second loading, and thereafter at loading numbers which were powers of two. The sixty-fourth loading was carried to failure of the cylinder. Very marked differences were found between the first and the second set of stress readings; after that, however, the readings remained constant or differed only by very small amounts well within the test accuracy. The twist readings increased slightly, but even here, the largest difference between the second and the last loading $\left(\text{about } 4 \times 10^{-4} \text{ radians}\right)$ was not much larger than the possible test error.

Figure 32 shows the stringer and the ring stresses during the first and the last loading. The buckling stress, judged by the appearance of these stresses, is lowered to less than one-half the original value. As a result, the stringer stresses at the last loading show a marked difference from those at the first loading at torques near the original buckling torque. On a relative basis, the same observation holds true for the ring stresses, but the differences are insignificant for the rings on an absolute basis. As the torque is increased in the last loading, the differences decrease again on a percentage basis; at torques equal to about three times the original buckling torque, the stresses in the last loading are again about the same as in the first loading.

Figure 32 shows also the computed curve of stringer stress, based on the theoretical buckling stress. If a similar curve based on the lowered buckling stress were computed for the second and subsequent loadings, the curve would move down and would have a smaller slope. The curve drawn through the test points for the last loading, on the other hand, has a steeper slope. It must be concluded, then, that it is not possible in general to make reliable stress predictions for a prebuckled

cylinder simply by using the experimental buckling stress in the calculations; in the case under consideration here, the predicted stresses would be roughly twice as large as the true stresses at high torques. This conclusion, of course, applies primarily in the range of low loading ratios $\left(\text{say } \frac{\tau}{\tau_{cr}} < 3\right)$, because the calculated stresses become more and more independent of the buckling stress as the loading ratio increases.

The actual stresses during subsequent loadings are about the same as those found on first loading, as noted previously, when the torque is more than about three times the original (or theoretical) buckling torque. This behavior is quite similar to that deduced by theory for a "flat" plate with initial eccentricity under compressive load (reference 13). It suggests that, for a cylinder intended to fail at a torque more than three times the theoretical buckling torque, the stresses near the ultimate load could be predicted by simply disregarding the fact that prebuckling has lowered the buckling stress. It is an open question, however, whether such a procedure would always give good results. The particular cylinder under consideration here shows, for instance, a much more gradual break in the torque-twist curve than the other cylinders for which such curves are available; it may therefore not be sufficiently typical.

Figure 33 shows the twist of cylinder 12a for the first and the last loading. The computed curve, valid for the first loading only, shows that the repeated torque was sufficiently high to bring the skin into the plastic region. As a result, there was a permanent set of about 5×10^{-3} radians after the first loading, with no significant additional set thereafter. In order to facilitate comparison of the slopes of the curves, the twist for the last loading is plotted with zero twist as origin; thus, the total twist at a torque of 660 inch-kips during the last loading is actually more, not less, than the corresponding twist during the first loading.

The figure indicates that the stiffness of the cylinder (as measured by the slope of the torque-twist curve) was considerably decreased in the low-load range by the previous loadings; at loads higher than the original buckling loads, however, it is somewhat greater. The remarks made concerning the possibilities of calculating the effects of prebuckling on the stringer stresses apply also to the calculation of the twist angles.

Figure 34 shows the observed and calculated twist curves for the ARL cylinders. Cylinder 14 was subjected to three loadings as indicated in the figure in order to obtain data on buckling before the final test run. Cylinder 15 was subjected to a first run for buckling tests, a semifinal run and a final run. Cylinders 20 and 21 were subjected to

one run before the final test. No significant effects of the "buckling runs" appear to have been observed; only the semifinal run on cylinder 15 produced large aftereffects, as shown in the figure. The difference between the curves for the semifinal and the final run is of the same nature as on NACA cylinder 12a (fig. 33). The predicted twist angles are too small in all cases by about 40 percent at torques well above the buckling value.

Figure 35 shows the twist curves for two cylinders reported in reference 12. These cylinders were used for extensive strain measurements, first under bending, then under torsional loads; the cylinders were thus subjected to many loads far beyond the buckling load. Three computed curves are shown; one is based on the theoretical buckling stress, one, on the experimental buckling stress quoted in the reference, and one, on pure diagonal tension. In the upper part of the load range, the measured angles of twist are larger than those computed, even when the condition of pure diagonal tension is assumed to exist throughout the load range. (It might be mentioned that a conservative estimate of the angle of twist cannot be obtained with certainty by simply assuming that a state of pure diagonal tension exists. When the diagonal tension is just beginning to develop, the angle α is very small; under this condition, the shear stiffness is very small, in spite of the low stresses in stringers and rings, and may be less than the stiffness that would exist if the diagonal tension were fully developed at the same torque.)

No satisfactory explanation of the discrepancies between calculated and observed angles of twist can be offered at present. All the cylinders for which twist data are shown in figures 34 and 35 failed at such low values of nominal shear stress that plasticity could account for only a very minor part of the discrepancy. Previous loading undoubtedly affected the cylinders of reference 12, and the final test on ARL cylinder 15. It is uncertain, however, whether the other ARL tests were seriously affected by the buckling test run. Furthermore, the discrepancies do not decrease at higher torque loads, as they did in NACA cylinder 12a in agreement with the theoretical behavior of a nearly flat plate.

There are some possible explanations other than prebuckling effects. In the ARL cylinders, the stringers were outside of the cylinder. Thus, the skin is hanging on the rivets, and as soon as the cross section assumes the polygon shape, large tensile forces on the rivets arise. These forces lead to dishing-in of the sheet around the rivets, which is equivalent to producing slack. It is not known whether this effect is of sufficient magnitude to explain the discrepancies.

In the cylinders of reference 12, the rings were floating on top of the cylinders. In the reference, a rather large amount of discussion is devoted to the fact that the stringers produced local squashing of the

rings; the author of the reference considered this effect to be sufficiently important to make an allowance for it in his stress calculations, based on the measured magnitude of the local deformations. Unfortunately, no details of these calculations are given in the reference. Local squashing of the rings facilitates radial inward displacements of the stringers and is therefore equivalent to an increase of ring hoop strain. In order to obtain some idea of whether this effect could explain the discrepancies, calculations were made on the arbitrary assumption that only the webs of the rings acted in hoop compression. The results of these calculations agreed fairly well with the test results for cylinder 3; for cylinder 4, the agreement was also much improved.

The discussions of this section may be summarized as follows:

It is obvious that the experimental evidence on the effect of previous buckling is too scanty to yield useful information. Previous buckling may lower the buckling stress markedly for subsequent loadings; when this happens, the stiffener stresses and the angles of twist will be increased markedly for torques near the original buckling torque. Unfortunately, it is not possible to predict quantitatively how much the buckling stress will be lowered, nor is it possible to calculate the stresses with any degree of accuracy even though the lowered buckling stress is known. There are indications, however, that a lowering of the buckling stress caused by previous buckling may not affect the predictions of ultimate strength seriously if the ratio τ/τ_{cr} at failure is more than 2 or 3.

In the ARL cylinders, the first buckling test runs apparently produced no discernible lowering of the buckling stress. If this observation is accepted at face value, the discrepancies between observed and calculated angles of twist indicate that the theoretical shear modulus for curved webs in incomplete diagonal tension may be unreliable. Other possible explanations for the discrepancies may exonerate the theory, but more adequate test data are needed to clarify the issue.

4. Ultimate Strength

4.1. Web strength.- All predictions discussed in this section are made in a manner similar to that used for flat webs: The basic allowable shear stress is corrected to typical material properties, and an increase of 10 percent is added to allow for the clamping effect of tight rivets. The actual strengths are then expected to range from 1.0 to 1.2 times the predicted strength (scatter band of the tests on flat webs in pure shear).

The ratios of actual to predicted failing loads for the NACA cylinders are shown in the last column of table 8. Most values are in parentheses,

however, to indicate that, according to the calculations, the web failure was secondary (forced crippling of the stringers being the primary failure). Thus, there are only two clear cases of web failure, with ratios of 1.08 and 1.01. However, two of the other four webs which ruptured in the tests also developed ratios larger than unity.

Additional evidence is furnished by the tests reported in reference 14. The test specimens included two cylinders and 10 beams with curved webs of 24S-T alloy. The webs were of construction similar to that of the cylinders; they comprised one-third of the circumference of the cylinder and were provided with steel flanges in order to be able to act as beams. The rings were formed Z-sections or angles inside the curved web. The stringers were extruded angles outside the web. In a subsequent series of 10 tests (not published), rings and stringers were rectangular bars symmetrical about the skin.

In these two test series, 8 web failures occurred. In the first series, 4 webs failed at ratios of 1.01, 1.18, 1.11, and 1.17. In the second series, 4 webs failed at ratios of 1.17, 1.08, 1.07, and 1.11. The difference in construction apparently had no effect on the strength developed. All the ratios fall in the expected range; the average ratio is 1.11, close to the expected average.

Four tests were available on curved-web systems of Alclad 24S-T3 alloy. The radii were 20 and 30 inches; hat-section stringers were inside, hat-section rings, outside of the web. The ratios of actual to predicted failing load ranged from 0.93 to 0.96; the predictions were thus from 7 to 4 percent unconservative. One of these failures (with a ratio 0.94) may be disregarded, because the failure was not in the curved web under test, but in the adjacent structure. The allowable stresses were based on typical material properties because the actual ones were not given; some possibility exists, therefore, that lower material properties might be partly responsible for the unconservative predictions. It is believed, however, that the main reason was inadequate stiffness of the edge flanges (corner angles). The flange-flexibility factors ωd were estimated to be about 3.2 for two specimens and about 1.6 for the third specimen which failed in the curved web. The configuration of the specimens was such that a quantitative evaluation is not justified; qualitatively, however, the estimates indicate that the edge flanges were sufficiently flexible to produce stress concentrations that would account for the unconservativeness of the predictions.

4.2. Stringer failure.- Table 8 lists the torques T_{FC} at which failure of the NACA cylinders is predicted to occur as the result of forced crippling. Comparison of these torques with those predicted to cause web rupture shows that stringer failure is held responsible for most of the cylinder failures.

The ratio of actual to predicted failing torque, shown in the next-to-the-last column of table 8, averages 1.29 and ranges from 0.98 to 1.70. (The value 0.98 for cylinder 1 is somewhat questionable because the load was in doubt; see section 3.1.) For plane-web systems with single uprights, predictions for forced crippling give an average ratio of about 1.25, ranging from 1.0 to 1.5, and the scatter band for double uprights appears to be about the same. It may be concluded that the formulas for forced crippling derived from tests on plane-web systems are applicable to curved systems but that the width of scatter band is somewhat larger and the average conservatism of prediction, somewhat higher.

Notable is the result for cylinder 9, which had 4 longerons consisting of two angles each (fig. 24). Although these angles had legs 0.119 inch thick, while the skin was 0.0244 inch thick, failure by forced crippling of the longerons was predicted to precede web rupture by a margin of 8 percent. The test log notes only web rupture and does not mention indications of distress of the longerons before failure. In view of this test observation, it should perhaps be regarded as an open question whether the formula for forced crippling is reliable at such a large thickness ratio $\left(\frac{t_U}{t} \approx 5\right)$.

Following a suggestion made by Moore and Wescoat (reference 11), flat-end column tests were made for the stringers of NACA cylinders 1 to 8. Each column consisted of two Z-sections riveted together and had an (actual) length equal to the ring spacing; three specimens were tested of each configuration. For cylinders 3, 4, and 7, which displayed no web failures, it was found that the calculated (average) stringer stresses σ_{ST} at failure were only 64, 69, and 70 percent, respectively, of the flat-end column stress. It will be noted in figure 27(a) from comparison with the measured values that the calculated stress σ_{ST} is fairly accurate for cylinders 3 and 4, and somewhat conservative for cylinder 7. It must be concluded, then, that the flat-ended column stress is not a reliable criterion of the stress at which a stringer will fail.

The suggestion made by Moore and Wescoat was based on the analysis of the stringer failures in their (ARL) cylinders 14, 20, and 21. A comparative analysis of these failures has been made by three methods as indicated by the following scheme:

Method	Applied stringer stress	Allowable stress
A	Measured, upper edge of scatter band	Flat-end column
B	Calculated (also measured, lower edge of scatter band)	Flat-end column
C	Calculated	Forced crippling

The scatter of the measured stresses may be seen in figure 29. The results obtained by the three methods are as follows:

Method	Ratio of actual to predicted failing torque for cylinder -		
	14	20	21
A	1.0	1.26	1.0
B	.78	1.11	.80
C	1.16	1.01	1.21

The ratios obtained by method A show that the stresses actually carried by the stringers were equal to, or somewhat higher than, the flat-end column stresses. Method B gives unconservative predictions for two cylinders, but the blame can obviously be placed on the fact that the stresses calculated by the theory of incomplete diagonal tension are too low. Moore and Wescoat were therefore justified in concluding that, for these tests, the flat-end column stresses could be used as a criterion for predicting cylinder failure. Unfortunately, the subsequent NACA tests discussed previously show that this conclusion may not be generalized.

Method C is the method of forced-crippling analysis as given in Part I and as applied to the NACA cylinders. This method gives conservative strength predictions for the ARL cylinders in spite of the fact that the predictions of stringer stress are unconservative. This success of the formula for forced crippling in spite of the unconservative stress prediction can possibly be explained by the inverted Ω-section used for the ARL stringers. The formula for forced crippling is based on tests of angle-, Z-, and J-section stiffeners. The inverted Ω-section is probably less susceptible to forced crippling than the other sections because the portion directly attached to the cylinder skin is very narrow and has both edges supported.

The test evidence available to date may be summarized as follows: The assumption that the stringers of a torsion cylinder will fail at the same stress as a corresponding flat-end column gives satisfactory strength predictions for the ARL cylinders, but unconservative predictions for the NACA cylinders. The assumption that the stringers fail by forced crippling gives conservative predictions for the ARL as well as the NACA cylinders; these predictions show a somewhat wider scatter band than those for plane-web systems and are thus somewhat more conservative on the average.

4.3. Ring failure.- In many of the test specimens discussed in this paper the rings were deliberately designed overstrength in order to preclude their failure; thus, little information on the subject of ring failure is available at present.

Among the tests of reference 14, the failures of two cylinders were attributed to general instability; the ratios of actual to predicted failing load were 1.10 and 1.25. Also attributed to general instability were the failures of two curved webs (15-in. radius) at ratios of 1.08 and 1.5.

Reference 15 reports results obtained in a series of tests made in the process of developing a fuselage design. All the failures were caused by local collapse of the ring at the place where it was notched in order to let a stringer pass through. Information is also given on the gain in strength obtained by clips and by additional rings acting as continuous clip angles. The information is difficult to evaluate, however, chiefly because the material is not specified.

4.4. Riveting.- In several reports on development tests of cylinders simulating fuselages with cut-outs, premature failures were reported on flush rivets. The rivets pulled through the sheet, a fact which indicates the necessity of applying some criterion for tensile strength. The reports are not sufficiently detailed to permit quantitative evaluation.

5. Combined Torsion and Compression

5.1. Test specimens.- A series of tests on cylinders in combined torsion and compression is reported in reference 16. The cylinders were designed to fail as the result of forced crippling of the stringers when loaded in pure torsion. The construction and nominal dimensions of the cylinders are shown in figure 36; the test setup is shown in figure 26. The material was 24S-T3 aluminum alloy. Clip angles (not shown in fig. 36) were used to connect the stringers to the rings. The actual dimensions are given in the following tabulation:

Cylinder	t (in.)	A_{ST} (sq in.)	A_{RG} (sq in.)
1	0.0253	0.0925	0.251
2	.0260	.0916	.254
3	.0248	.0918	.254
4	.0250	.0915	.257
5	.0248	.0915	.257

5.2. Stresses.- Stresses were measured on three stringers (120° apart) at the gage locations shown in figure 37. The average from all 36 gages is plotted in figure 37 against applied load. No significant variation of stress either across the section or along the length of a stringer was noted until rather high loads were reached. As the failing load was approached, the stresses in the free flanges of the stringers stopped increasing and then started to decrease; the stresses in the stringer webs correspondingly increased at a more and more rapid rate.

Detailed calculations for two of the cylinders are given in section 13 of Part I in the form of numerical examples. Figure 37 shows systematic discrepancies between observed and calculated stresses at loads just above the buckling value. They arise from the fact that the use of the Kármán-Sechler formula for effective width results in a sudden increase in calculated stress just beyond the buckling load, whereas the actual stresses show no such sudden increase. However, at loads more than about twice the buckling load, the agreement between observed and calculated stresses is very satisfactory.

5.3. Ultimate strength.- The ultimate loads and the corresponding load ratios are shown in the following tabulation:

Cylinder	T_{ult} (in.-kips)	P_{ult} (kips)	R^{T}_{ult}	R^{C}_{ult}
1	388.0	0	1.00	0
2	0	42.0	0	1.00
3	255.9	26.4	.581	.629
4	129.6	34.6	.334	.825
5	303.0	13.5	.781	.322

Figure 38 shows the load ratios plotted for comparison with the interaction curve proposed for design used in Part I. It may be seen that the curve is slightly conservative.

At the failing load, the stringer stress in cylinder 1 (pure torsion) was calculated as 20.6 ksi and measured as 20.2 ksi. Tested as a flat-end column of the same length as the ring spacing, the stringer failed at a stress of 26.7 ksi (average of six tests). The flat-end column test is therefore an unconservative method of estimating the failing stress in this case, as it was for other NACA cylinders (section 4.2).

Langley Aeronautical Laboratory
National Advisory Committee for Aeronautics
Langley Field, Va., January 22, 1952

REFERENCES

1. Kuhn, Paul, Peterson, James P., and Levin, L. Ross: A Summary of Diagonal Tension. Part I - Methods of Analysis. NACA TN 2661, 1952.

2. Kuhn, Paul, and Peterson, James P.: Strength Analysis of Stiffened Beam Webs. NACA TN 1364, 1947.

3. Levin, L. Ross, and Sandlin, Charles W., Jr.: Strength Analysis of Stiffened Thick Beam Webs. NACA TN 1820, 1949.

4. Kuhn, Paul, and Chiarito, Patrick T.: The Strength of Plane Web Systems in Incomplete Diagonal Tension. NACA ARR, Aug. 1942.

5. Levin, L. Ross, and Nelson, David H.: Effect of Rivet or Bolt Holes on the Ultimate Strength Developed by 24S-T and Alclad 75S-T Sheet in Incomplete Diagonal Tension. NACA TN 1177, 1947.

6. Levin, L. Ross: Ultimate Stresses Developed by 24S-T and 75S-T Aluminum Alloy Sheet in Incomplete Diagonal Tension. NACA TN 1756, 1948.

7. Anon.: Strength of Aircraft Elements. ANC-5, Army-Navy-Civil Committee on Aircraft Design Criteria. Revised ed., Dec. 1942; Amendment 1, Oct. 22, 1943.

8. Anon.: Riveting Alcoa Aluminum and Its Alloys. Aluminum Co. of America (Pittsburgh, Pa.), 1946.

9. Kuhn, Paul, and Moggio, Edwin M.: The Longitudinal Shear Strength Required in Double-Angle Columns of 24S-T Aluminum Alloy. NACA RB 3E08, 1943.

10. Kuhn, Paul, and Griffith, George E.: Diagonal Tension in Curved Webs. NACA TN 1481, 1947.

11. Moore, R. L., and Wescoat, C.: Torsion Tests of Stiffened Circular Cylinders. NACA ARR 4E31, 1944.

12. Schapitz, E.: The Twisting of Thin-Walled, Stiffened Circular Cylinders. NACA TM 878, 1938.

13. Hu, Pai C., Lundquist, Eugene E., and Batdorf, S. B.: Effect of Small Deviations from Flatness on Effective Width and Buckling of Plates in Compression. NACA TN 1124, 1946.

14. Chiarito, Patrick T.: Some Strength Tests of Stiffened Curved Sheets Loaded in Shear. NACA RB L4D29, 1944.

15. Thorn, K.: Spannungsmessungen an gekrümmten Schubwänden eines Schalenrumpfes. Jahrb. 1937 der deutschen Luftfahrtforschung, R. Oldenbourg (Munich), pp. I 459 - I 463.

16. Peterson, James P.: Experimental Investigation of Stiffened Circular Cylinders Subjected to Combined Torsion and Compression. NACA TN 2188, 1950.

TABLE 1.- PROPERTIES OF TEST BEAM SERIES I to IV

Beam	h_e (in.)	h_U (in.)	t (in.)	d (in.)	A_U (sq in.)	A_{U_e} (sq in.)	$\frac{A_U}{dt}$	$\frac{A_{U_e}}{dt}$	ρ (in.)	$\frac{R}{R_R}$	Flanges ($2\angle s$) (in.) (a)	αd	Material	
													Web	Upright
I-40-1D	40.0	38.6	0.0425	10.0	0.338	0.338	0.795	0.795	0.256	0.705	$2 \times 2 \times \frac{1}{4}$	0.88	24S-T	24S-T
I-40-2D	40.0	38.6	.0425	10.0	.384	.384	.903	.903	.490	.522	$2 \times 2 \times \frac{1}{4}$	.88	24S-T	24S-T
I-40-3D	41.4	38.6	.0392	20.0	.384	.384	.490	.490	.490	.472	$3 \times 3 \times \frac{5}{16}$	1.20	24S-T	24S-T
I-40-4Da	41.4	38.6	.0390	20.0	.353	.353	.454	.454	.351	.545	$3 \times 3 \times \frac{5}{16}$	1.20	24S-T	24S-T
I-40-4Db	41.4	38.6	.0390	20.0	.353	.353	.454	.454	.351	.832	$3 \times 3 \times \frac{5}{16}$	1.20	24S-T	24S-T
I-40-4Dc	41.4	38.6	.0390	20.0	.353	.353	.454	.454	.351	1.58	$3 \times 3 \times \frac{5}{16}$	1.20	24S-T	24S-T
I-25-1D	25.0	23.9	.0102	10.0	.123	.123	1.206	1.206	.232	.665	$2 \times 2 \times \frac{3}{16}$	.98	24S-T	24S-T
I-25-2D	25.0	23.9	.0105	20.0	.123	.123	.586	.586	.232	.734	$2 \times 2 \times \frac{3}{16}$	1.97	24S-T	24S-T
I-25-3D	25.0	23.9	.0116	10.0	.110	.110	.952	.952	.167	.776	$2 \times 2 \times \frac{3}{16}$	1.02	17S-T	24S-T
I-25-4D	25.0	23.9	.0153	10.0	.114	.114	.747	.747	.182	.770	$2 \times 2 \times \frac{3}{16}$	1.09	24S-T	24S-T
I-25-5D	25.0	23.9	.0150	20.0	.269	.269	.897	.897	.247	.320	$2 \times 2 \times \frac{3}{16}$	2.14	24S-T	24S-T
I-25-6D	25.0	23.9	.0162	20.0	.206	.206	.635	.635	.241	.805	$2 \times 2 \times \frac{3}{16}$	2.19	24S-T	24S-T
I-25-7D	25.0	23.9	.0402	10.0	.101	.101	.252	.252	.291	1.63	$2 \times 2 \times \frac{3}{16}$	1.38	24S-T	24S-T
II-25-1S	24.3	23.3	.0265	20.0	.212	.0955	.400	.180	.309	-----	$2 \times 2 \times \frac{3}{16}$	2.52	24S-T	24S-T
II-25-2S	24.3	23.3	.0265	20.0	.195	.0756	.368	.143	.407	-----	$2 \times 2 \times \frac{1}{4}$	2.36	24S-T	24S-T
II-25-3S	24.3	23.3	.0224	10.0	.153	.0776	.684	.346	.357	-----	$2 \times 2 \times \frac{3}{16}$	1.20	24S-T	24S-T
II-25-4S	24.3	23.3	.0257	10.0	.121	.0640	.471	.249	.314	-----	$2 \times 2 \times \frac{1}{4}$	1.17	24S-T	24S-T
II-25-5S	24.3	23.3	.0249	10.0	.194	.0740	.778	.297	.377	-----	$2 \times 2 \times \frac{3}{16}$	1.24	24S-T	24S-T
II-25-6S	24.3	23.3	.0248	20.0	.212	.0955	.427	.192	.309	-----	$2 \times 2 \times \frac{3}{16}$	2.46	24S-T	24S-T
II-25-7S	24.3	23.3	.0248	20.0	.108	.0407	.217	.0820	.582	-----	$2 \times 2 \times \frac{1}{4}$	2.32	24S-T	24S-T
II-25-8S	24.3	23.3	.0248	10.0	.109	.0427	.439	.172	.611	-----	$2 \times 2 \times \frac{1}{4}$	1.16	24S-T	24S-T
II-25-9S	24.3	23.3	.0245	10.0	.156	.0795	.637	.324	.358	-----	$2 \times 2 \times \frac{3}{16}$	1.23	24S-T	24S-T
III-25-1S	24.3	23.3	.0210	20.0	.105	.0354	.249	.0843	.541	-----	$2 \times 2 \times \frac{1}{4}$	2.18	Alclad 75S-T	Alclad 75S-T
III-25-2S	24.3	23.3	.0208	10.0	.108	.0376	.517	.181	.556	-----	$2 \times 2 \times \frac{3}{16}$	1.16	Alclad 75S-T	Alclad 75S-T
III-25-3S	24.3	23.3	.0395	10.0	.108	.0371	.273	.0940	.556	-----	$2 \times 2 \times \frac{1}{4}$	1.27	Alclad 75S-T	Alclad 75S-T
III-25-4D	24.3	23.3	.0206	10.0	.136	.136	.659	.659	.231	.765	$2 \times 2 \times \frac{3}{16}$	1.16	Alclad 75S-T	Alclad 75S-T
III-25-5S	24.3	23.3	.0204	10.0	.102	.0479	.496	.235	.318	-----	$2 \times 2 \times \frac{1}{4}$	1.08	Alclad 75S-T	Alclad 75S-T
III-25-6D	24.3	23.3	.0295	15.0	.107	.107	.242	.242	.283	1.23	$2 \times 2 \times \frac{3}{16}$	1.91	Alclad 75S-T	Alclad 75S-T
III-25-7D	24.3	23.3	.0303	15.0	.100	.100	.220	.220	.221	1.44	$2 \times 2 \times \frac{3}{16}$	1.92	Alclad 75S-T	Alclad 75S-T
III-25-8S	24.3	23.3	.0206	10.0	.152	.0742	.741	.360	.359	-----	$2 \times 2 \times \frac{1}{4}$	1.09	Alclad 75S-T	Alclad 75S-T
IV-72-1D	73.7	64.3	.1237	18.0	.762	.762	.342	.342	.594	2.08	(b)	.60	24S-T	24S-T
IV-72-2S	73.7	64.3	.1219	18.0	1.137	.371	.518	.169	1.110	-----	(b)	.60	24S-T	24S-T
IV-72-3D	73.7	64.3	.1227	18.0	1.176	1.176	.533	.533	.939	2.39	(b)	.60	24S-T	24S-T
IV-72-4S	73.7	64.3	.1239	18.0	1.092	.417	.490	.187	1.618	-----	(b)	.60	24S-T	24S-T

[a]Flanges of I-40 and IV-72 beams are steel; all others are 24S-T alloy.

[b]See figure 9(a).

TABLE 2.- TEST DATA AND RESULTS FOR TEST BEAM SERIES I TO IV

Beam	$\tau_{cr_{calc}}$ (ksi)	P_{ult} (kips)	$\tau_{ult} = \frac{P_{ult}}{h_e t}$ (ksi)	$\frac{\tau_{ult}}{\tau_{cr}}$	k	Predicted P_{ult} (a)			Observed failure	$\frac{P_{ult}}{P_C}$	$\frac{P_{ult}}{P_{FC}}$	$\frac{P_{ult}}{P_W}$
						P_C (kips)	P_{FC} (kips)	P_W (kips)				
I-40-1D	1.88	27.4	16.1	8.57	0.435	30.7	57.7	46.8	Column	0.89	----	------
I-40-2D	1.85	39.3	23.1	12.5	.500	85.7	61.2	46.6	Flange	----	----	------
I-40-3D	.423	37.0	22.8	54.0	.699	43.3	39.1	42.8	Web (defective)	----	0.95	(0.86)
I-40-4Da	.416	30.3	18.8	45.2	.680	28.5	37.4	42.4	Column	1.06	----	------
I-40-4Db	.416	32.1	19.9	47.9	.685	29.3	37.4	42.4	Column	1.10	----	------
I-40-4Dc	.416	35.7	22.1	53.0	.698	29.7	37.4	42.4	Column	1.20	----	------
I-25-1D	.113	6.8	26.6	235	.830	9.67	13.4	6.71	Web	----	----	1.01
I-25-2D	.0393	6.3	24.0	610	.885	4.76	7.70	6.45	Column	1.32	----	------
I-25-3D	.146	7.6	26.2	179	.809	5.36	11.9	6.58	Web	1.42	----	(1.15)
I-25-4D	.254	7.8	20.4	80.3	.740	6.93	12.7	10.1	Column	1.13	----	------
I-25-5D	.0808	10.9	29.1	360	.855	9.25	16.9	9.15	None	----	----	------
I-25-6D	.0943	10.0	24.7	262	.836	8.64	13.0	9.84	Column	1.16	----	------
I-25-7D	.114	12.7	12.6	11.03	.480	24.0	13.3	27.1	Forced crippling	----	.95	------
II-25-1S	.206	13.2	20.5	99.5	.761	------	11.9	13.9	(b)	----	1.11	(.95)
II-25-2S	.206	11.4	17.7	86.0	.747	------	9.65	14.3	Forced crippling	----	1.18	------
II-25-3S	.402	13.9	25.4	63.1	.715	------	13.3	13.6	Web	----	1.04	(1.02)
II-25-4S	.520	13.5	21.6	41.5	.669	------	11.7	15.7	Forced crippling	----	1.15	------
II-25-5S	.496	15.5	25.6	51.6	.695	------	13.4	15.4	Web	----	1.16	(1.01)
II-25-6S	.190	13.6	22.6	119	.777	------	11.4	13.0	Web	----	1.19	(1.05)
II-25-7S	.167	6.7	11.1	66.5	.722	------	6.15	13.6	Forced crippling	----	1.09	------
II-25-8S	.447	10.2	16.9	37.8	.657	------	8.75	15.3	Forced crippling	----	1.17	------
II-25-9S	.490	15.4	25.8	52.6	.696	------	13.9	15.3	Web	----	1.11	(1.01)
III-25-1S	.125	6.7	13.0	104	.765	------	6.34	14.1	Forced crippling	----	1.06	------
III-25-2S	.327	9.5	18.7	57.1	.705	------	9.24	14.8	Forced crippling	----	1.03	------
III-25-3S	.700	14.8	15.4	22.0	.585	------	13.0	29.8	Forced crippling	----	1.14	------
III-25-4D	.472	14.3	28.5	60.4	.712	14.2	17.7	15.0	Column	1.01	----	------
III-25-5S	.334	13.5	27.2	81.5	.741	------	11.1	15.0	Forced crippling	----	1.21	------
III-25-6D	.410	11.4	15.8	38.6	.662	14.8	12.2	20.5	Forced crippling	----	.93	------
III-25-7D	.430	10.5	14.3	33.2	.642	9.80	12.1	21.1	Column	1.07	----	------
III-25-8S	.340	14.2	28.5	84.0	.745	------	15.6	14.9	Web	----	----	.95
IV-72-1D	3.58	178.5	19.6	5.48	.353	212	168	244	Forced crippling	----	1.06	------
IV-72-2S	3.07	212	23.6	7.69	.415	------	163	240	(b)	----	1.30	(.88)
IV-72-3D	4.05	255	28.2	6.96	.397	460	210	247	Forced crippling	----	1.22	------
IV-72-4S	1.89	160	17.5	9.25	.450	------	134	241	Forced crippling	----	1.19	------
									[c]Average	1.14	1.11	0.98

[a]Subscripts have the following meanings:

C column failure
FC forced-crippling failure
W web failure

[b]Failure of web that had previously failed by rivet pulling through web.

[c]Average disregards values in parentheses.

TABLE 3.- PROPERTIES OF TEST BEAM SERIES V

[All material 24S-T aluminum alloy]

Beam	h_e (in.)	h_c (in.)	t (in.)	d (in.)	Uprights (in.)	A_U (sq in.)	A_{U_e} (sq in.)	$\frac{A_U}{dt}$	$\frac{A_{U_e}}{dt}$	Flanges (2 ∠s) (in.)	ωd
V-12-1D	11.38	9.38	0.1000	2.75	$\frac{1}{2} \times \frac{1}{2} \times 0.0666$	0.1260	0.1260	0.458	0.458	$1\frac{3}{4} \times 1\frac{3}{4} \times \frac{5}{16}$	0.58
V-12-2S	11.38	10.88	.1005	2.75	$\frac{1}{2} \times \frac{1}{2} \times 0.0690$	.0640	.0266	.233	.096	$1\frac{3}{4} \times 1\frac{3}{4} \times \frac{5}{16}$	.58
V-12-3D	11.38	9.38	.1010	2.75	$\frac{5}{8} \times \frac{5}{8} \times 0.0397$	.0948	.0948	.342	.342	$1\frac{3}{4} \times 1\frac{3}{4} \times \frac{5}{16}$	.58
V-12-4S	11.57	10.13	.1018	2.75	$\frac{5}{8} \times \frac{5}{8} \times 0.0398$	.0478	.0239	.171	.086	$2 \times 2 \times \frac{1}{4}$	.54
V-12-5D	11.57	9.13	.1015	2.75	$\frac{5}{8} \times \frac{5}{8} \times 0.0931$	.2546	.2546	.912	.912	$2 \times 2 \times \frac{1}{4}$	.54
V-12-6S	11.57	10.13	.1029	2.75	$\frac{5}{8} \times \frac{5}{8} \times 0.0977$	.1170	.0487	.413	.172	$2 \times 2 \times \frac{1}{4}$	.54
V-12-7S	11.58	9.88	.1005	7.00	$1\frac{1}{8} \times 1\frac{1}{8} \times 0.1249$	.2709	.1202	.387	.171	$2 \times 2 \times \frac{5}{16}$	1.37
V-12-8S	11.58	9.88	.1044	7.00	$\frac{3}{4} \times \frac{3}{4} \times 0.1315$	.1820	.0695	.249	.095	$2 \times 2 \times \frac{5}{16}$	1.37
V-12-9D	11.58	9.13	.1025	7.00	$\frac{5}{8} \times \frac{5}{8} \times 0.1280$	.2860	.2860	.399	.399	$2 \times 2 \times \frac{5}{16}$	1.37
V-12-10S	11.58	9.88	.1043	7.00	$\frac{5}{8} \times \frac{5}{8} \times 0.1283$	.1443	.0498	.198	.068	$2 \times 2 \times \frac{5}{16}$	1.37
V-12-11D	11.58	9.13	.1025	7.00	$\frac{5}{8} \times \frac{5}{8} \times 0.0976$	.2340	.2340	.326	.326	$2 \times 2 \times \frac{5}{16}$	1.37
V-12-12S	11.58	9.88	.0987	7.00	$\frac{1}{2} \times \frac{1}{2} \times 0.0604$	.0589	.0216	.085	.031	$2 \times 2 \times \frac{5}{16}$	1.37
V-12-13D	11.58	9.13	.1000	7.00	$\frac{1}{2} \times \frac{1}{2} \times 0.0627$	.1214	.1214	.173	.173	$2 \times 2 \times \frac{5}{16}$	1.37
V-12-14S	11.58	9.88	.1007	7.00	$\frac{5}{8} \times \frac{5}{8} \times 0.0902$	.1082	.0404	.154	.057	$2 \times 2 \times \frac{5}{16}$	1.37
V-12-15D	11.58	9.13	.1057	7.00	$\frac{5}{8} \times \frac{5}{8} \times 0.0664$	.1622	.1622	.220	.220	$2 \times 2 \times \frac{5}{16}$	1.37

TABLE 4.- TEST DATA AND RESULTS FOR TEST BEAM SERIES V

Beam	$\tau_{cr_{calc}}$ (ksi)	$\tau_{cr_{meas}}$ (ksi)	$\frac{\tau_{cr_{meas}}}{\tau_{cr_{calc}}}$	P_{ult} (kips)	$\tau_{ult} = \frac{P_{ult}}{2h_e t}$ (ksi)	$\frac{\tau_{ult}}{\tau_{cr_{calc}}}$	k	Predicted P_{ult} (a)		Observed failure	$\frac{P_{ult}}{P_{FC}}$	$\frac{P_{ult}}{P_W}$
								P_{FC} (kips)	P_W (kips)			
V-12-1D	28.2	23.3	0.83	74.6	32.7	1.16	0.031	76.1	71.6	Forced crippling	(0.98)	1.04
V-12-2S	22.2	17.0	.77	57.8	25.3	1.14	.028	59.5	69.8	Forced crippling	.97	------
V-12-3D	25.8	----	----	69.4	30.2	1.17	.034	65.6	71.3	Forced crippling	1.06	------
V-12-4S	12.2	12.5	1.02	51.1	21.7	1.78	.125	39.2	66.2	Forced crippling	1.30	------
V-12-5D	30.2	23.7	.78	89.0	37.9	1.25	.048	100.1	71.7	Web	------	1.24
V-12-6S	26.1	23.4	.90	75.0	31.5	1.21	.041	74.6	75.0	Forced crippling	1.01	------
V-12-7S	15.3	15.5	1.01	71.2	30.6	2.00	.149	62.3	65.2	Web	1.14	(1.09)
V-12-8S	16.4	15.4	.94	72.0	29.8	1.82	.130	63.9	72.0	Web	1.13	(1.00)
V-12-9D	19.6	16.8	.86	80.0	33.8	1.72	.117	76.5	72.0	Web	------	1.11
V-12-10S	16.1	16.3	1.01	69.0	28.6	1.77	.123	61.2	71.6	Web	1.13	(.96)
V-12-11D	17.9	17.2	.96	79.6	33.5	1.87	.135	65.8	71.5	Web	1.21	(1.11)
V-12-12S	9.9	12.3	1.24	51.0	22.3	2.25	.175	39.5	64.2	Forced crippling	1.29	------
V-12-13D	13.7	13.1	.96	59.5	25.7	1.87	.135	47.3	67.2	Forced crippling	1.26	------
V-12-14S	13.6	13.2	.97	59.2	25.4	1.87	.135	51.2	67.7	Forced crippling	1.16	------
V-12-15D	15.2	15.7	1.03	67.5	27.6	1.82	.130	53.9	71.8	Forced crippling	1.25	------
										[b]Average	1.16	1.13

[a]Subscripts have the following meanings:
FC forced-crippling failure
W web failure

[b]Average disregards values in parentheses.

TABLE 5.- DIMENSIONS, TEST DATA, AND RESULTS FOR

24S-T ALUMINUM-ALLOY SHEAR WEBS

Specimen	d (in.)	Rows of holes	t (in.)	b (in.)	L (in.)	τ_{cr} (ksi)	P (kips)	τ_g (ksi)	$\frac{\tau_g}{\tau_{cr}}$	k	σ_{ult} (ksi) (a)	τ_g (ksi) Corrected (b)	τ_n (ksi) Corrected (b)
k ≈ 0.017													
1	3/16	2	0.0409	5.0	51.25	31.6	72.50	34.85	1.100	0.020	69.60	31.05	38.20
2	3/16	2	.0413	5.0	51.25	31.6	72.76	34.60	1.095	.020	69.60	30.80	38.00
3	3/16	2	.0384	5.0	51.25	31.2	70.25	35.70	1.145	.030	70.07	31.60	38.90
4	3/16	1	.0414	5.0	51.25	31.6	71.00	33.60	1.062	.012	69.60	29.92	36.85
5	3/16	1	.0414	5.0	51.25	31.6	68.40	32.40	1.026	.002	69.60	28.85	35.50
6	1/4	2	.0391	5.0	51.25	31.2	70.00	34.90	1.120	.022	70.07	30.85	41.20
7	1/4	1	.0391	5.0	51.25	31.2	65.20	32.65	1.047	.012	70.07	28.90	38.50
8	1/4	1	.0412	5.0	51.25	31.6	72.00	34.30	1.085	.018	69.60	30.55	40.70
9	1/4	1	.0413	5.0	51.25	31.6	72.70	34.50	1.092	.020	69.60	30.70	40.90
10	1/4	1	.0413	5.0	51.25	31.6	69.10	32.70	1.035	.008	69.60	29.10	38.90
11	1/4	1	.0385	5.0	51.25	31.2	65.40	33.15	1.063	.012	70.07	29.30	39.10
12	5/16	2	.0384	5.0	51.25	31.2	66.20	33.65	1.079	.016	70.07	29.75	43.30
13	5/16	1	.0391	5.0	51.25	31.2	67.40	33.65	1.079	.016	70.07	29.75	43.30
14	5/16	1	.0412	5.0	51.25	31.6	72.00	34.30	1.085	.018	69.60	30.55	44.30
15	5/16	1	.0407	5.0	51.25	31.6	68.80	33.10	1.048	.012	69.60	29.50	42.80
16	3/8	2	.0390	5.0	51.25	31.2	68.60	34.40	1.102	.020	70.07	30.42	48.70
17	3/8	1	.0396	5.0	51.25	31.3	69.00	34.00	1.087	.018	70.07	30.10	48.20
18	3/8	1	.0408	5.0	51.25	31.6	71.80	34.50	1.092	.020	69.60	30.72	49.20
19	3/8	1	.0412	5.0	51.25	31.6	72.80	34.70	1.098	.020	69.60	30.90	49.30
k ≈ 0.35													
20	3/16	2	0.0411	5.0	51.25	5.62	65.9	31.4	5.59	0.36	69.6	28.0	34.5
21	3/16	2	.0407	5.0	51.25	5.51	64.4	31.0	5.62	.35	69.6	27.5	33.9
22	3/16	2	.0390	5.0	51.25	5.07	61.8	31.0	6.11	.37	70.1	27.4	33.8
23	3/16	1	.0414	5.0	51.25	5.71	62.4	29.5	5.17	.34	69.6	26.3	32.5
24	3/16	1	.0413	5.0	51.25	5.70	62.7	29.7	5.22	.34	69.6	26.5	32.5
25	3/16	1	.0413	5.0	51.25	5.70	58.1	27.6	4.84	.33	69.6	24.6	30.2
26	1/4	2	.0392	5.0	51.25	5.12	58.5	29.1	5.69	.36	70.1	25.7	34.4
27	1/4	1	.0389	5.0	51.25	5.03	59.3	29.8	5.92	.37	70.1	26.3	35.1
28	1/4	1	.0408	5.0	51.25	5.55	60.1	29.0	5.22	.34	69.6	25.8	34.3
29	1/4	1	.0413	5.0	51.25	5.70	59.3	28.1	4.93	.33	69.6	25.1	33.4
30	5/16	2	.0391	5.0	51.25	5.09	58.1	29.0	5.69	.36	70.1	25.7	37.3
31	5/16	1	.0385	5.0	51.25	4.93	58.4	29.7	6.02	.37	70.1	26.2	38.1
32	5/16	1	.0412	5.0	51.25	5.64	61.1	29.1	5.17	.34	69.6	25.9	37.7
33	5/16	1	.0413	5.0	51.25	5.70	59.4	28.2	4.95	.33	69.6	25.1	36.6
34	3/8	2	.0384	5.0	51.25	4.91	54.8	27.9	5.68	.36	70.1	24.7	39.5
35	3/8	1	.0389	5.0	51.25	5.03	55.3	27.7	5.51	.35	70.1	24.5	39.3
36	3/8	1	.0410	5.0	51.25	5.59	58.6	28.1	5.03	.34	69.6	25.1	39.9
37	3/8	1	.0406	5.0	51.25	5.48	57.2	27.7	5.05	.34	69.6	24.7	39.4
k ≈ 0.55													
38	3/16	2	0.0264	6.0	49.63	1.61	37.2	27.4	17.0	0.55	70.2	24.3	29.9
39	1/4	2	.0265	6.0	49.63	1.61	39.5	30.0	18.6	.56	70.2	26.5	35.4
40	1/4	1	.0261	6.0	49.63	1.61	39.1	30.1	18.7	.56	70.2	26.6	35.6
41	5/16	1	.0263	6.0	49.63	1.61	37.2	28.4	17.6	.55	69.7	25.3	36.8
42	3/8	1	.0265	6.0	49.63	1.61	35.0	26.6	16.5	.54	69.7	23.7	37.9
k ≈ 0.72													
43	3/16	2	0.0265	12.0	49.63	0.403	38.5	29.2	72.5	0.73	70.2	25.8	31.8
44	1/4	2	.0262	12.0	49.63	.403	35.8	27.5	68.1	.72	69.7	24.4	32.7
45	1/4	1	.0263	12.0	49.63	.403	36.4	27.8	69.0	.72	69.7	24.7	33.0
46	5/16	1	.0264	12.0	49.63	.403	34.4	26.2	65.0	.72	70.2	23.1	33.8
47	3/8	1	.0262	12.0	49.63	.403	33.5	25.7	63.8	.72	70.2	22.7	36.4

[a] Actual tensile strength of material.

[b] Stresses corrected to σ_{ult} = 62 ksi.

TABLE 6.- DIMENSIONS, TEST DATA, AND RESULTS FOR

ALCLAD 75S-T ALUMINUM-ALLOY SHEAR WEBS

Specimen	d (in.)	Rows of holes	t (in.)	b (in.)	L (in.)	τ_{cr} (ksi)	P (kips)	τ_g (ksi)	$\frac{\tau_g}{\tau_{cr}}$	k	σ_{ult} (ksi) (a)	τ_g (ksi) Corrected (b)	τ_n (ksi) Corrected (b)
k ≈ 0.057													
1	3/16	2	0.0390	5.0	51.25	31.2	77.6	38.8	1.24	0.050	78.6	35.6	43.8
2	1/4	2	.0390	5.0	51.25	31.2	81.0	40.6	1.30	.058	78.6	37.2	49.6
3	1/4	1	.0393	5.0	51.25	31.2	81.0	40.3	1.29	.058	78.6	36.9	49.2
4	5/16	2	.0390	5.0	51.25	31.2	83.6	41.8	1.34	.065	78.6	38.3	55.7
5	5/16	1	.0390	5.0	51.25	31.2	81.0	40.6	1.30	.058	78.6	37.2	54.1
6	3/8	2	.0390	5.0	51.25	31.2	78.6	39.3	1.26	.050	78.6	36.0	57.7
7	3/8	1	.0397	5.0	51.25	31.2	83.5	41.1	1.32	.060	78.6	37.6	60.2
k ≈ 0.40													
8	3/16	2	0.0390	5.0	51.25	5.05	73.6	36.9	7.30	0.41	78.6	33.8	41.5
9	1/4	2	.0383	5.0	51.25	4.88	66.8	34.1	6.98	.40	78.6	31.2	41.5
10	1/4	1	.0396	5.0	51.25	5.21	71.2	35.1	6.74	.39	78.6	32.1	42.8
11	5/16	2	.0390	5.0	51.25	5.05	69.0	34.6	6.85	.39	78.6	31.7	46.0
12	5/16	1	.0389	5.0	51.25	5.02	68.6	34.4	6.86	.39	78.6	31.5	45.9
13	3/8	2	.0386	5.0	51.25	4.98	68.1	34.5	6.92	.40	78.6	31.6	50.5
14	3/8	1	.0396	5.0	51.25	5.22	70.2	34.6	6.63	.39	78.6	31.7	50.8
k ≈ 0.59													
15	3/16	2	0.0201	5.0	51.25	1.39	35.4	35.5	25.6	0.61	79.6	32.1	39.5
16	3/16	2	.0205	5.0	49.68	1.42	36.0	35.4	25.0	.60	79.6	32.0	39.4
17	3/16	2	.0496	12.0	49.68	1.61	87.5	35.6	22.1	.58	79.9	32.1	39.5
18	3/16	2	.0500	12.0	49.68	1.61	82.1	33.1	20.5	.58	79.9	29.9	36.7
19	3/16	2	.0489	12.0	49.68	1.56	78.0	32.1	20.6	.58	78.9	29.3	36.1
20	3/16	2	.0242	6.0	49.68	1.61	42.4	35.2	21.8	.58	70.8	35.8	44.1
21	1/4	2	.0204	5.0	49.68	1.42	35.1	34.7	24.5	.60	79.6	31.3	41.7
22	1/4	2	.0203	5.0	49.68	1.42	38.1	37.8	26.7	.61	79.6	34.5	46.0
23	1/4	2	.0203	5.0	49.68	1.42	34.8	34.5	24.6	.60	79.6	31.2	41.6
24	1/4	1	.0239	6.0	49.68	1.61	37.8	31.8	19.7	.57	70.8	32.3	43.0
25	1/4	2	.0241	6.0	49.68	1.61	38.8	32.4	20.1	.57	70.8	32.9	43.9
26	1/4	2	.0489	12.0	49.68	1.56	75.7	31.2	20.0	.57	78.9	28.5	37.9
27	5/16	1	.0244	6.0	49.68	1.61	38.4	31.7	19.7	.57	68.8	33.1	48.2
28	5/16	1	.0202	5.0	49.68	1.42	35.0	34.9	24.6	.60	79.6	31.6	45.8
29	5/16	1	.0204	5.0	49.68	1.42	34.2	33.8	23.8	.60	79.6	30.6	44.4
30	5/16	1	.0204	5.0	49.68	1.42	39.0	38.5	27.2	.61	79.6	34.9	50.7
31	5/16	1	.0486	12.0	49.68	1.56	80.6	33.5	21.4	.58	78.9	30.6	44.4
32	5/16	1	.0491	12.0	49.68	1.56	91.6	37.7	24.1	.60	79.9	34.0	49.3
33	5/16	1	.0497	12.0	49.68	1.61	89.3	36.3	22.5	.59	79.9	32.7	47.6
34	5/16	1	.0493	12.0	49.68	1.56	83.0	33.9	21.7	.58	79.9	30.6	44.4
35	3/8	1	.0207	5.0	49.68	1.43	39.0	38.1	26.6	.61	79.1	34.7	55.4
36	3/8	1	.0203	5.0	49.68	1.42	33.8	33.6	23.7	.59	79.1	30.6	49.0
37	3/8	1	.0486	12.0	49.68	1.56	71.2	29.5	18.9	.57	78.1	27.2	43.5
38	3/8	1	.0495	12.0	49.68	1.56	72.0	29.3	18.8	.57	78.1	27.1	43.3
39	3/8	1	.0488	12.0	49.68	1.56	74.3	30.7	19.7	.57	78.1	28.3	45.3
40	3/8	1	.0485	12.0	49.68	1.56	71.8	29.9	19.2	.57	78.1	27.6	44.2
41	3/8	1	.0239	6.0	49.68	1.61	35.4	29.8	18.5	.56	68.8	31.3	50.0
k ≈ 0.74													
42	3/16	2	0.0243	12.0	49.63	0.403	40.5	33.5	83.2	0.74	70.8	34.0	41.9
43	3/16	2	.0213	12.0	49.63	.290	33.9	32.1	110.6	.77	75.8	30.5	37.5
44	3/16	2	.0214	12.0	49.63	.290	30.6	28.8	99.2	.76	75.8	27.1	33.4
45	1/4	2	.0241	12.0	49.63	.403	35.4	29.5	73.2	.73	68.8	31.0	41.3
46	1/4	1	.0241	12.0	49.63	.403	38.3	32.0	79.3	.74	68.8	33.4	44.6
47	5/16	1	.0243	12.0	49.63	.403	37.1	31.0	76.9	.74	70.8	31.5	45.8
48	3/8	1	.0234	12.0	49.63	.403	32.8	28.2	70.0	.73	70.8	28.7	45.9

[a] Actual tensile strength of material.

[b] Stresses corrected to σ_{ult} = 72 ksi.

TABLE 7.- PROPERTIES OF NACA CYLINDERS 1 TO 12

[All material 24S-T aluminum alloy]

Cylinder	t (in.)	R (in.)	d (in.)	h (in.)	t_{ST} (in.)	t_{RG} (in.)	A_{ST} (sq in.)	A_{RG} (sq in.)	$\frac{A_{ST}}{ht}$	$\frac{A_{RG}}{dt}$
1	0.0248	15.04	15.00	7.87	0.052	0.061	0.230	0.197	1.180	0.530
2	.0266	15.03	7.50	7.87	.050	.064	.221	.202	1.055	1.015
3	.0265	15.02	15.00	7.86	.033	.063	.155	.198	.744	.498
4	.0266	15.02	7.50	7.86	.033	.068	.153	.216	.732	1.083
5	.0393	15.03	15.00	7.87	.081	.104	.335	.320	1.080	.544
6	.0394	15.05	7.50	7.88	.080	.104	.332	.317	1.070	1.073
7	.0428	15.04	15.00	7.87	.053	.102	.239	.318	.710	.495
8	.0399	15.06	7.50	7.88	.053	.102	.239	.321	.762	1.072
9	.0244	15.02	7.50	23.57	.119	.081	.512	.252	.892	1.38
10	.0260	15.03	7.50	7.87	.040	.061	.145	.138	.709	.710
11	.0400	15.04	21.00	5.25	.040	.101	.142	.320	.675	.381
12	.0250	15.02	5.00	4.72	.093	.078	.192	.246	1.628	1.97

TABLE 8.- TEST DATA AND RESULTS FOR NACA CYLINDERS 1 TO 12

Cylinder	$\tau_{cr_{calc}}$ (ksi)	T_{ult} (in.-kips)	τ_{ult} (ksi)	$\frac{\tau_{ult}}{\tau_{cr}}$	k	T_{ult} (a)		Observed failure	$\frac{T_{ult}}{T_{FC}}$	$\frac{T_{ult}}{T_W}$
						T_{FC} (in.-kips)	T_W (in.-kips)			
1	3.36	669	19.8	5.90	0.806	680	723	Web	0.98	(0.93)
2	4.46	944	25.0	5.60	.649	853	929	Web	1.11	(1.02)
3	3.74	468	12.9	3.44	.670	373	766	Forced crippling	1.26	-------
4	4.46	732	19.4	4.35	.588	572	931	Forced crippling	1.28	-------
5	6.04	1261	23.6	3.91	.828	1002	1140	Web	1.26	(1.11)
6	8.34	1528	27.3	3.27	.592	1420	1420	Web	----	1.08
7	7.16	1113	19.2	2.68	.740	657	1240	Forced crippling	1.70	-------
8	8.35	1503	26.6	3.19	.586	1034	1410	Web and forced crippling	1.45	-------
9	2.97	820	23.6	7.95	.870	783	850	Web	1.05	(.97)
10	2.84	656	18.6	6.55	.850	430	796	Forced crippling	1.53	-------
11	7.88	840	15.1	1.92	.533	674	1190	Forced crippling	1.25	-------
12	6.54	972	28.0	4.28	.572	1860	960	Web	----	1.01
								[b]Average	1.29	1.04

[a]Subscripts have the following meanings:
FC forced-crippling failure
W web failure

[b]Average disregards values in parentheses.

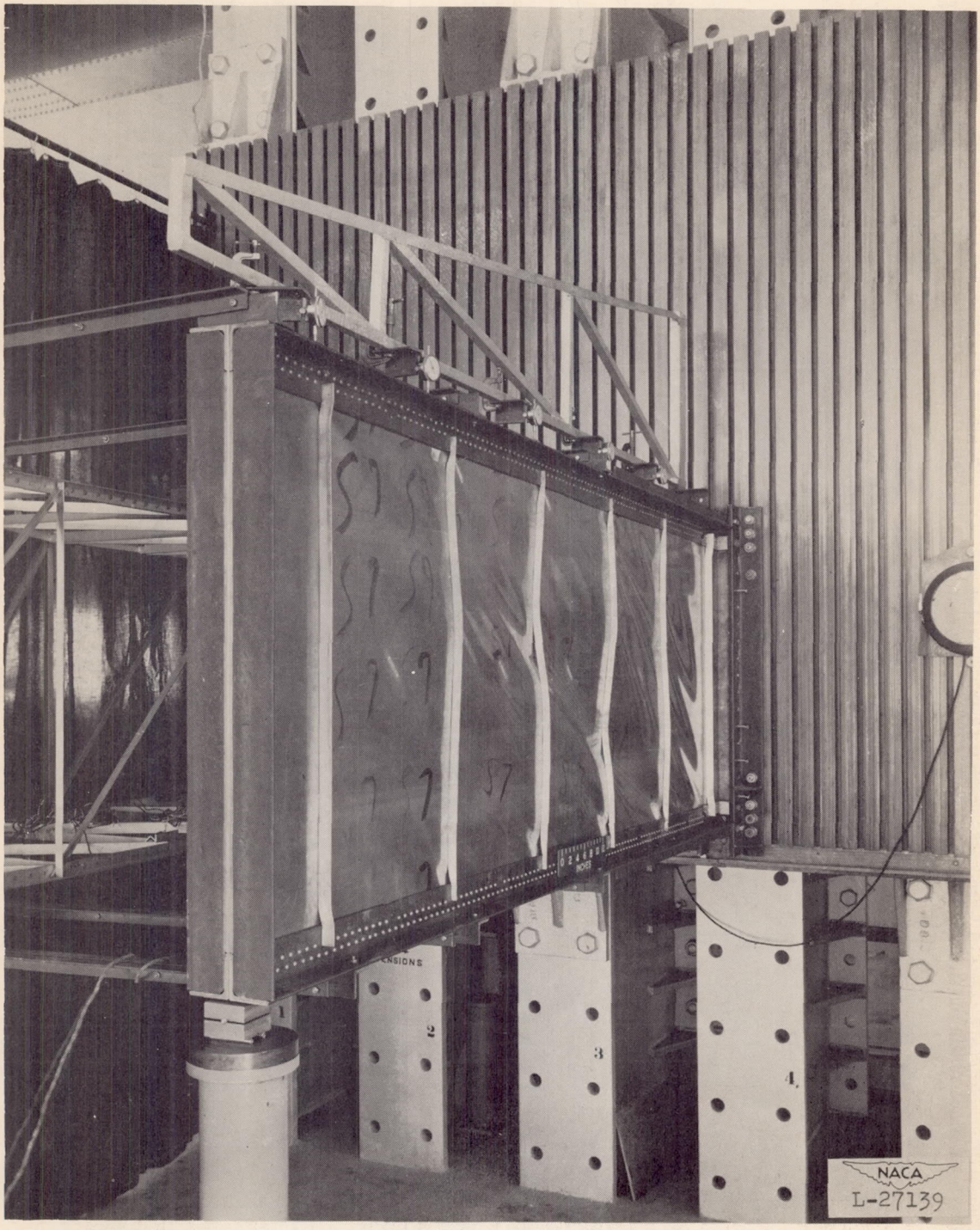

Figure 1.- Test setup for medium-size beam.

Figure 2.- Test setup for small, heavily loaded beam.

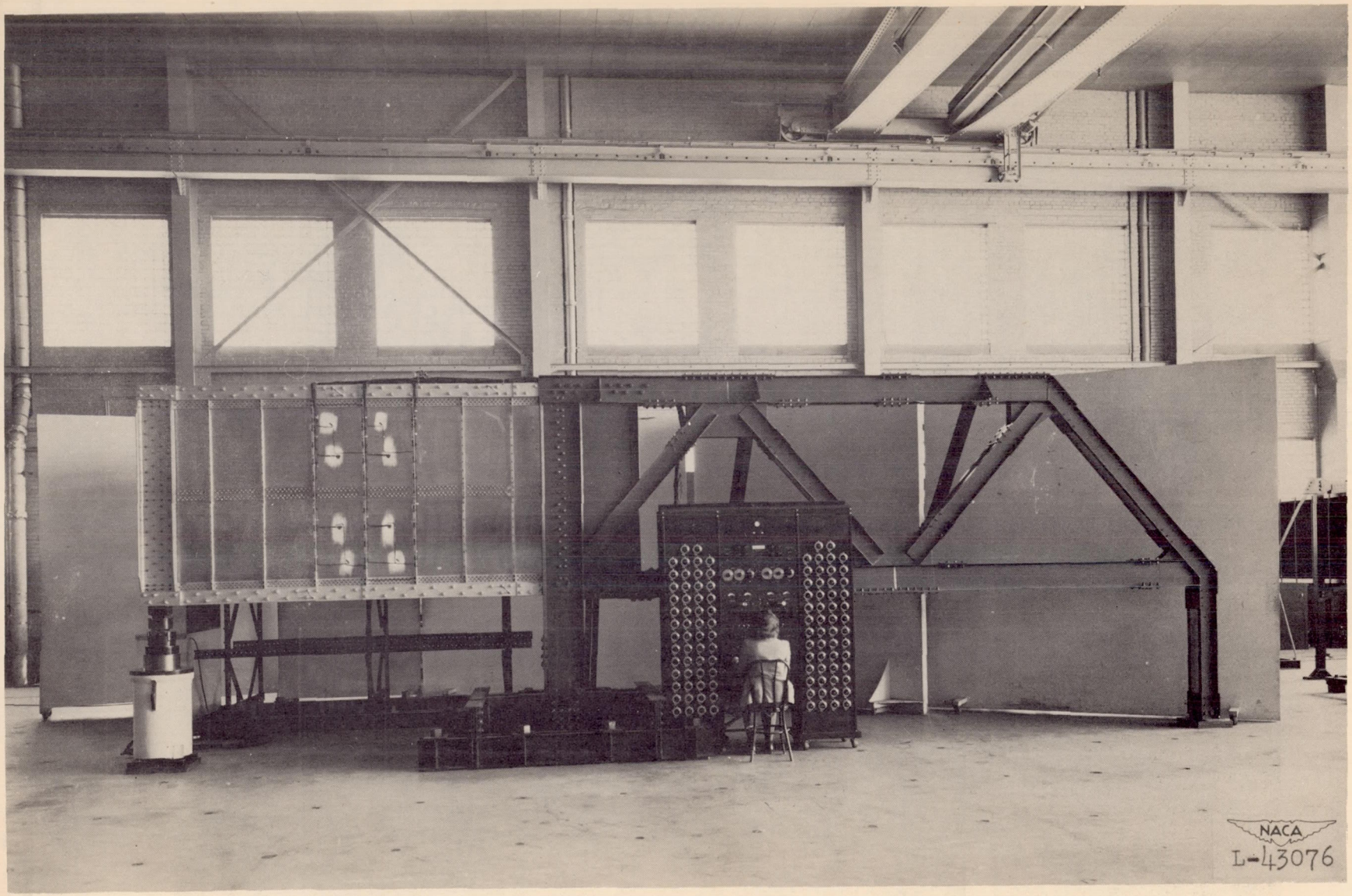

Figure 3.- Test setup for large beam. Front view.

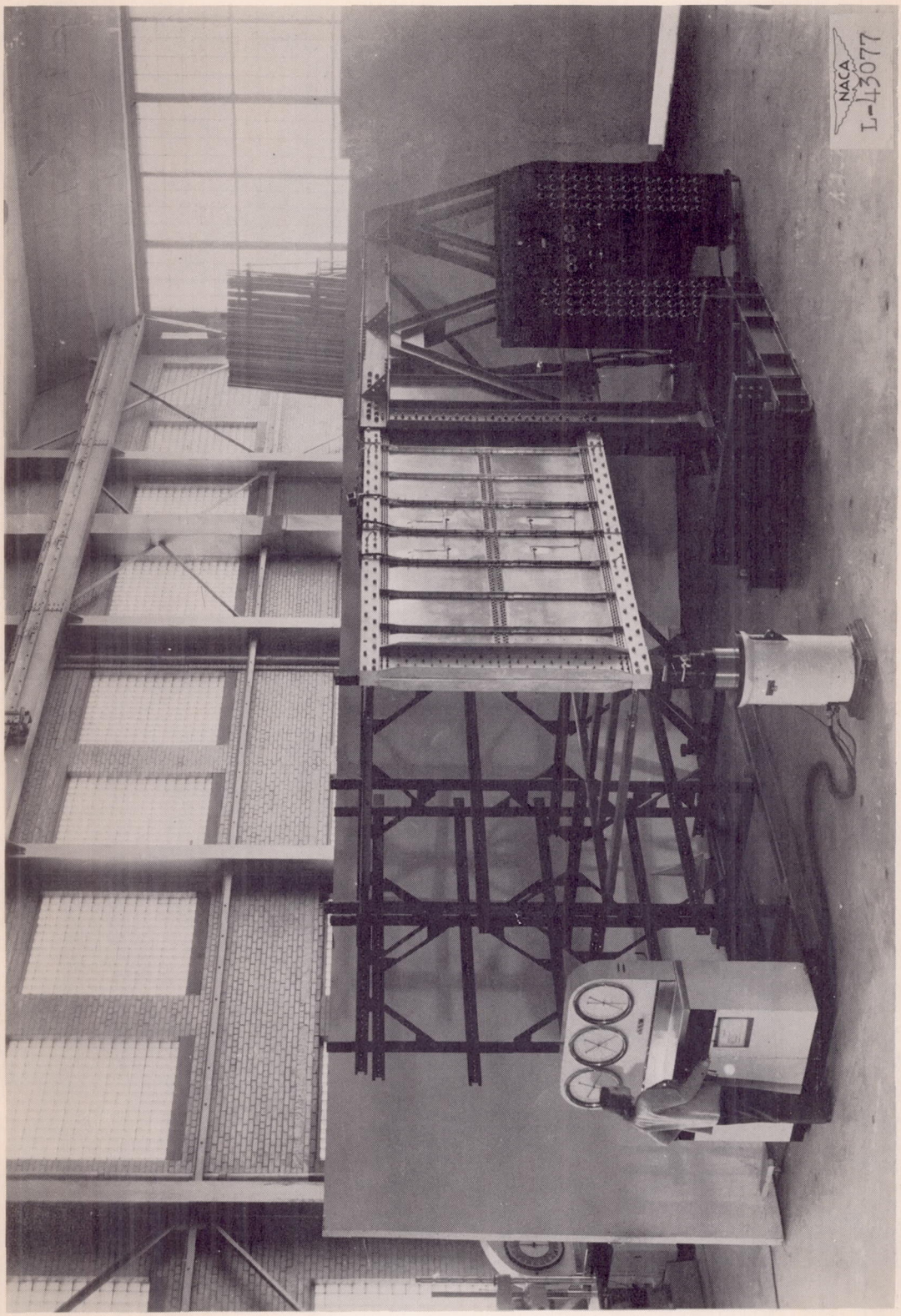

Figure 4.- Test setup for large beam. One-quarter end view.

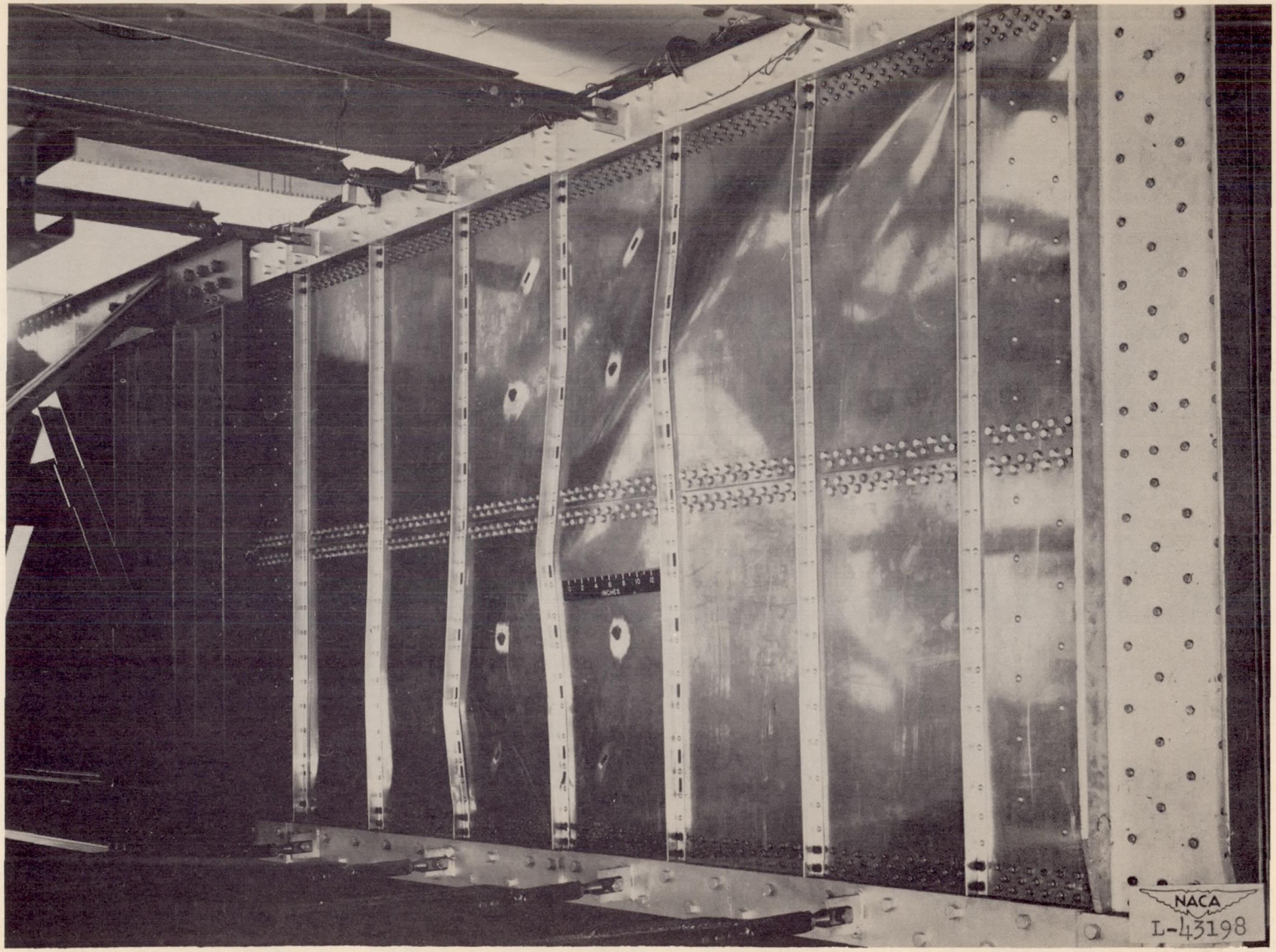

Figure 5.- Failure by column bowing of uprights on large beam.

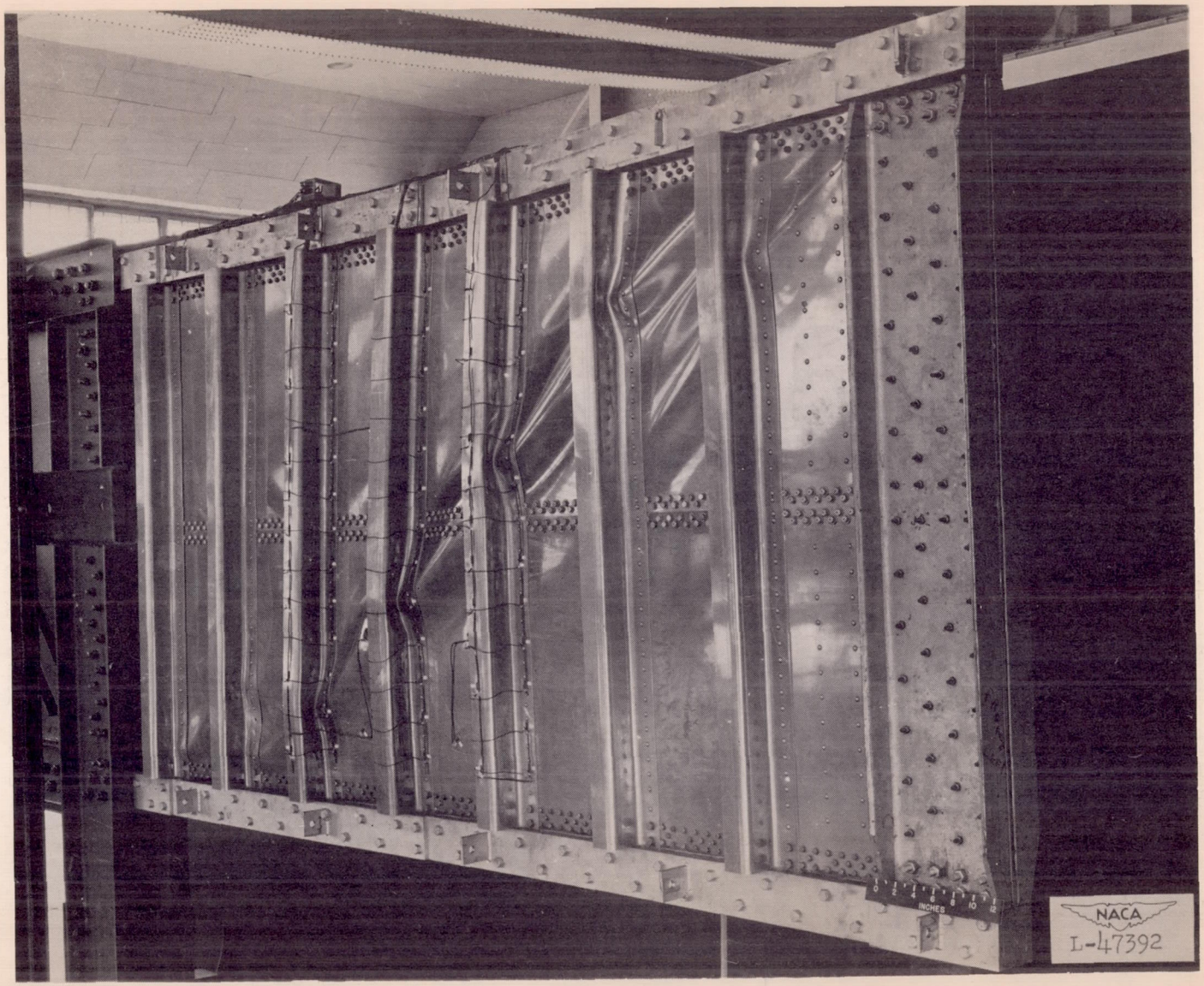

Figure 6.- Failure by forced crippling of uprights on large beam.

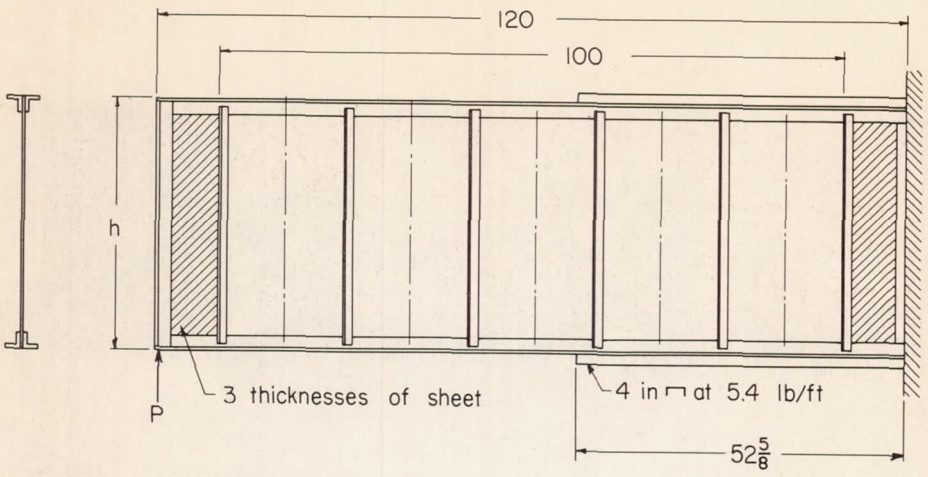

40-inch beams - series I (For beams 1D and 2D, h = 41.1; for beams 3D and 4D, h = 43.1)

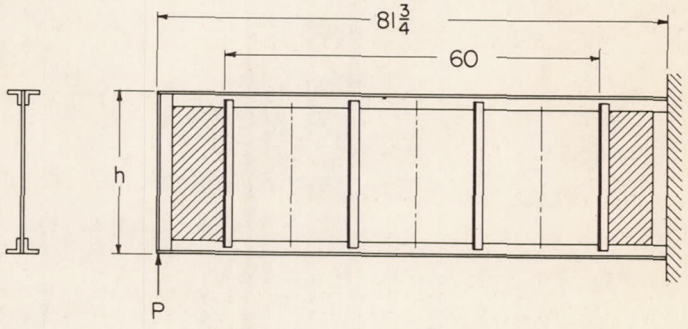

25-inch beams - series I, II-25-6S, II-25-9S, III-25-4D, III-25-6D and III-25-7D. (For series I, h = 26.1; for series II and III, h = 25.5)

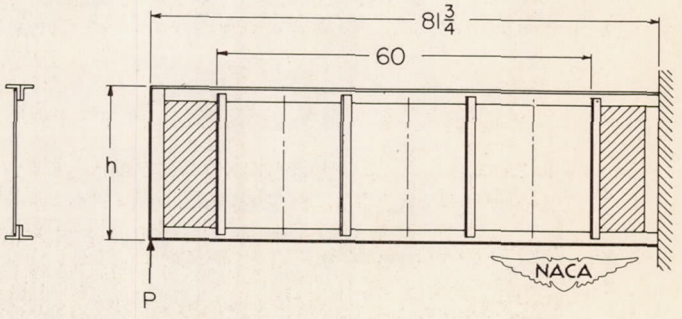

25-inch beams - series II and III. (h = 25.5)

Figure 7. - Test beams, series I to III.

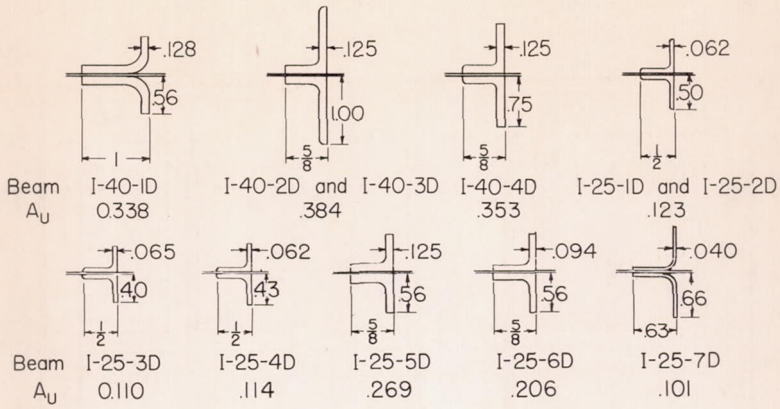

Series I

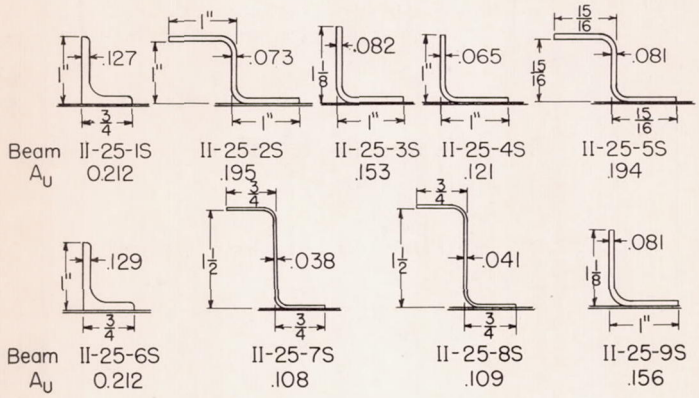

Series II

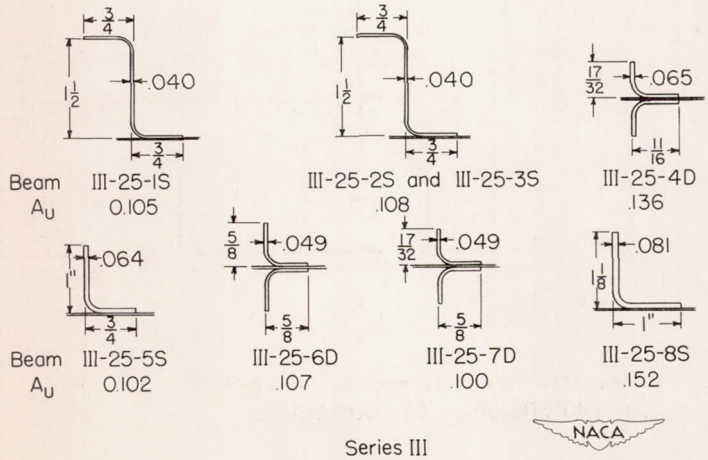

Series III

Figure 8.- Sections of uprights, beam series I to III.

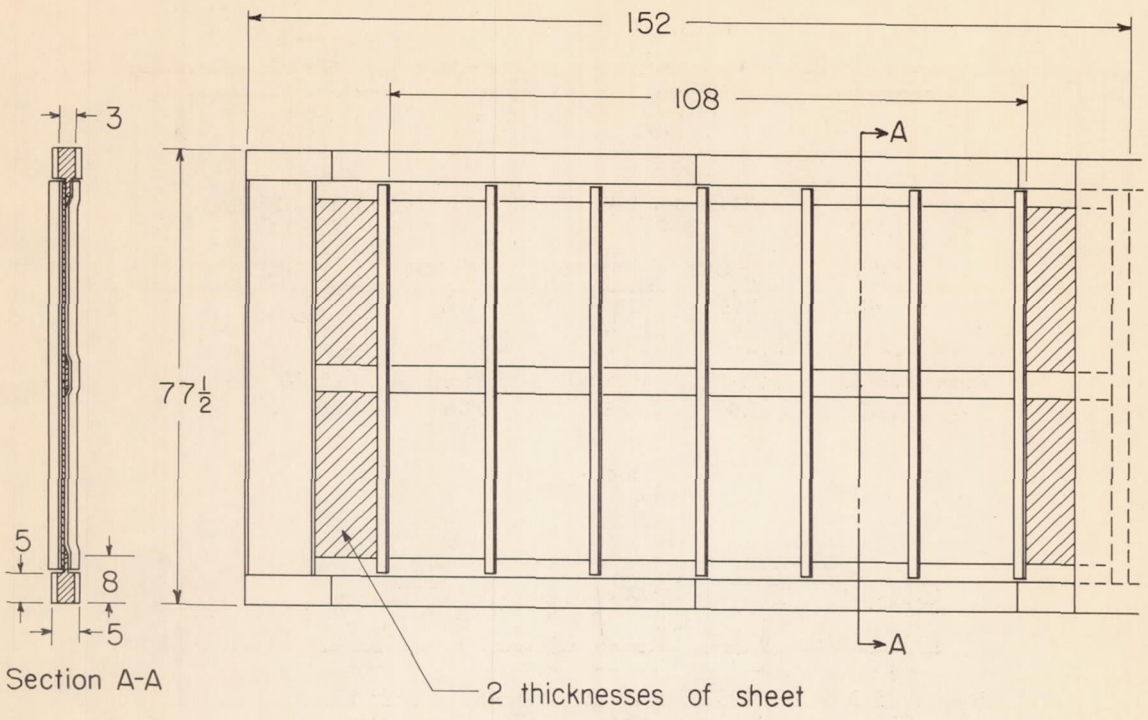

(a) General dimensions of test beams.

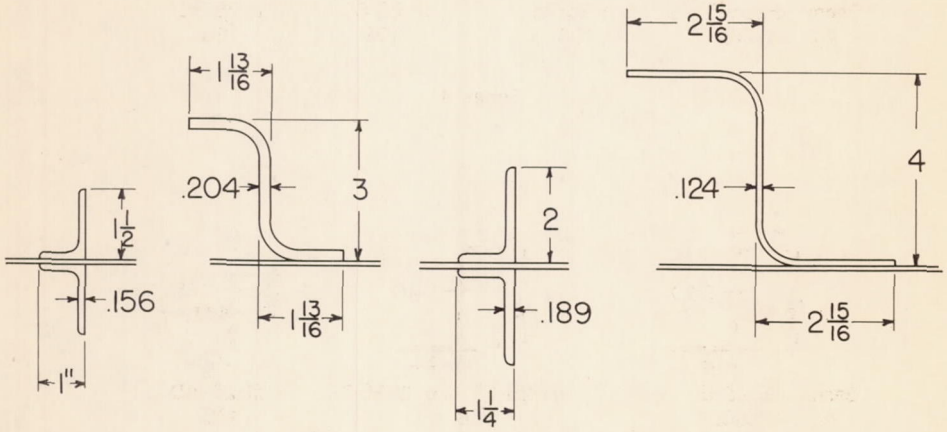

Beam	IV-72-1D	IV-72-2S	IV-72-3D	IV-72-4S
A_U	0.762	1.137	1.176	1.092

(b) Dimensions of uprights.

Figure 9.- Test beams, series IV.

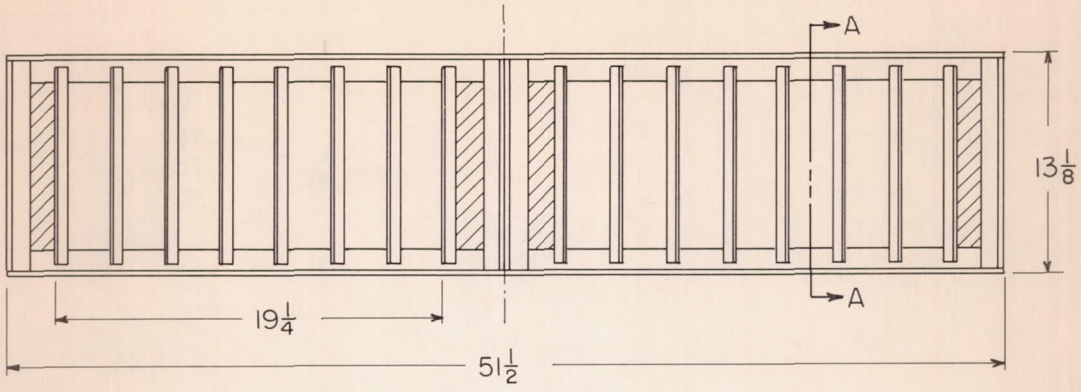

$\frac{d}{h} = 0.25$

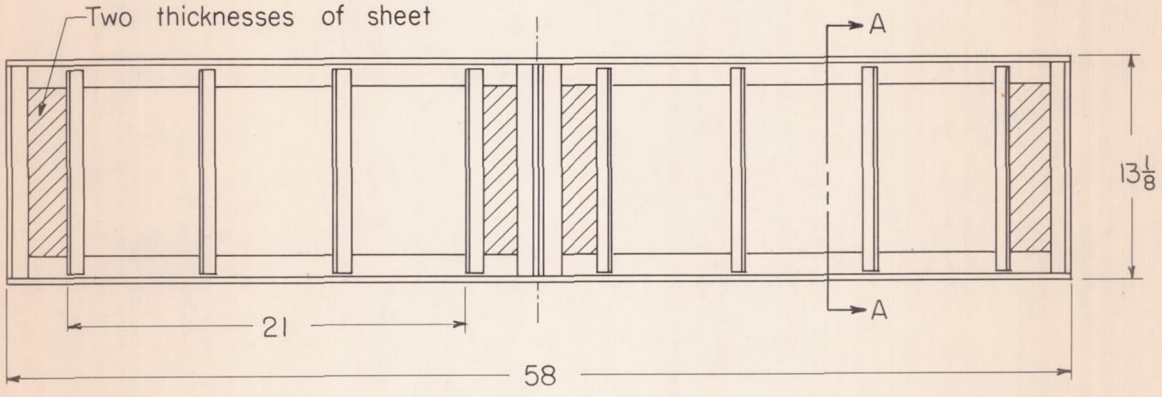

$\frac{d}{h} = 0.70$

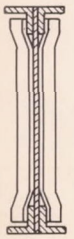

Section A-A
Double uprights

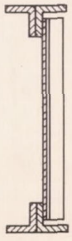

Section A-A
Single uprights

Figure 10.- Test beams, series V.

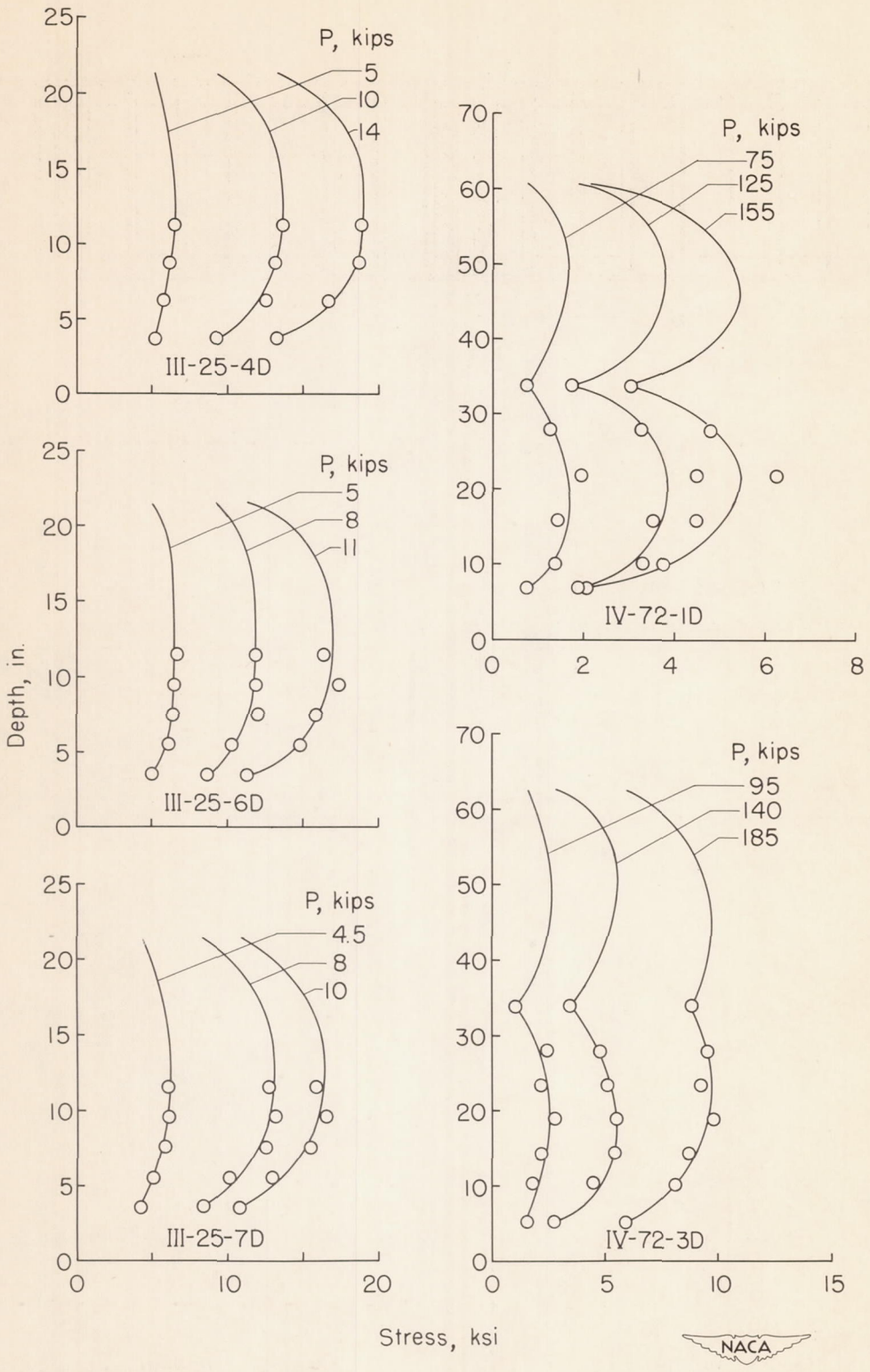

Figure 11.- Distribution of experimental upright stresses along length of uprights.

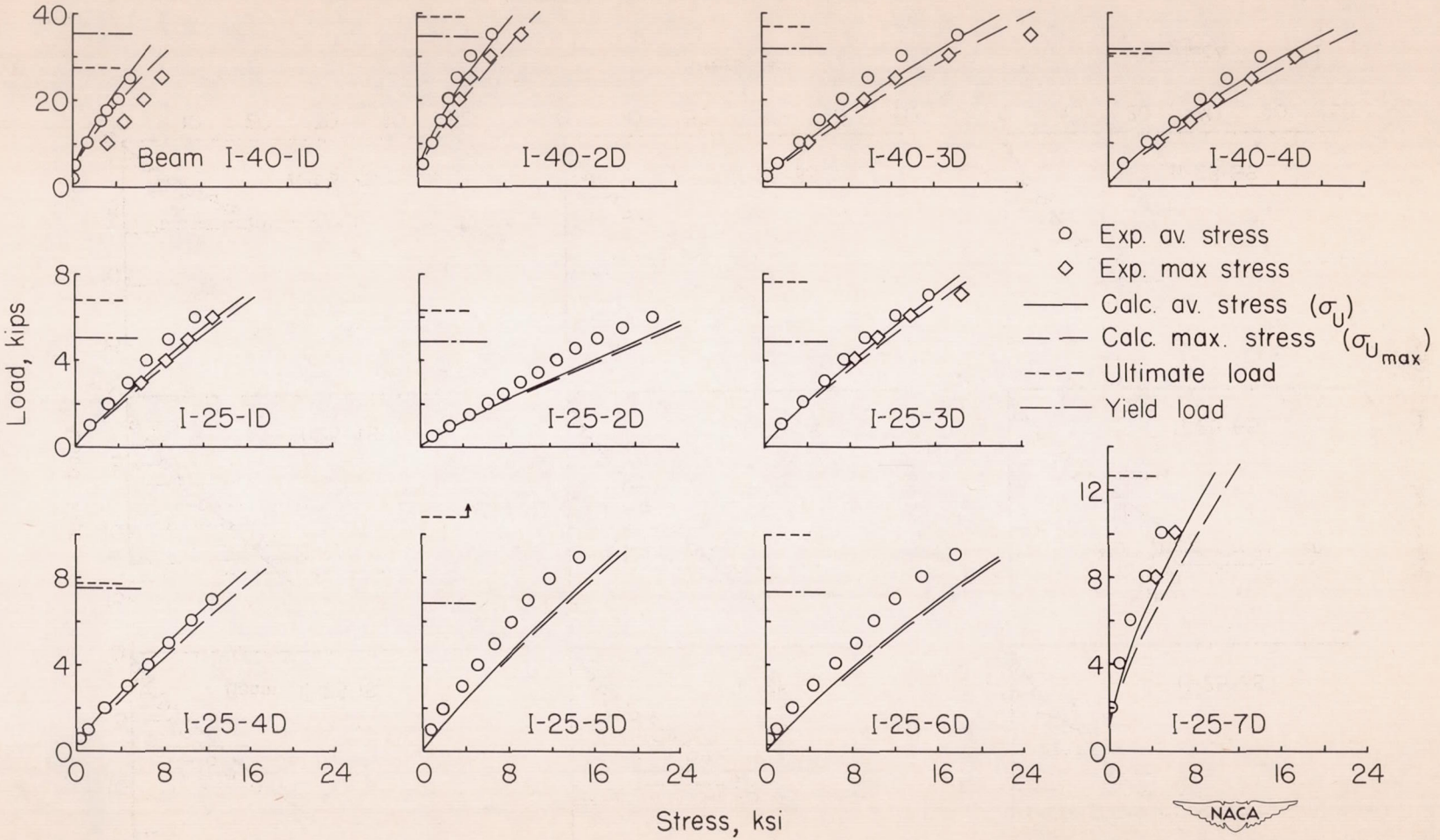

Figure 12.- Upright stresses, beam series I.

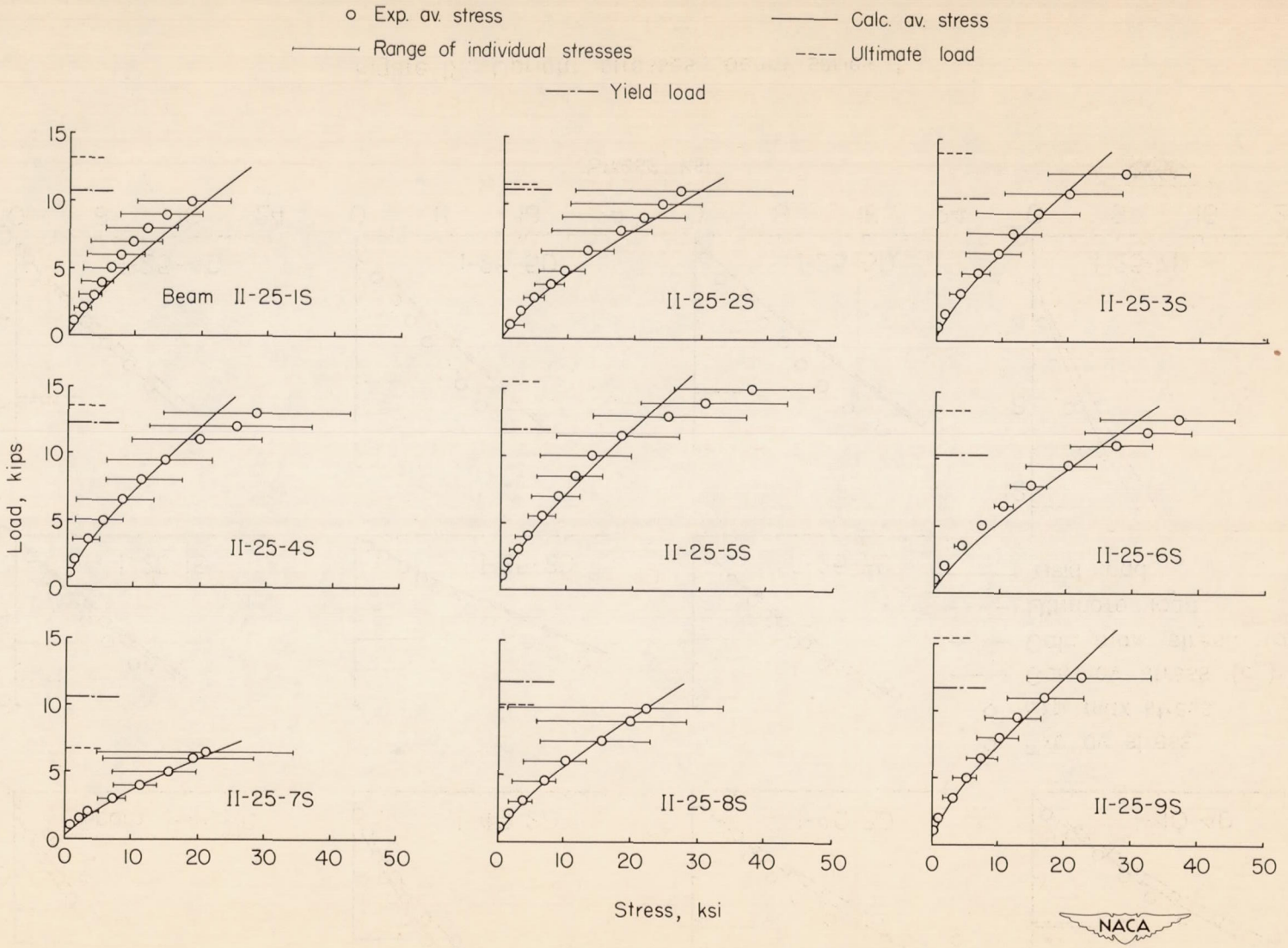

Figure 13.- Upright stresses, beam series II.

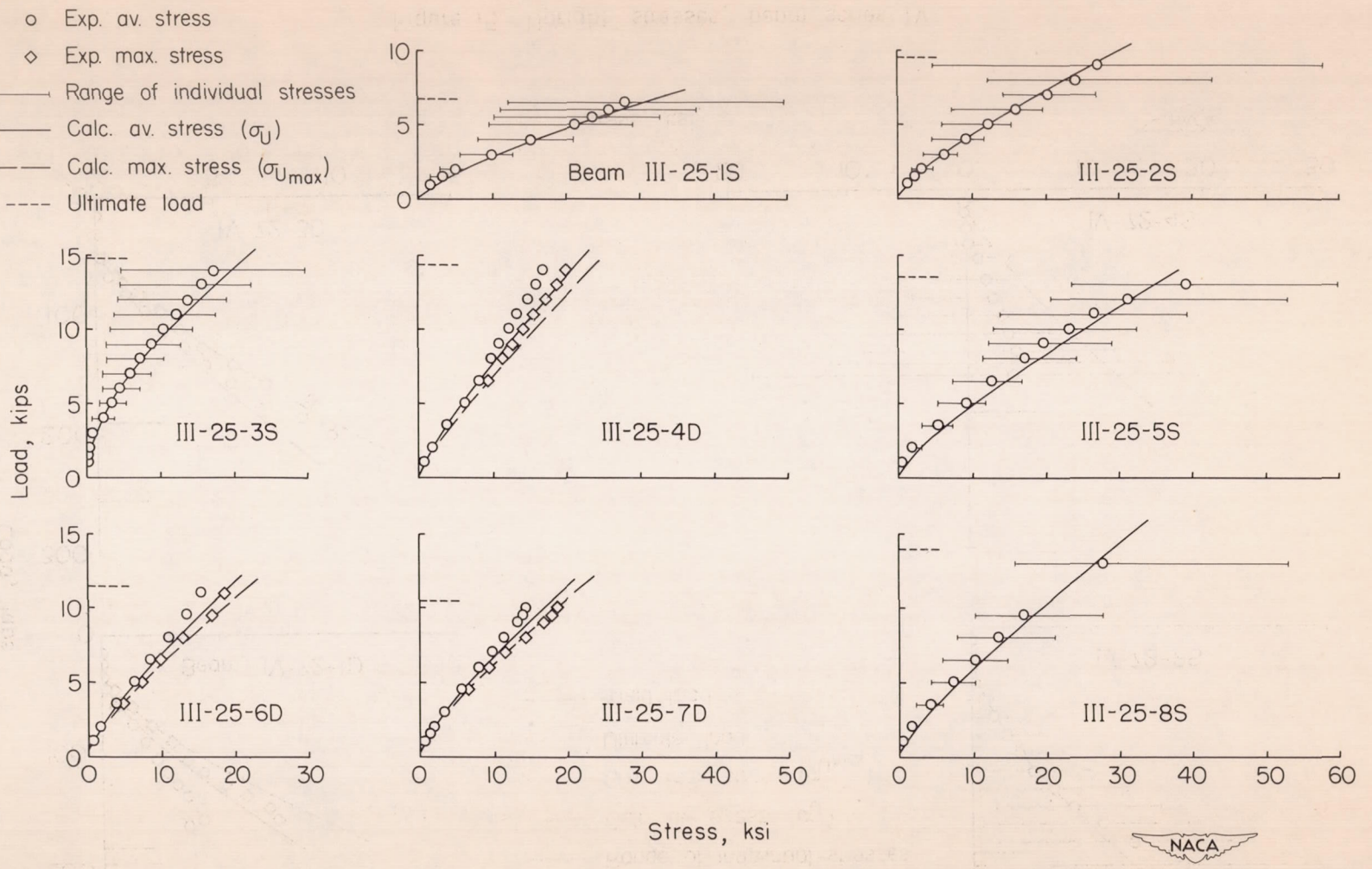

Figure 14.- Upright stresses, beam series III.

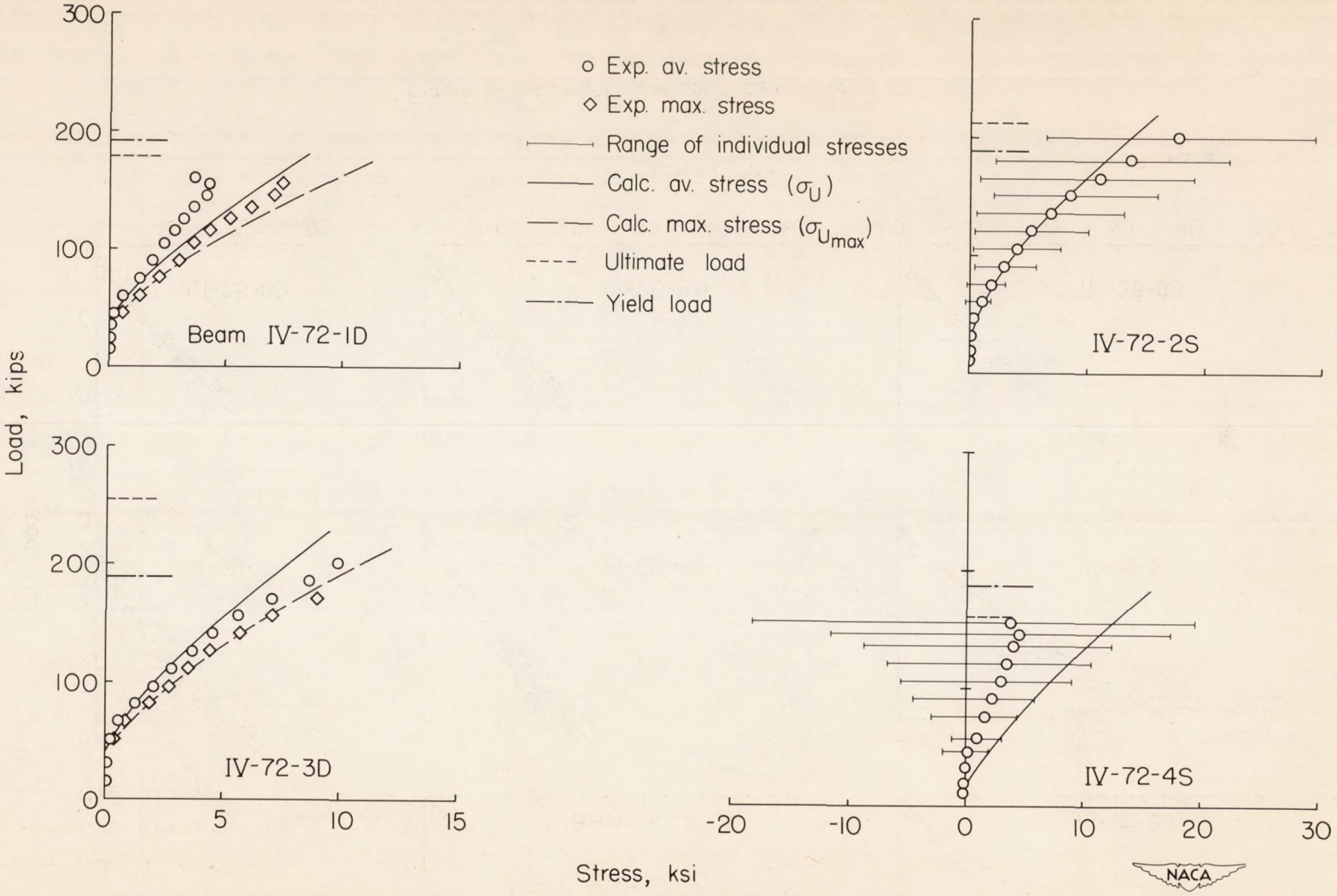

Figure 15.- Upright stresses, beam series IV.

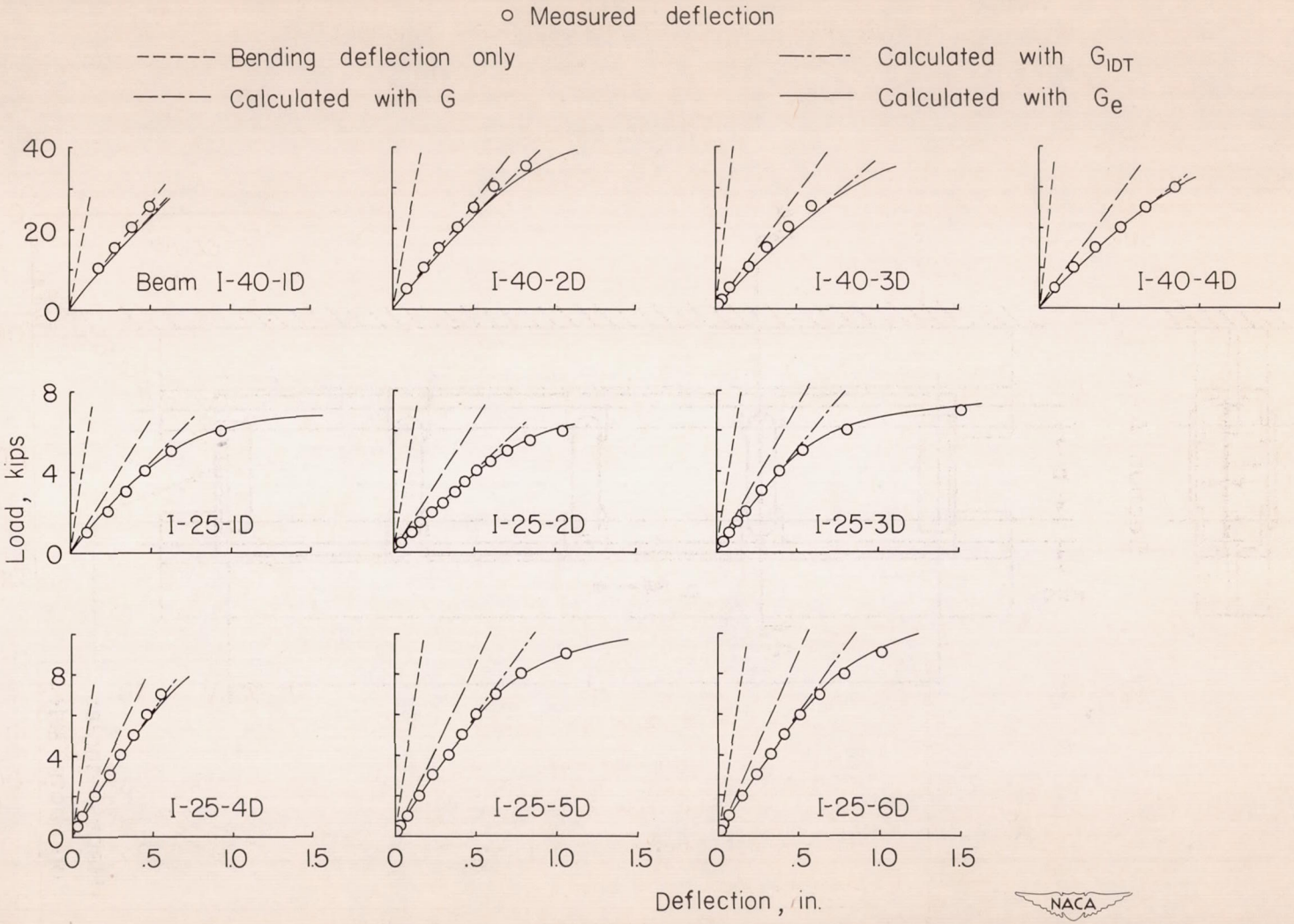

Figure 16.- Beam deflections, beam series I.

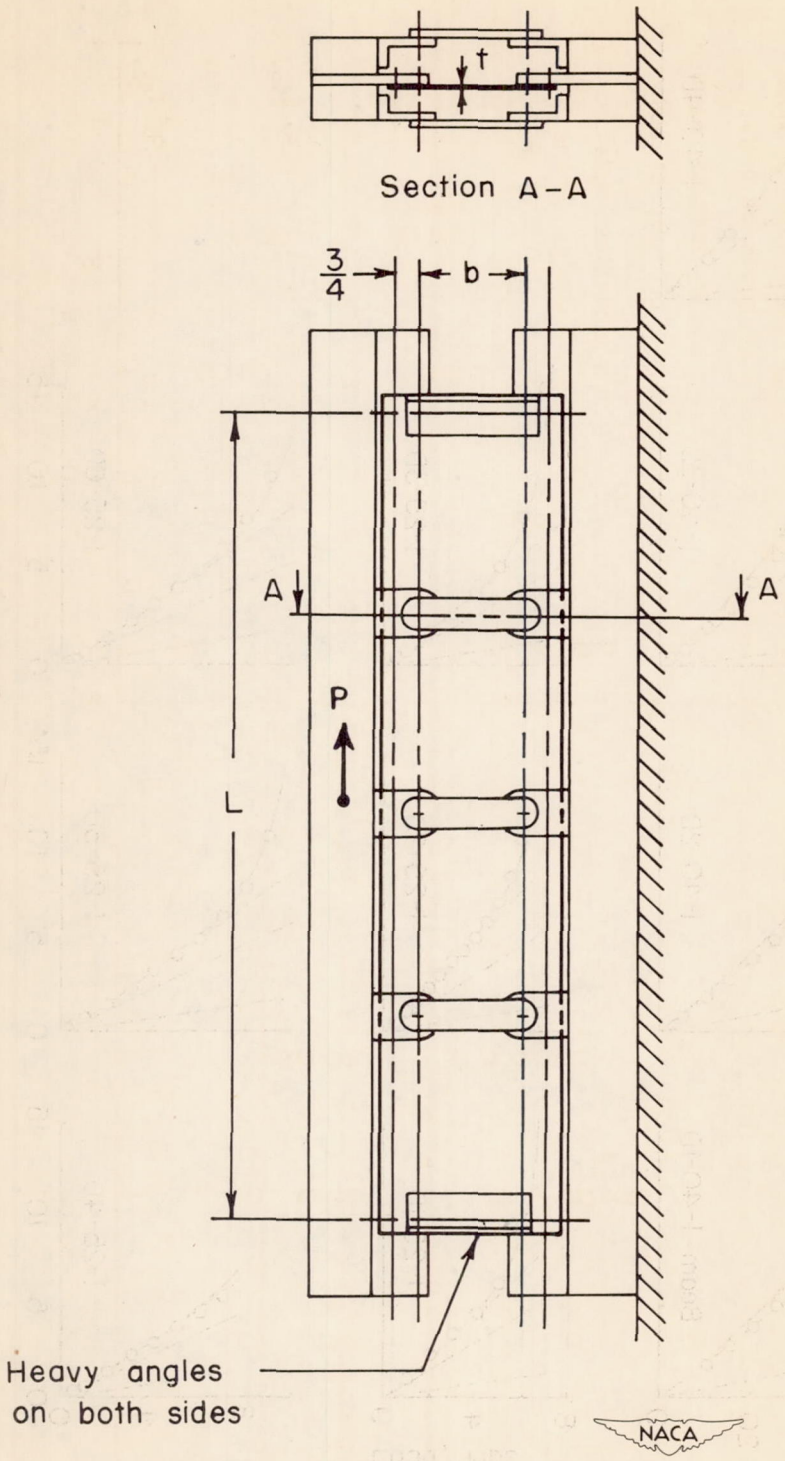

Figure 17.- Jig for shear-web tests

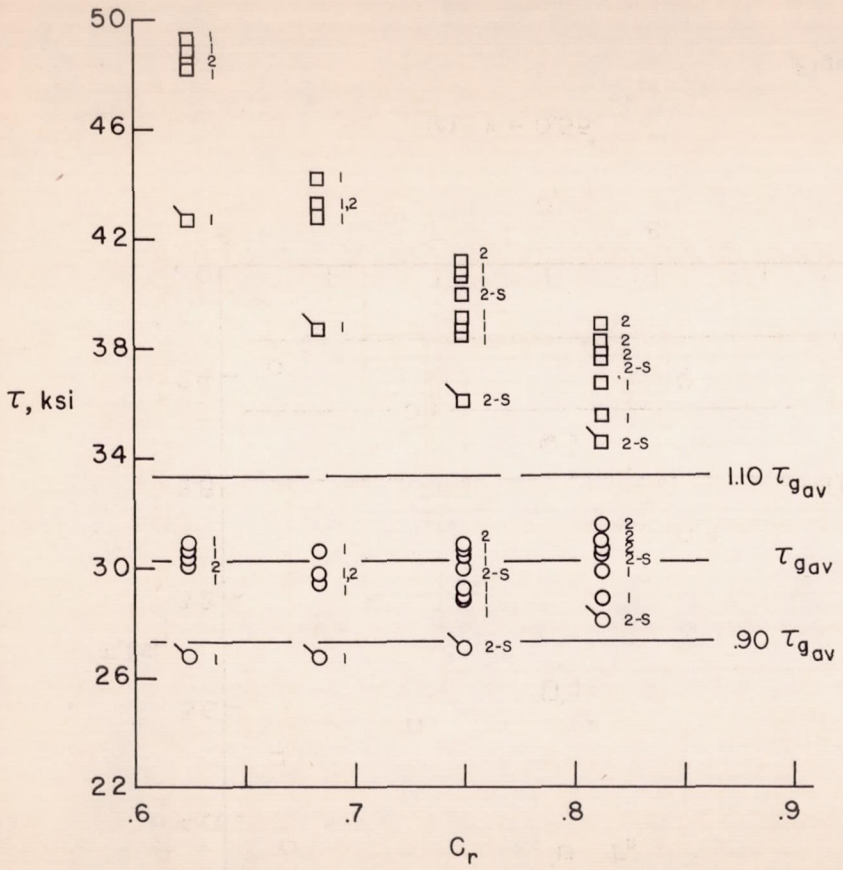

(a) k = 0.017.

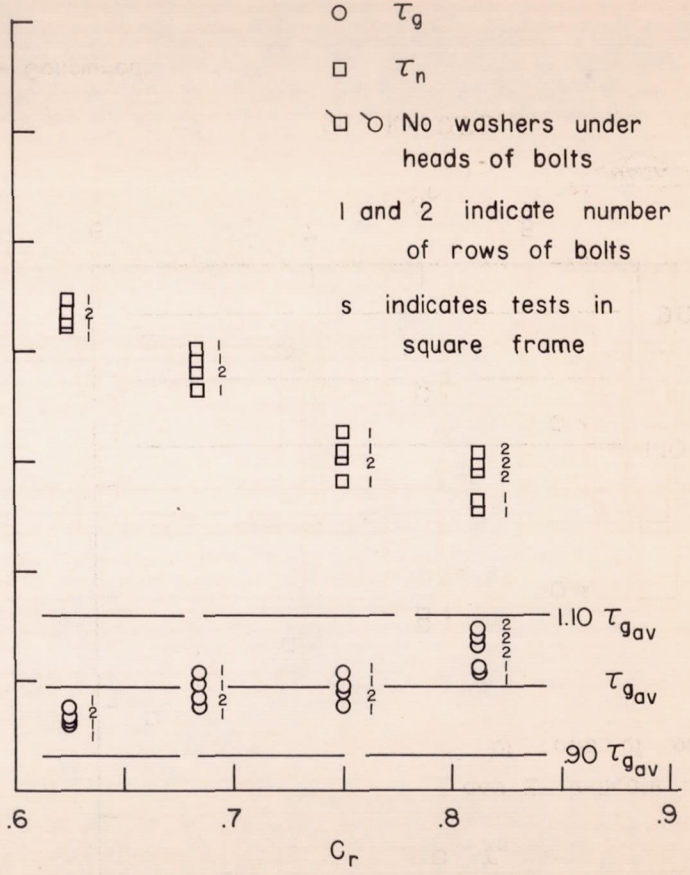

(b) k = 0.35.

Figure 18.— Ultimate stresses in shear webs of 24S-T3 aluminum alloy. (All stresses corrected to σ_{ult} = 62 ksi.)

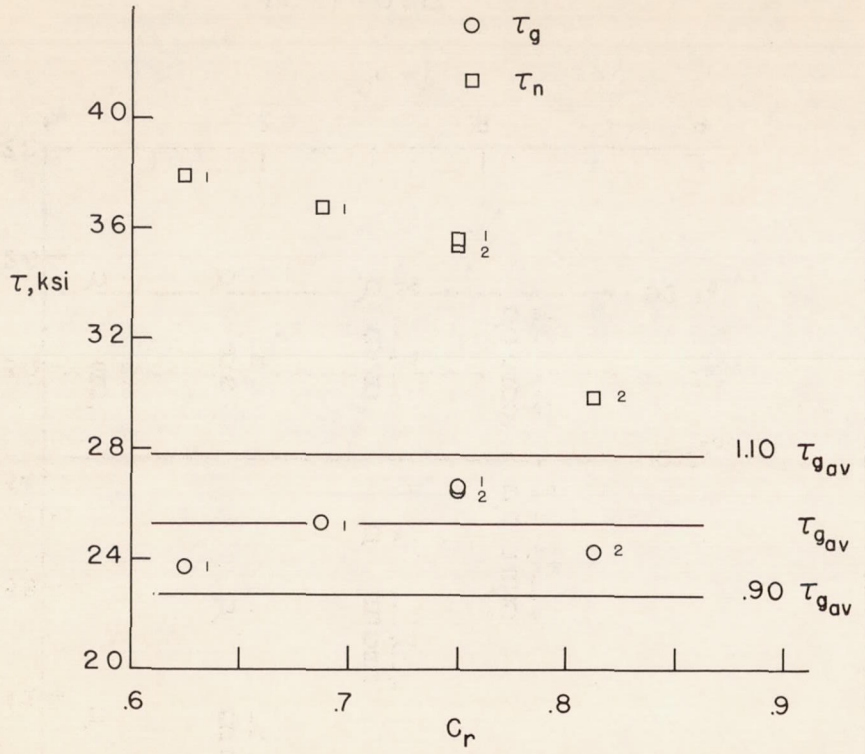

(c) $k \approx 0.55$.

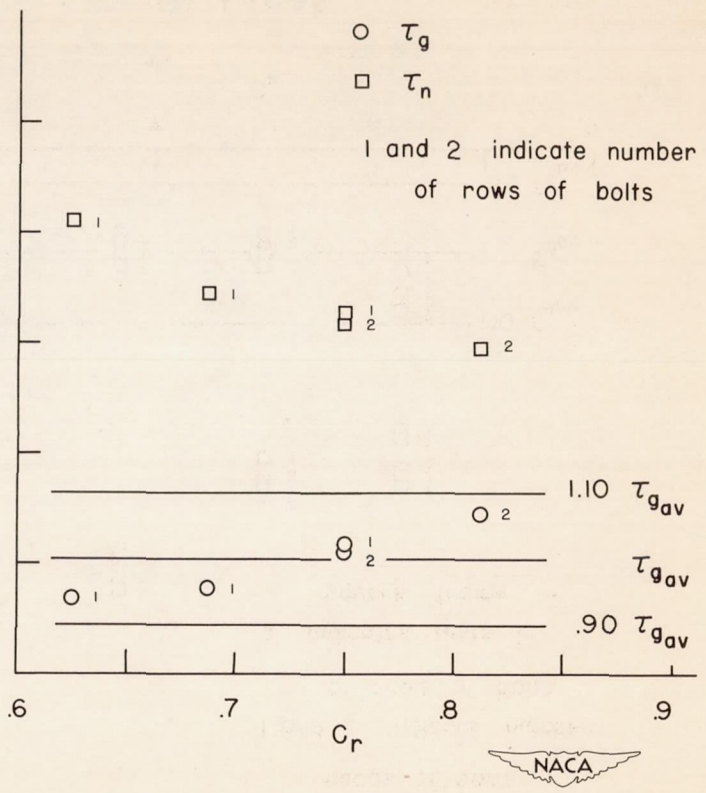

(d) $k \approx 0.72$.

Figure 18.— Concluded.

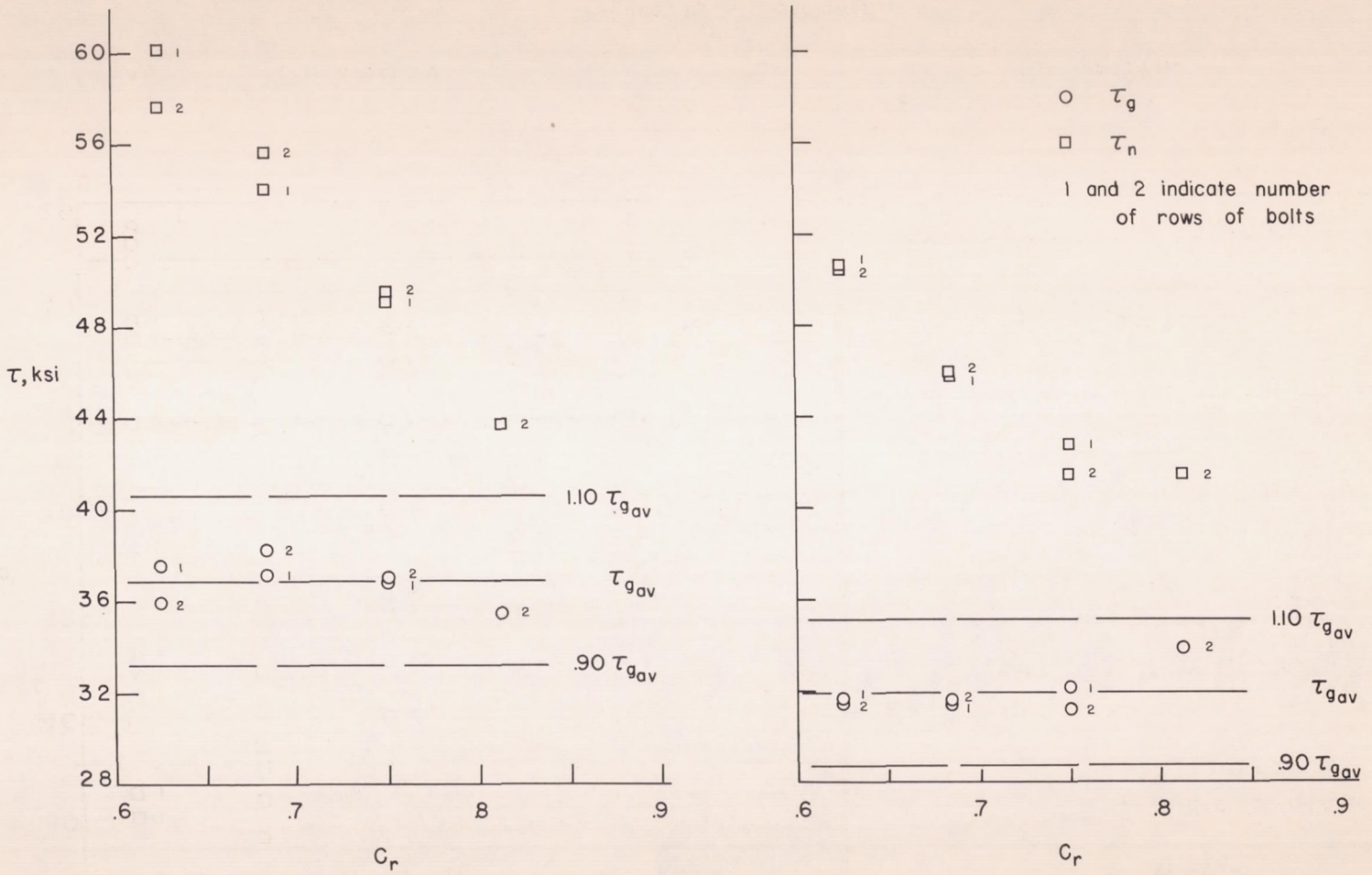

Figure 19.— Ultimate stresses in shear webs of Alclad 75S-T6 aluminum alloy. (All stresses corrected to σ_{ult} = 72 ksi.)

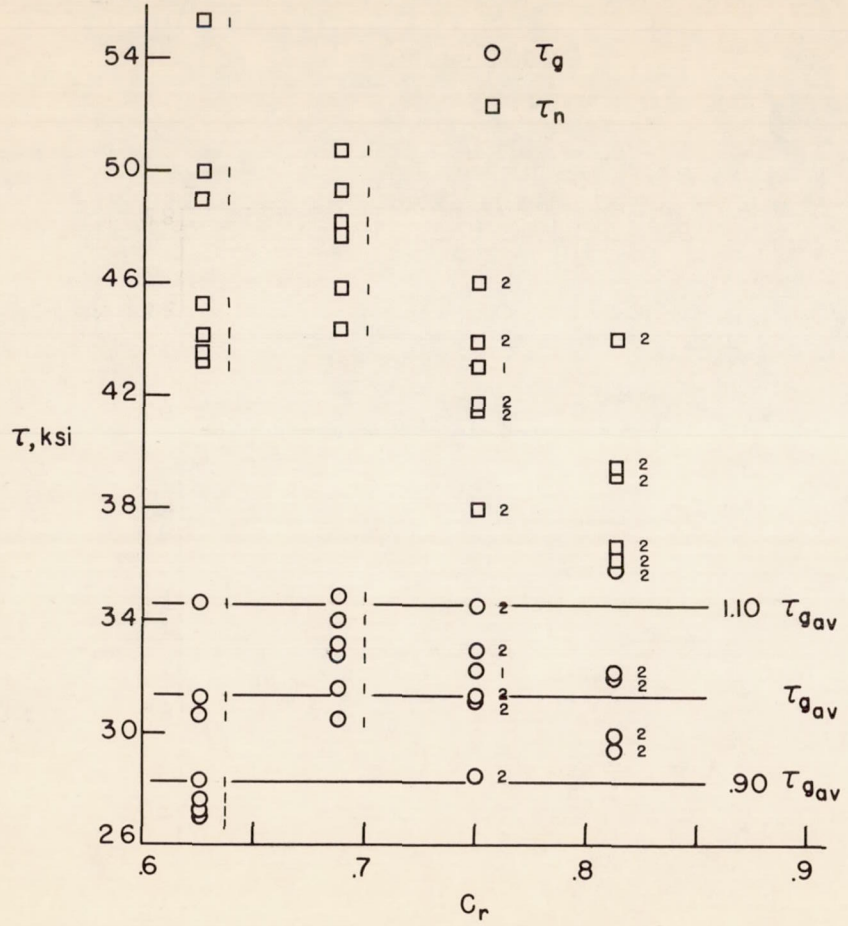

(c) k ≈ 0.59.

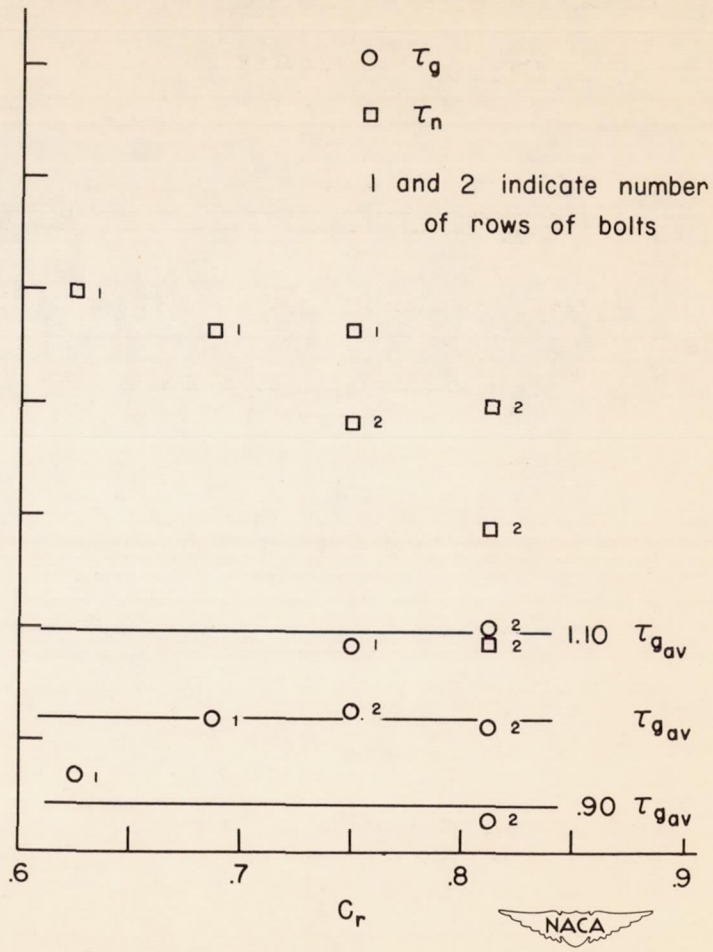

(d) k ≈ 0.74.

Figure 19.— Concluded.

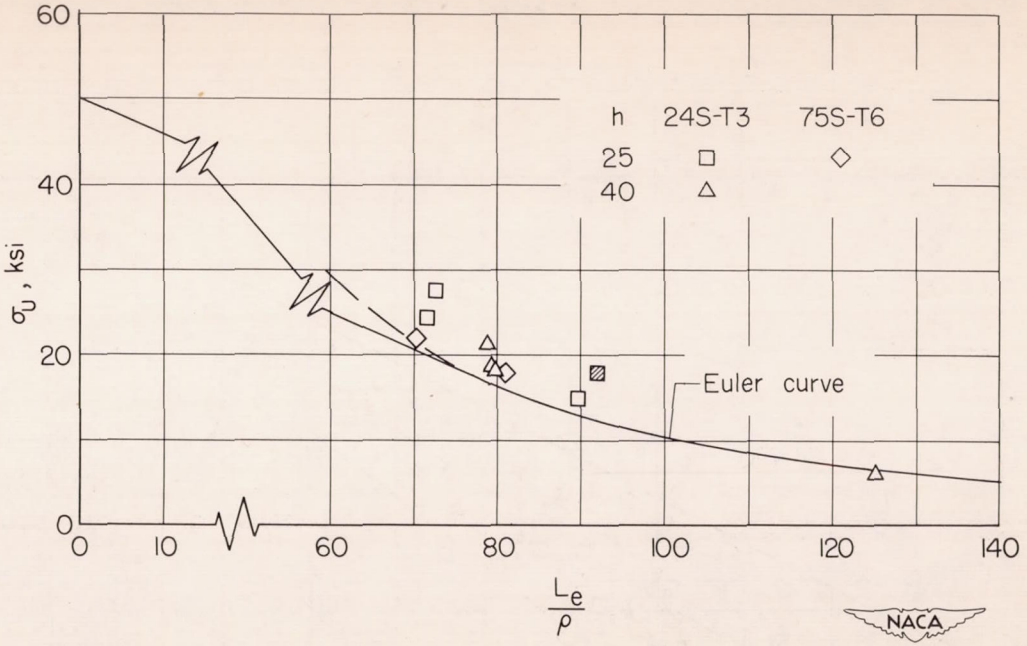

Figure 20.- Upright failures by column bowing. The shaded symbols represent web failures.

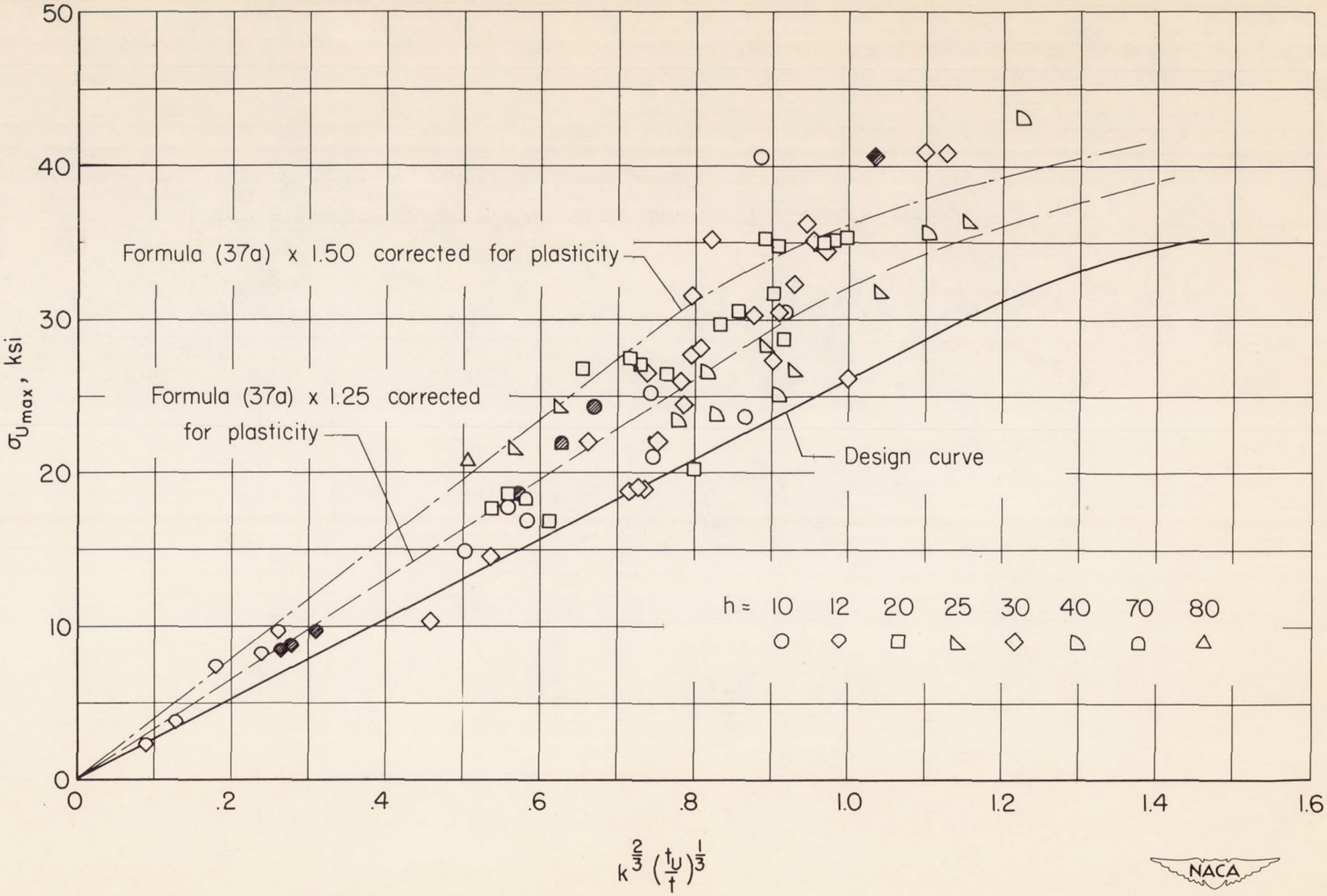

Figure 21.- Upright failures by forced crippling. Single uprights, 24S-T3 aluminum alloy. The shaded symbols represent web failures.

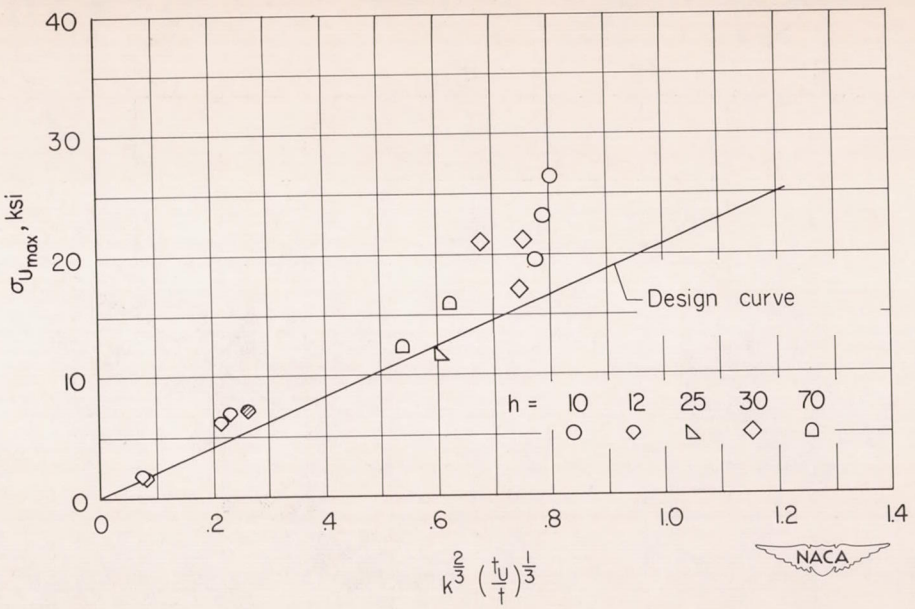

Figure 22.- Upright failures by forced crippling. Double uprights, 24S-T3 aluminum alloy. The shaded symbols represent web failures.

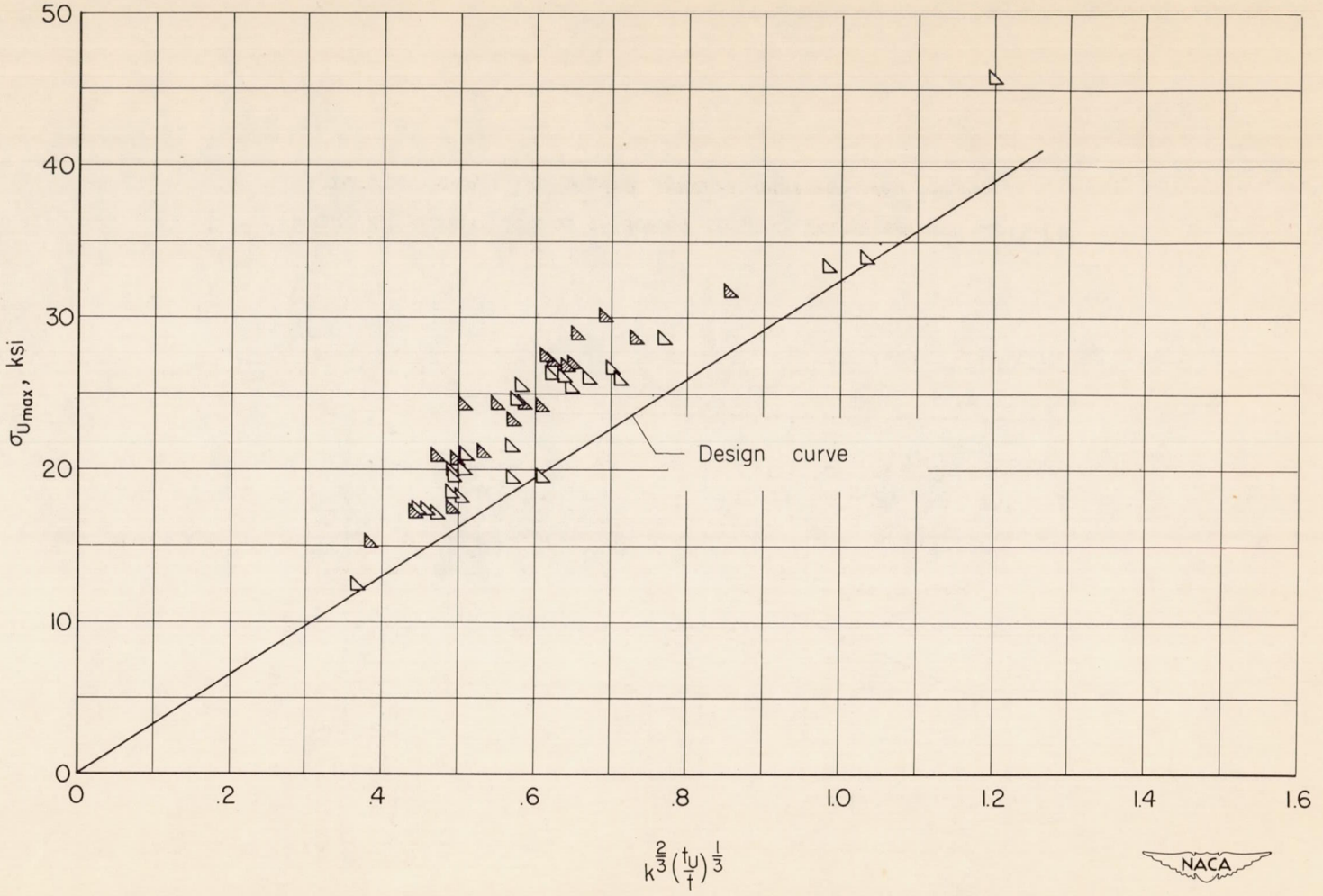

Figure 23.- Upright failures by forced crippling. Single uprights, 75S-T6 aluminum alloy, h = 25 inches. The shaded symbols represent web failures.

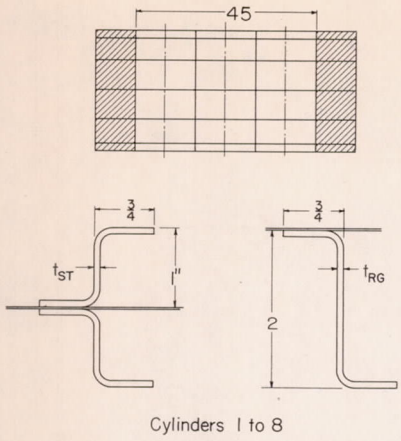

Cylinder	t_{ST}	t_{RG}	A_{ST}	A_{RG}
1	.052	.061	.230	.197
2	.050	.064	.221	.202
3	.033	.063	.155	.198
4	.033	.068	.153	.216
5	.081	.104	.335	.320
6	.080	.104	.332	.317
7	.053	.102	.239	.318
8	.053	.102	.239	.321

Cylinders 1 to 8

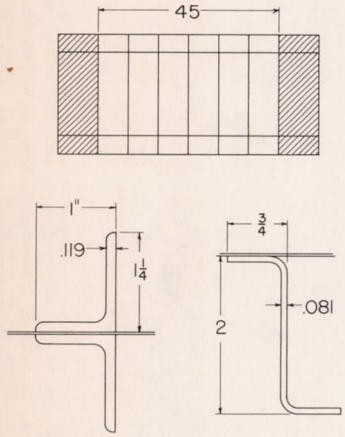

A_{ST} = .512 A_{RG} = .252

Cylinder 9

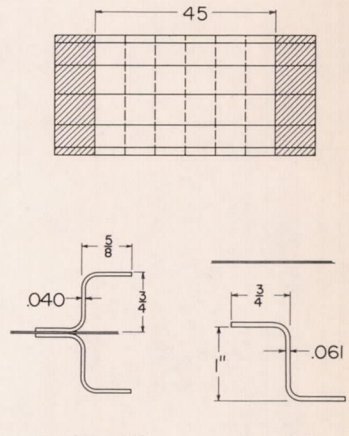

A_{ST} = .145 A_{RG} = .138

Cylinder 10

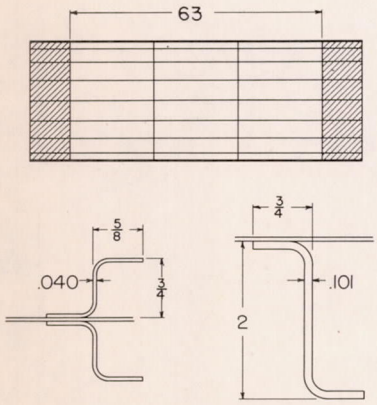

A_{ST} = .142 A_{RG} = .320

Cylinder 11

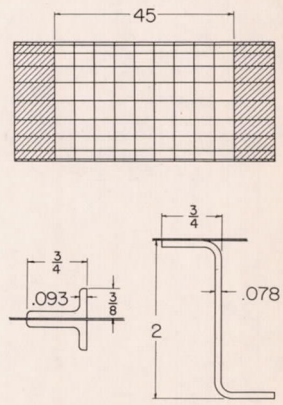

A_{ST} = .192 A_{RG} = .246

Cylinder 12

Figure 24.- Cylinders for torsion tests.

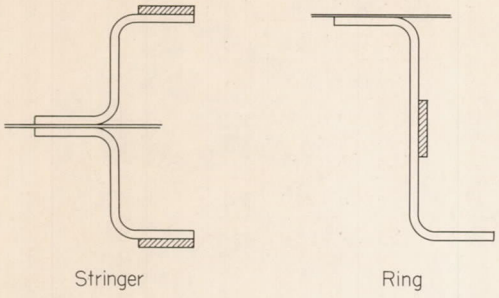

Cylinders 1 to 8

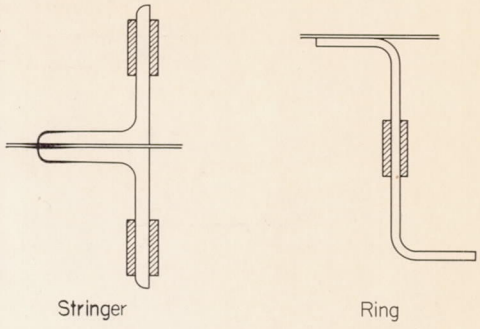

Cylinder 9

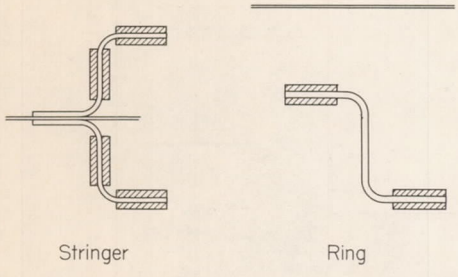

Cylinder 10

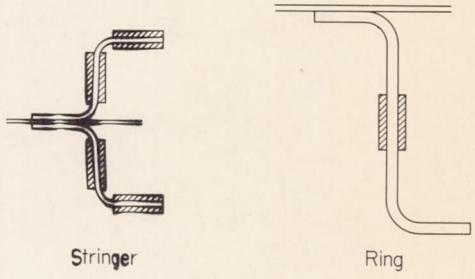

Cylinder 11

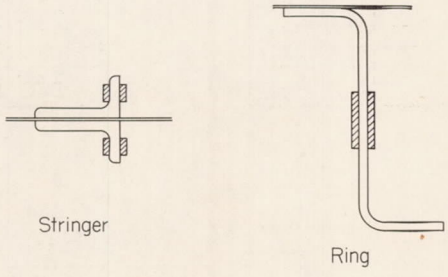

Cylinder 12

Figure 25.- Location of strain gages on cylinder stiffeners.

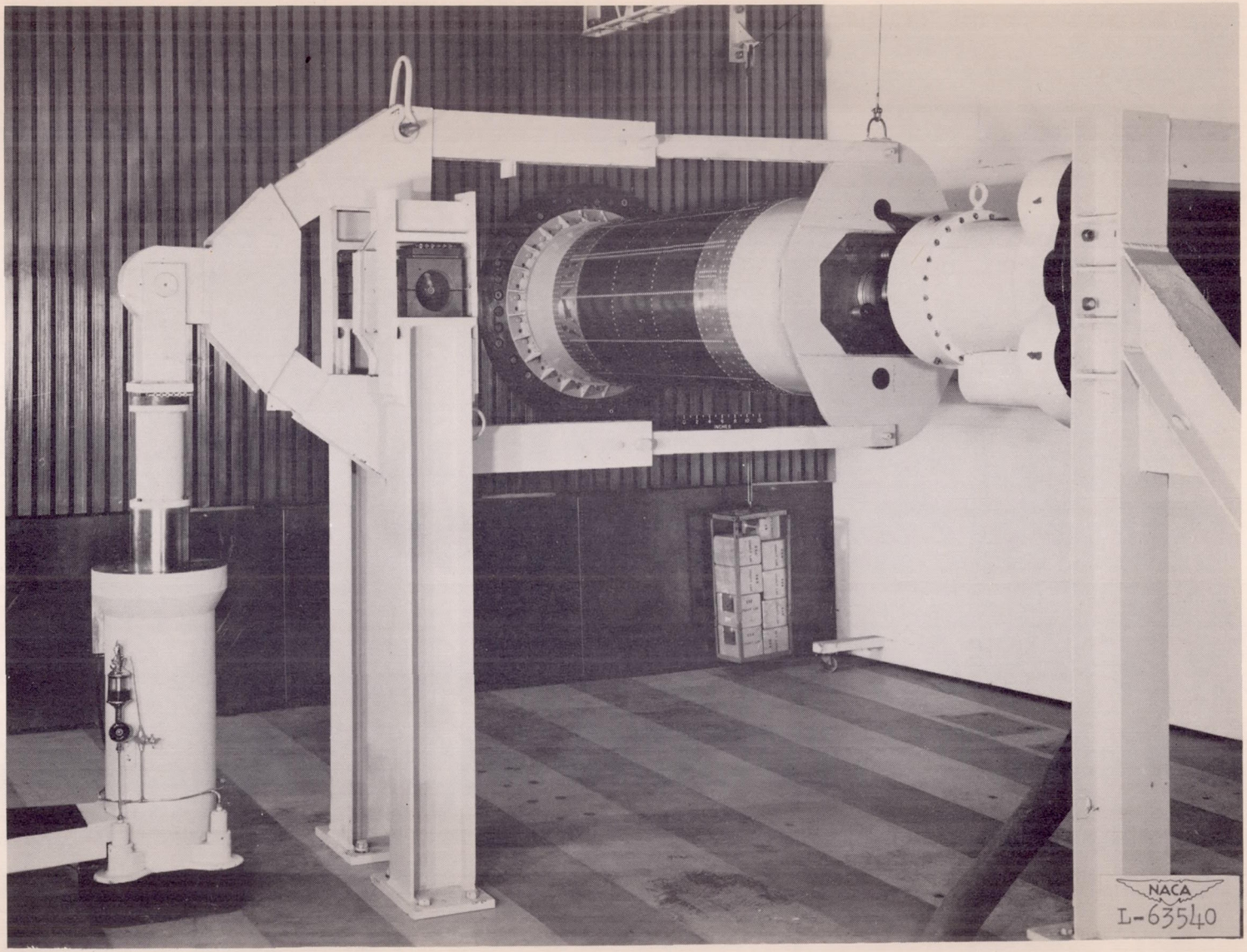

Figure 26.- Setup for test of cylinder in combined torsion and compression.

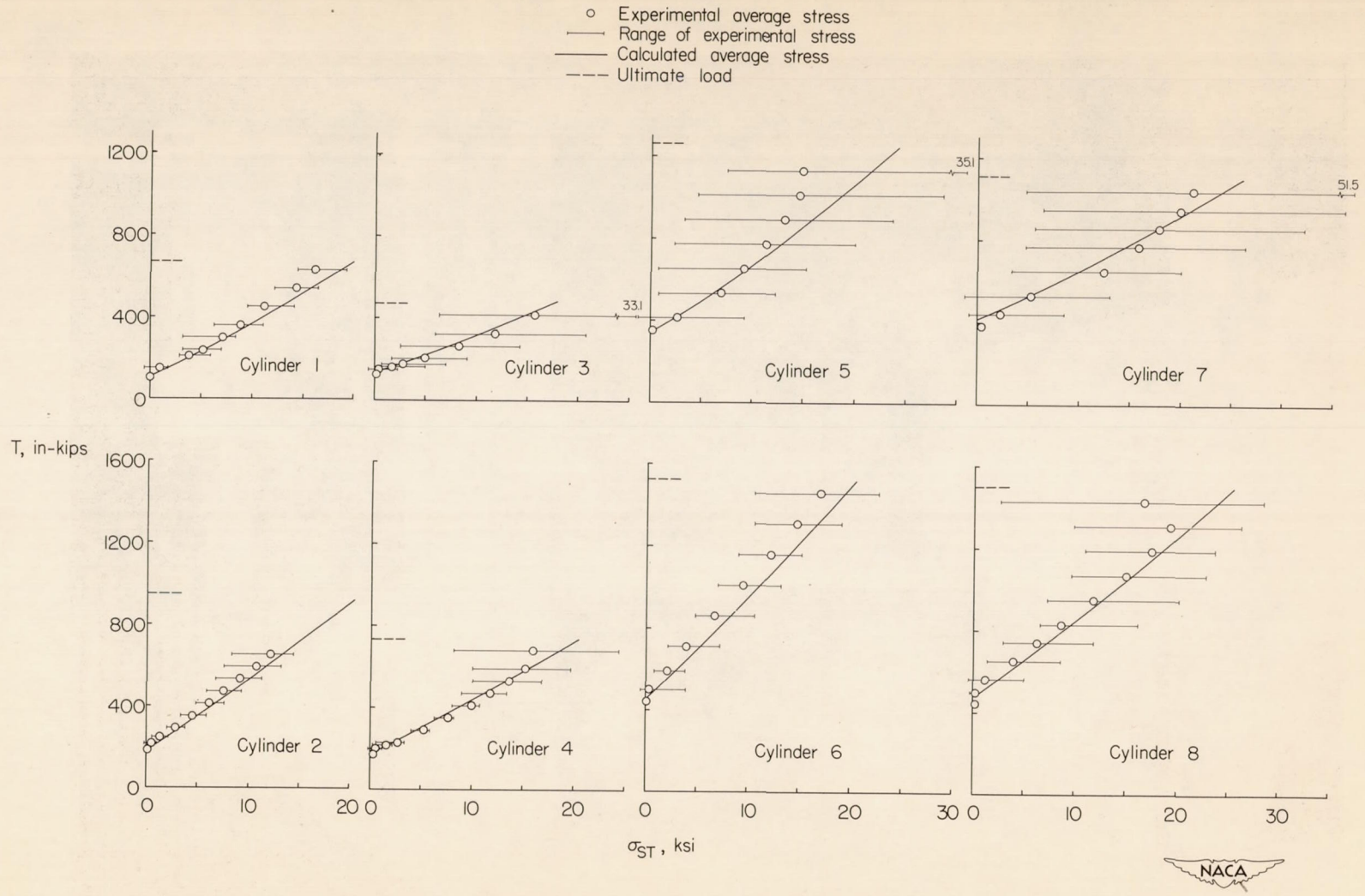

(a) Stringer stresses.

Figure 27.-Stiffener stresses in torsion cylinders 1 to 8.

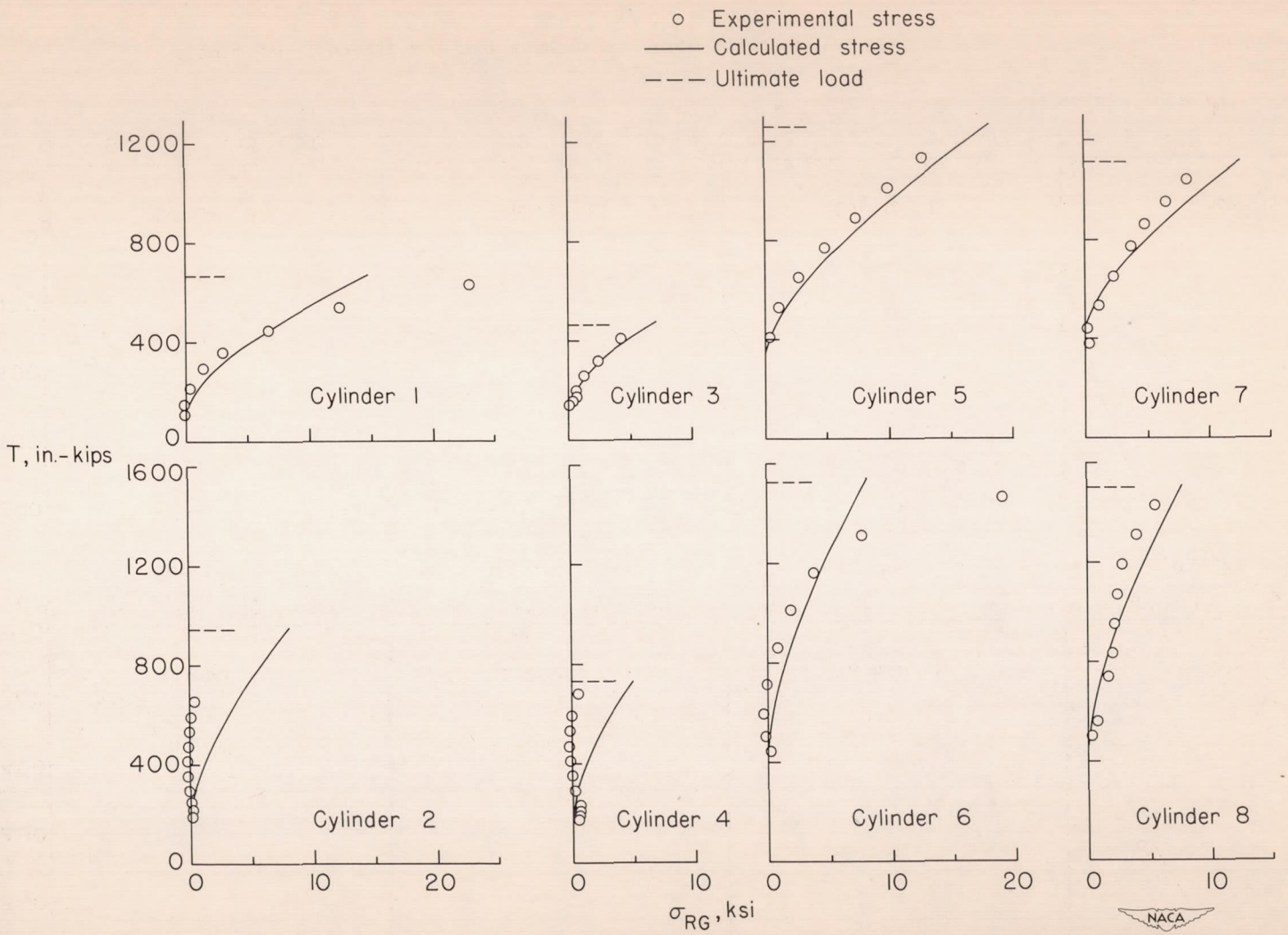

(b) Ring stresses

Figure 27.- Concluded.

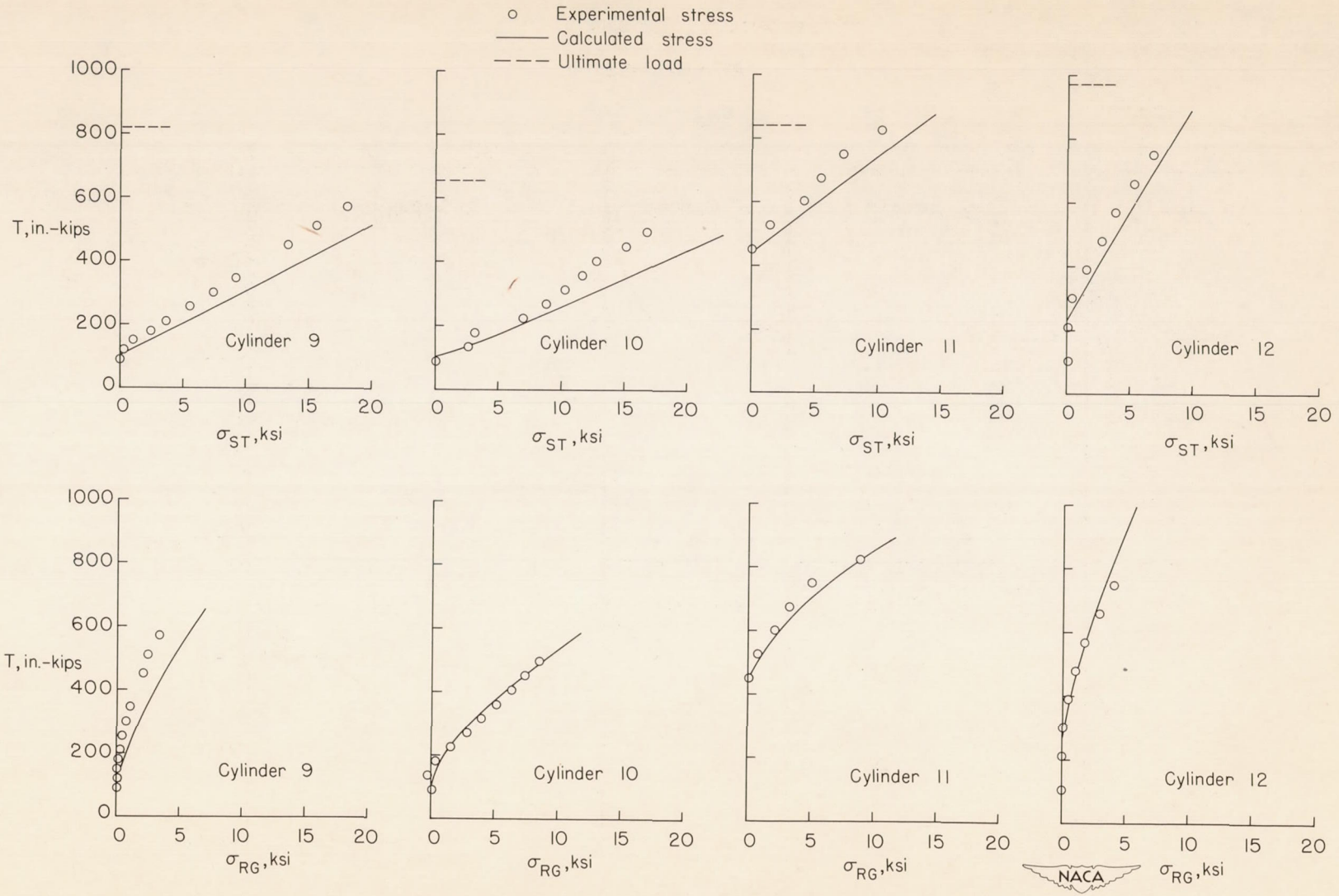

Figure 28.- Stringer and ring stresses in torsion cylinders 9 to 12.

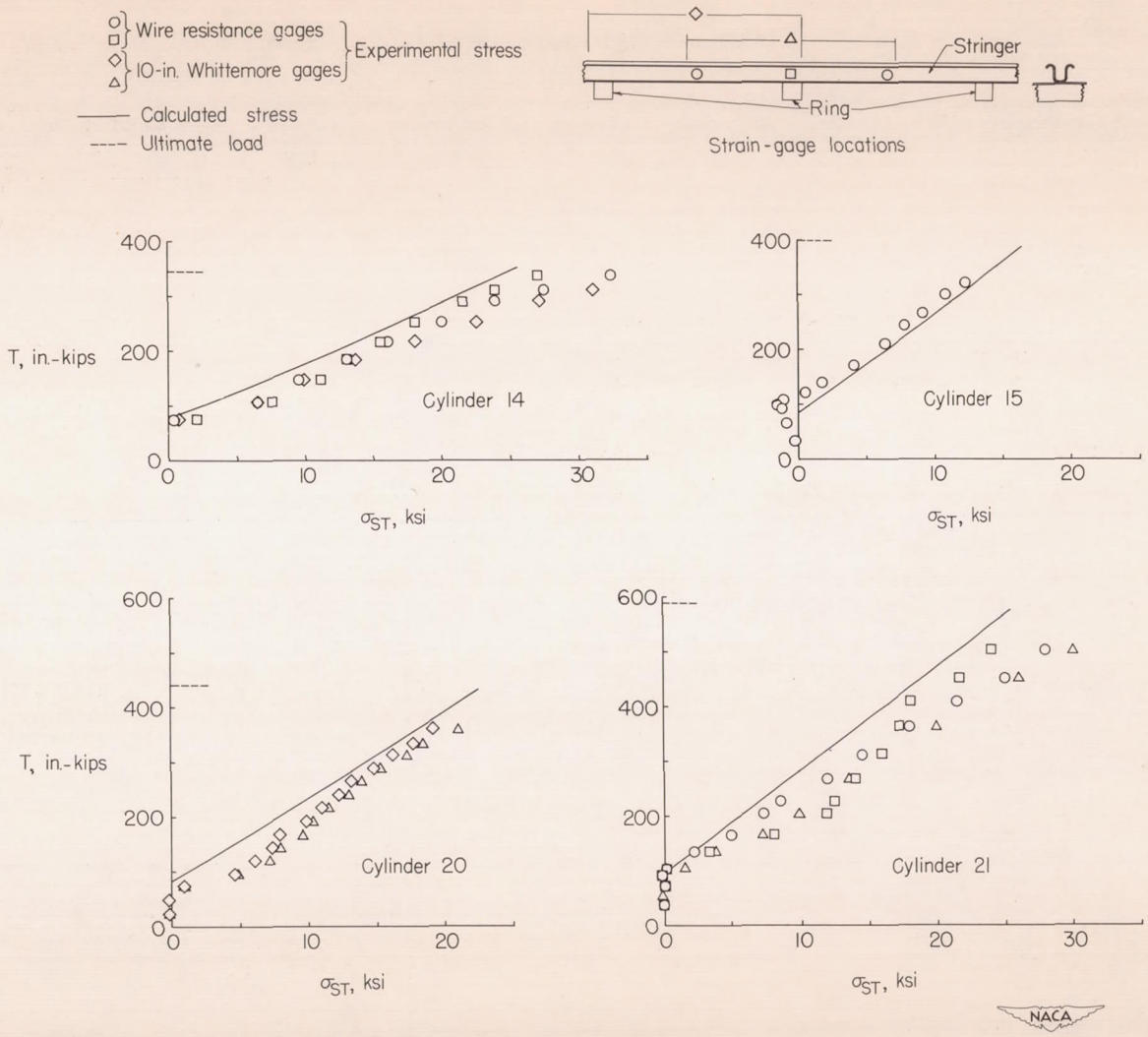

Figure 29.-Stringer stresses in ARL cylinders.

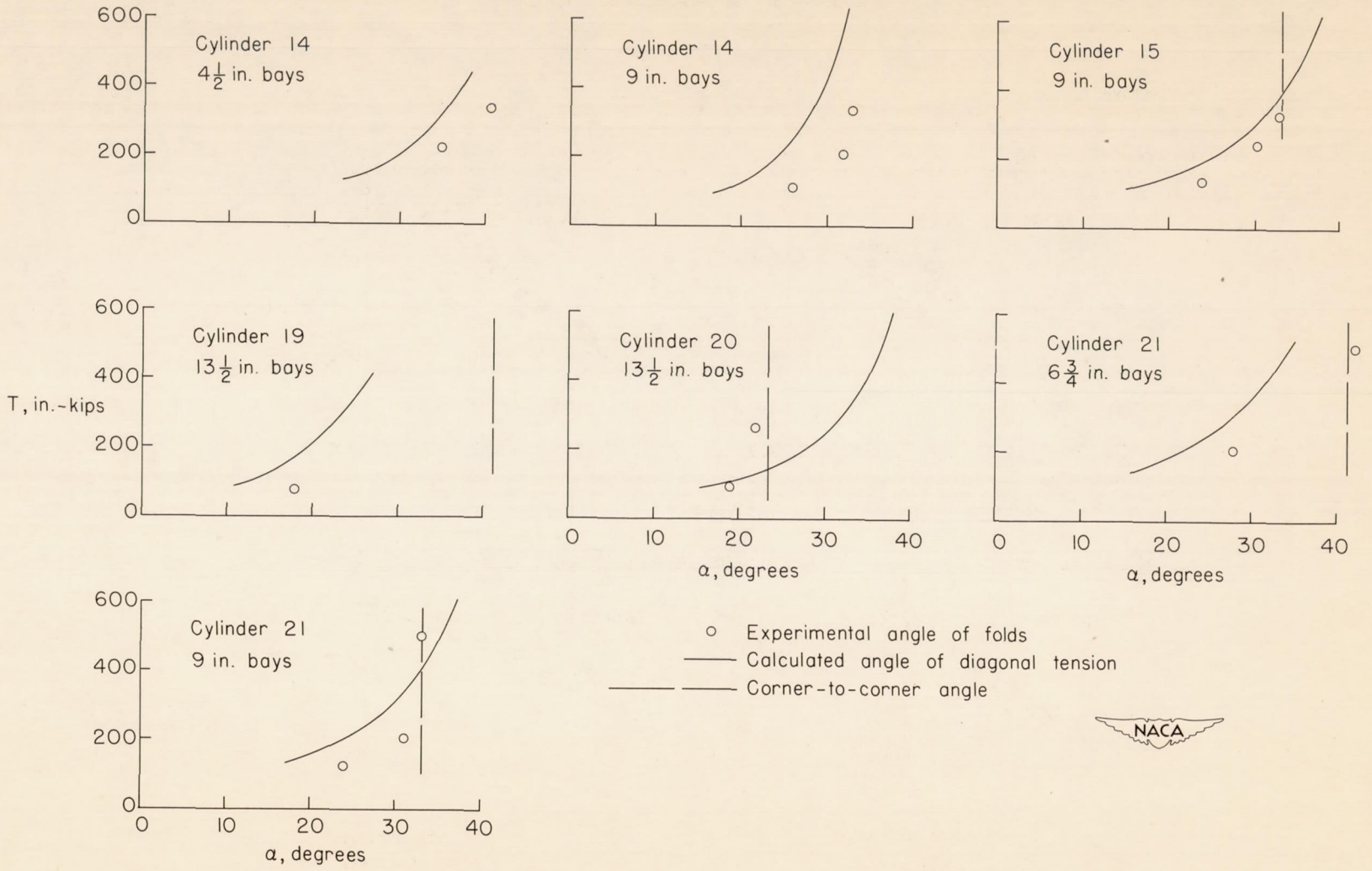

Figure 30.- Angle of folds (ARL cylinders).

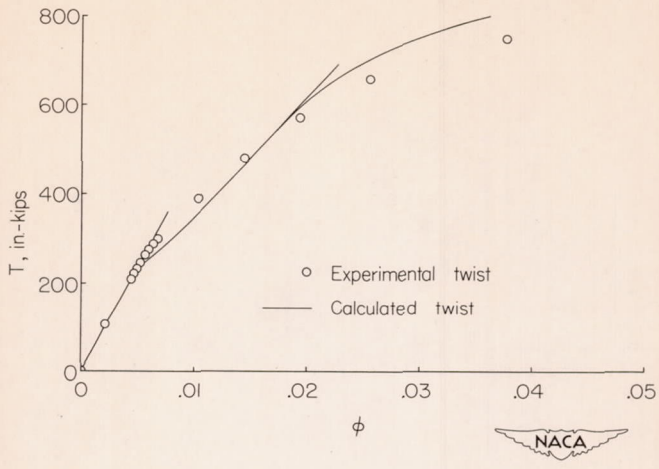

Figure 31.- Angle of twist of cylinder 12.

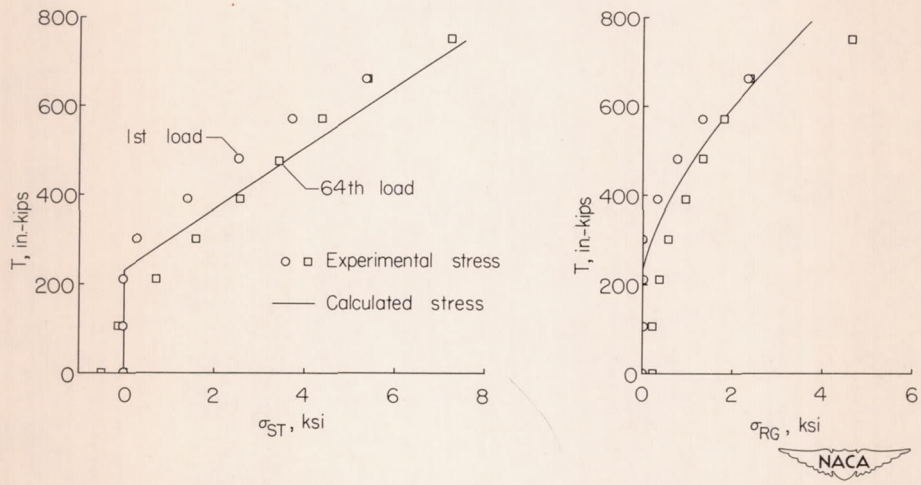

Figure 32.- Stresses in stringers and rings of cylinder 12a, first and last loading.

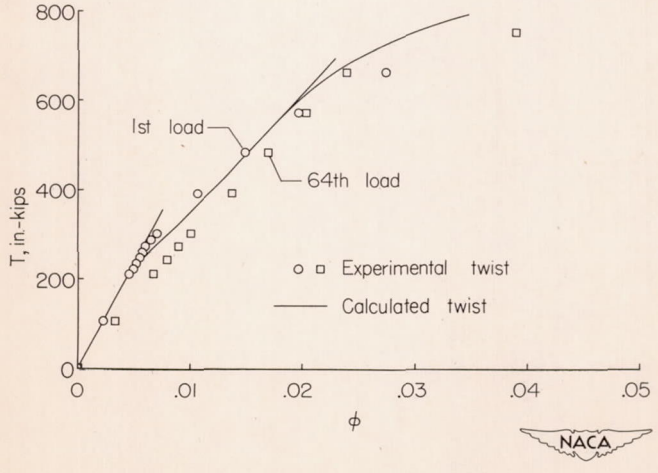

Figure 33.- Twist of cylinder 12a, first and last loading.

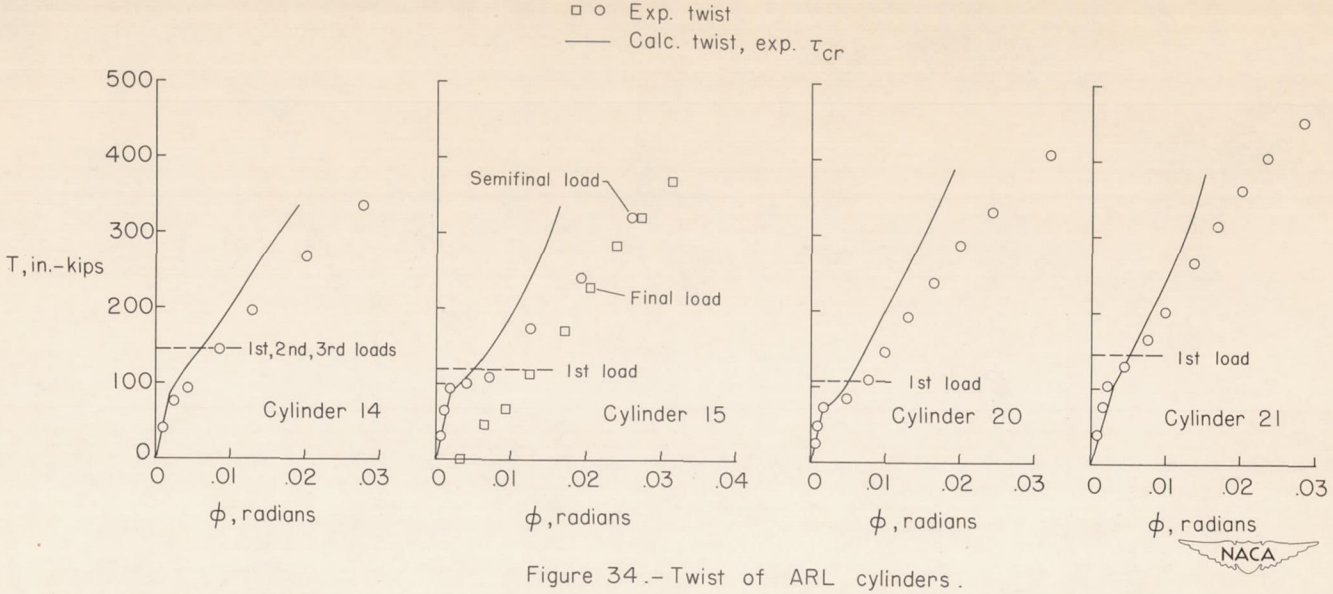

Figure 34.- Twist of ARL cylinders.

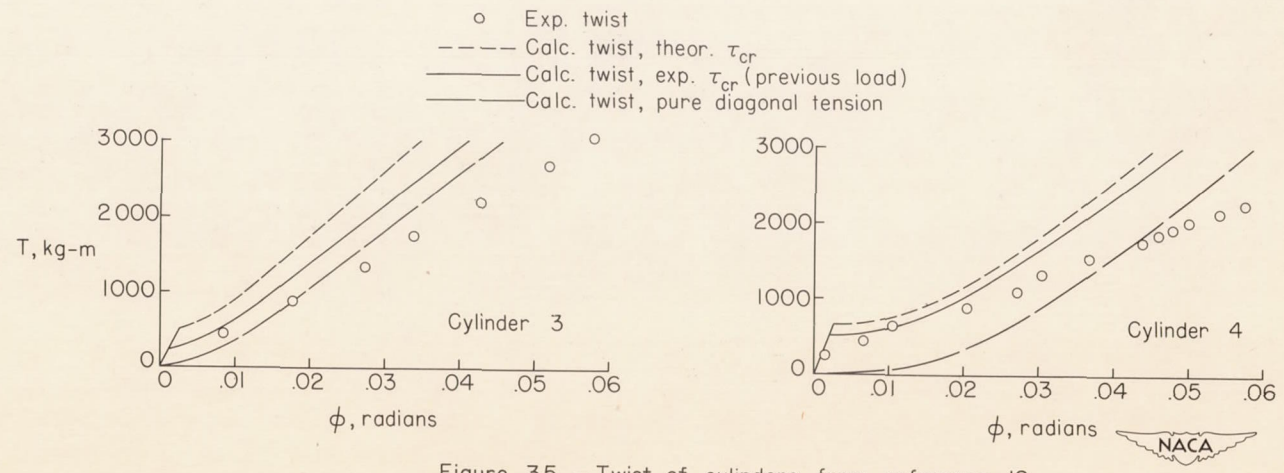

Figure 35.- Twist of cylinders from reference 12.

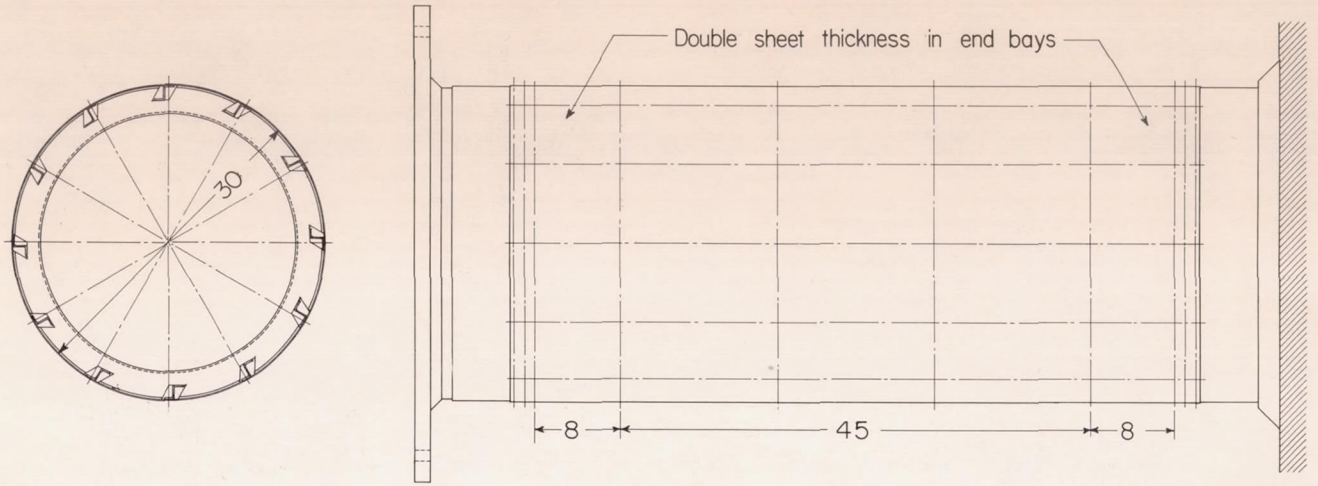

(a) Cylinder dimensions.

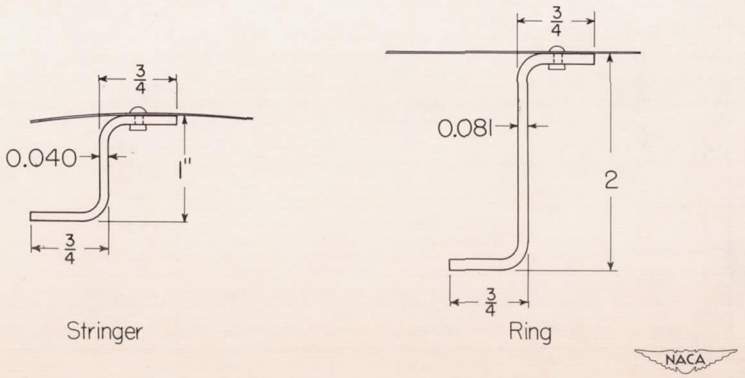

(b) Stiffener dimensions.

Figure 36.- Nominal dimensions of cylinders for combined-load tests.

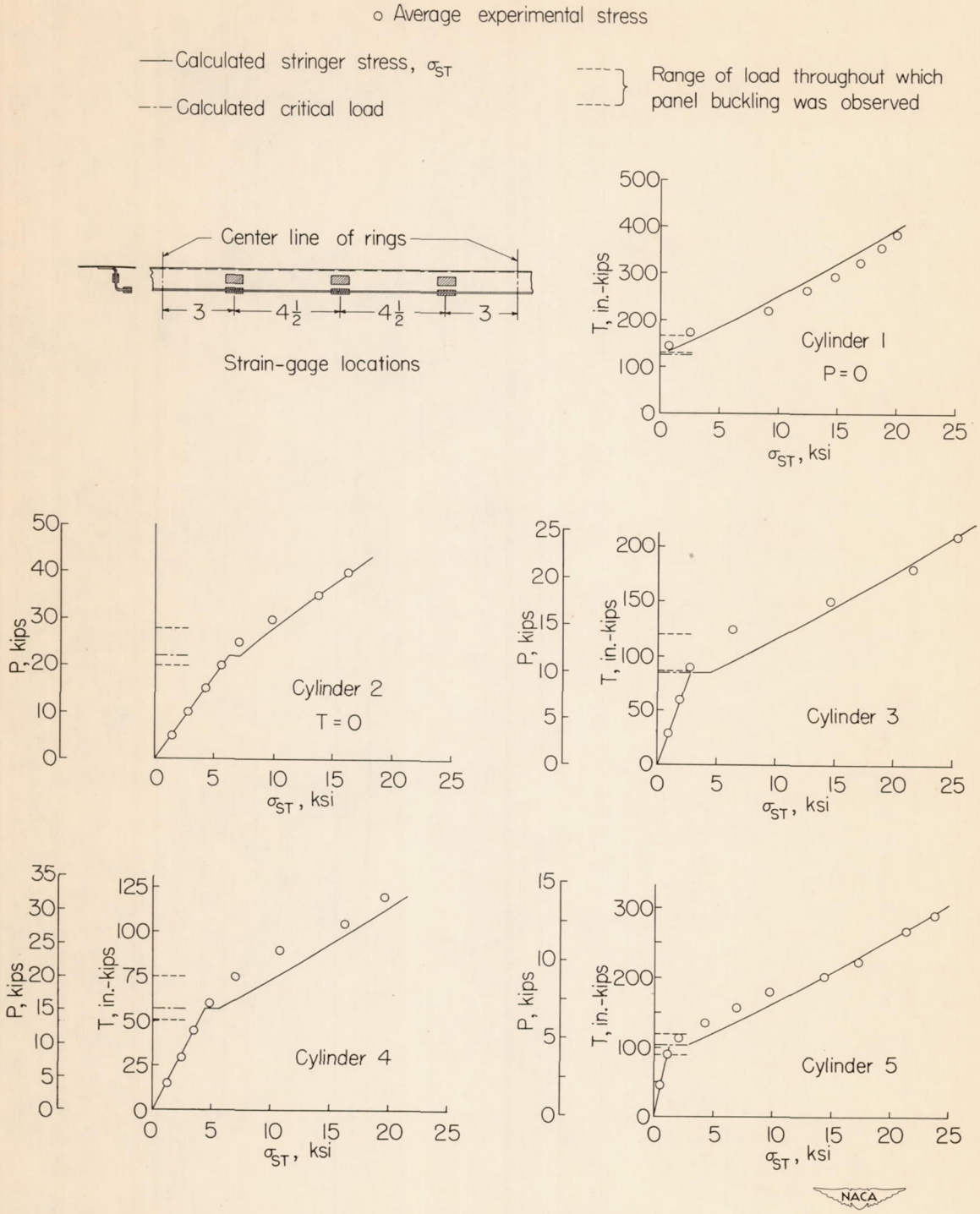

Figure 37.-Stresses in cylinders under combined loading.

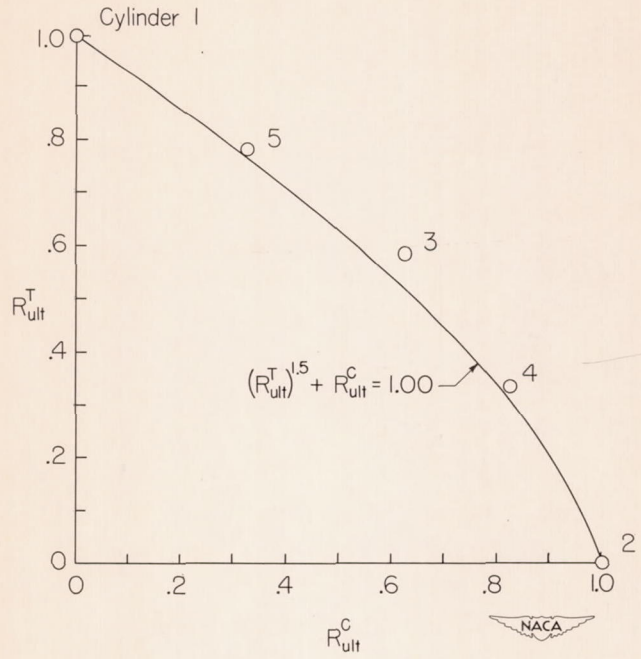

Figure 38.- Interaction curve for strength of cylinders under combined loading.